

Electronic Thesis and Dissertation Repository

8-24-2012 12:00 AM


Water Treatment Using Advanced Oxidation Processes: Application Perspectives

Charles R. Gilmour
The University of Western Ontario

Supervisor
Dr. Madhumita Ray
The University of Western Ontario

Graduate Program in Chemical and Biochemical Engineering
A thesis submitted in partial fulfillment of the requirements for the degree in Master of
Engineering Science
© Charles R. Gilmour 2012

Follow this and additional works at: <https://ir.lib.uwo.ca/etd>

 Part of the [Catalysis and Reaction Engineering Commons](#), and the [Environmental Engineering Commons](#)

Recommended Citation

Gilmour, Charles R., "Water Treatment Using Advanced Oxidation Processes: Application Perspectives" (2012). *Electronic Thesis and Dissertation Repository*. 836.
<https://ir.lib.uwo.ca/etd/836>

This Dissertation/Thesis is brought to you for free and open access by Scholarship@Western. It has been accepted for inclusion in Electronic Thesis and Dissertation Repository by an authorized administrator of Scholarship@Western. For more information, please contact wlsadmin@uwo.ca.

WATER TREATMENT USING ADVANCED OXIDATION PROCESSES:
APPLICATION PERSPECTIVES

(Spine title: Water Treatment Using Advanced Oxidation Processes)

(Thesis format: Monograph)

by

Charles Gilmour

Graduate Program in Engineering Science
Department of Chemical and Biochemical Engineering

A thesis submitted in partial fulfillment
of the requirements for the degree of
Masters in Engineering Science

The School of Graduate and Postdoctoral Studies
The University of Western Ontario
London, Ontario, Canada

© Charles Gilmour 2012

THE UNIVERSITY OF WESTERN ONTARIO
School of Graduate and Postdoctoral Studies

CERTIFICATE OF EXAMINATION

Supervisor

Examiners

Dr. Mita Ray

Dr. Lars Rehmann

Dr. José E. Herrera

Dr. Jason I. Gerhard

The thesis by

CHARLES GILMOUR

entitled:

**Water Treatment using Advanced Oxidation Processes: Application
Perspectives**

is accepted in partial fulfillment of the requirements for the degree of
Masters in Engineering Sciences

Date

Chair of the Thesis Examination Board

Abstract

Advanced oxidation processes (AOPs) using hydroxyl radicals and other oxidative radical species are being studied extensively for removal of organic compounds from various waste streams. However, large scale applications of these highly effective technologies in water and wastewater treatment are still very limited due to cost and inadequate information about the resultant water quality. This study focuses on the evaluation of the upstream processing and downstream post treatment analysis of selective AOPs. In the first stage of research, the performance of a proprietary catalyst (VN-TiO₂) was compared with the industry standard P25 TiO₂, for the use in a pilot-scale immobilized photocatalytic reactor. Using a dip coated fibreglass disk support in the VN-TiO₂ solution and calcining, porous films with high surface area were produced. Although films formed by VN-TiO₂ on fibreglass disks had a reaction rate 50% lower than that of P25, the VN-TiO₂ disks were mechanically robust in the reactor, compared to those coated with P25. The addition of 15% P25 in the VN-TiO₂ solution increased the reaction rate by 40%, while maintaining the mechanical stability. Reuse potential of both catalysts (VN-TiO₂ and P25) was tested, and the rates of deactivation were comparable for both catalysts. Deactivation occurred possibly due to sustained adsorption of intermediates as well as loss of active sites due to heat treatment for reactivation. The low cost of the fibreglass, as compared to commonly used borosilicate glass, in combination with the VN-TiO₂ catalyst is ideal for testing pilot scale reactor designs.

In the second stage of the study two bioassays were used to evaluate and compare the toxicity of bisphenol A, and its degradation intermediates formed in three AOPs, namely UV/H₂O₂, ozonation, and photocatalysis. Two assays were used in evaluating water quality, namely the Ames Test for mutagenicity and the YES assay for estrogenicity. Both UV/H₂O₂ and ozonation removed less than 10% of the initial total organic carbon (TOC), whereas photocatalysis resulted in a 50% reduction of TOC indicating a significant difference in intermediate formation. No mutagenicity was found over the entire tested range of BPA degradation in any of the AOPs. Estrogenicity steadily decreased in accordance with BPA degradation, and was below the limit of detection for photocatalysis. UV/H₂O₂ and ozonation results indicated the possible formation of intermediates with slight estrogenic activity as estrogenicity reached a plateau with a constant value at 15% of initial estrogenicity, while

BPA continued to degrade with time. The work demonstrated effective use of bioassay tools in determining performances of AOPs.

Keywords

Photocatalysis, BPA, water treatment, advanced oxidation processes, Ames Test, YES assay

Dedication

To my loving wife

Acknowledgments

I would like to start by giving my complete gratitude to my supervisor, Dr. Mita Ray, for taking me on two years ago; your exceptional academic and scientific guidance has guided me towards success and hopefully a very bright future.

I would like to thank Sura Ali, for performing the YES and Ames Test for my research, without your help I could have never completed my thesis. As well, I would like to give my gratitude to Dr. Lars Rehmann for letting me use his laboratory equipment and for always being willing to help explain many challenging concepts.

At the lowest point in my research, Mehran Andalib provided the strict, but motivating leadership and guidance to help get my thesis back on track. As well, I would like to thank Noshin Hashim for, if you had not been willing to communicate with me two years ago and introduced me to Dr. Ray, I would have never gotten this far. I would also like to thank my laboratory colleagues Charu Chawla and Shubhajit Sarkar.

Finally, as has been the fact for more than six years, I could have never accomplished any of my successes without my beautiful and loving wife, Rosie. I owe you so much for all of your love, support, and sacrifice.

Table of Contents

CERTIFICATE OF EXAMINATION	ii
Abstract	iii
Dedication	v
Acknowledgments	vi
Table of Contents	vii
List of Tables	xi
List of Figures	xii
Chapter 1	1
1 Introduction	1
1.1 Background	1
Chapter 2	5
2 Literature Review	5
2.1 Background	5
2.2 Advanced Oxidation Processes	5
2.2.1 Ozonation	6
2.2.2 UV/H ₂ O ₂	7
2.3 Semi-Conductor Photocatalysis	8
2.3.1 Photocatalytic Mechanism	8
2.3.2 Photocalysis Model Compound – Methylene Blue	10
2.3.3 Immobilisation of Titanium Dioxide	11
2.3.4 Immobilisation Procedures	12
2.3.5 Titanium Dioxide Thin Films from Sol-Gel	13
2.4 Bioassays for AOP Water Quality Analysis	13
2.5 Model Compound - BPA	14

2.6	Application of AOPs for BPA Degradation.....	16
2.7	Mutagenicity Analysis of Water	20
2.7.1	The Ames Test	20
2.8	Yeast Estrogen Screen	22
2.9	Summary of Literature Review and Literature Gaps	22
Chapter 3	24
3	Photocatalytic Performance of Titanium Dioxide Thin Films from Polymer Encapsulated Titania	24
3.1	Introduction.....	24
3.2	Experimental.....	26
3.2.1	Preparation of Support Mediums and Coating Procedures	26
3.2.2	Characterization of Titanium Dioxide Films	27
3.2.3	Photocatalytic Activity Measurement	28
3.3	Results and Discussion	30
3.3.1	Proprietary Titanium Dioxide Catalyst.....	30
3.3.2	Support Material and Coating Procedure	32
3.3.2.1	Glass Plate with Spray Coatings.....	33
3.3.2.2	Inorganic Fibres with Dip Coating.....	36
3.3.2.2.1	TGA & DSC Analysis.....	36
3.3.2.2.2	Surface Morphology.....	38
3.3.2.2.3	XRD	41
3.3.2.2.4	Surface Area and Pore Size Distribution.....	43
3.3.3	Photocatalytic Performance.....	47
3.3.4	Mechanical Stability of the Films	51
3.3.5	Long-Term Photocatalytic Performance	52
3.3.6	Photocatalytic Degradation Mechanism of Methylene Blue.....	56

3.3.7 Effect of Calcination Temperature	59
3.4 Summary and Economic Consideration for Proposed Application	60
Chapter 4	63
4 Assessment of the Mutagenicity and Estrogenicity of BPA Following Advanced Oxidation Treatment	63
4.1 Introduction.....	63
4.2 Experimental.....	65
4.2.1 Chemicals.....	65
4.2.2 HPLC Analysis.....	65
4.2.3 Other Analyses	66
4.2.4 Ozonation	66
4.2.5 UV/H ₂ O ₂	67
4.2.6 Photocatalysis.....	68
4.2.7 The Ames Test Protocol.....	68
4.2.8 Yeast Estrogen Screen.....	69
4.2.8.1 Calculation of Sample Response.....	71
4.3 Results and Discussion	72
4.3.1 BPA Degradation	72
4.3.2 Degree of Mineralisation and Intermediate Formation.....	73
4.3.3 Mutagenicity Comparison.....	76
4.3.4 Removal of Estrogenicity	79
Chapter 5	80
5 Conclusions and Recommendations	80
5.1 Conclusions.....	80
5.2 Recommendations.....	82
References.....	83

Curriculum Vitae 97

List of Tables

Table 2.1: Properties of methylene blue.	11
Table 2.2: General properties of bisphenol A.	15
Table 2.3: Detected primary intermediates for BPA degradation by AOPs.	19
Table 3.1: Surface characteristics and crystal properties of VN-TiO ₂ and hybrid films.	47
Table 3.2: Change in mass for coated fibreglass disks after reusability testing.	53
Table 3.3: Fibreglass versus glass for use in an immobilised photocatalysis reactor.	62

List of Figures

Figure 2.1: Photo-induced formation of electron–hole pair and corresponding reaction pathways in a spherical TiO ₂ particle..	9
Figure 2.2: Ozonation degradation mechanism of BPA.	17
Figure 2.3: UV/TiO ₂ degradation mechanism of BPA.	18
Figure 2.4: Frameshift mutation mechanism.	21
Figure 2.5: Base pair substitution resulting in a missense mutation.	22
Figure 3.1: Image of blank fibreglass and quartz wool disks.	27
Figure 3.2: Cross-sectional diagram of swirl flow reactor.	29
Figure 3.3: Photograph of coated fibreglass disk in swirl flow reactor.	30
Figure 3.4: General scheme of VN-TiO ₂ synthesis procedure.	31
Figure 3.5: PDDA and titanium precursor chemical structure.	31
Figure 3.6: TEM image and size distribution of VN-TiO ₂ encapsulated nano-particles in solution.	32
Figure 3.7: SEM of coatings on borosilicate glass.	34
Figure 3.8: EDX of coatings on borosilicate glass.	35
Figure 3.9: Dissociation of PDDA monomer	37
Figure 3.10: TGA and DSC curve for VN-TiO ₂ dried powder sample.	37
Figure 3.11: SEM of coatings on fibreglass.	40
Figure 3.12: EDX of coatings on fibreglass.	41
Figure 3.13: X-ray diffraction spectra of different types of films on fibreglass disks.	42

Figure 3.14: X-ray diffraction spectra of VN-TiO ₂ and hybrid films removed from glass disks.	43
Figure 3.15: Pore size distribution of each thin film coating, P25 as powder.	44
Figure 3.16: Adsorption/desorption isotherms for each coating, scraped from glass and P25 as powder.	45
Figure 3.17: Film characteristics of two separately prepared VN-TiO ₂ films, adsorption/desorption isotherm and pore size distribution curve.	46
Figure 3.18: Removal of MB for immobilised P25.	48
Figure 3.19: Optimal loadings for VN-TiO ₂ and P25 on fibreglass disks.	49
Figure 3.20: MB degradation curve for various coatings on fibreglass.	50
Figure 3.21: Effect of P25 mass loading on hybrid VN-TiO ₂ coated fibreglass disks.	51
Figure 3.22: Image of coated fibreglass disks.	52
Figure 3.23: Reusability tests for VN-TiO ₂ coated fibreglass.	54
Figure 3.24: Reusability tests for P25 coated fibreglass.	54
Figure 3.25: Images of the effect of long-term testing and regeneration on the apparent colour of coated fibreglass disks.	55
Figure 3.26: First order rate constants for regenerated fibreglass disks compared to initial rate of degradation.	56
Figure 3.27: Comparison in the degree of blue shifting relative to MB conversion for different catalysts on fibreglass.	57
Figure 3.28: N-demethylation products of methylene blue.	58
Figure 3.29: Degradation mechanism of methylene blue through breakage of aromatic ring.	58

Figure 3.30: Effect of calcination temperature for VN-TiO ₂ films on quartz wool disk.....	60
Figure 4.1: Experimental set-up for ozonation.	67
Figure 4.2: Experimental set-up for UV/H ₂ O ₂	68
Figure 4.3: Estradiol 50 µg/L standard curve using methanol.....	70
Figure 4.4: Degradation curves for BPA in each AOP tested.....	72
Figure 4.5: Determination of apparent first order rate constant, k (min ⁻¹) for each AOP BPA degradation experiment.....	73
Figure 4.6: Degree of mineralization for BPA removal in each AOP	74
Figure 4.7: HPLC chromatogram of BPA degradation.	76
Figure 4.8: Mutagenicity analysis using the Ames Test for BPA degradation in different advanced oxidation processes.	78
Figure 4.9: Analysis of estrogenic activity of BPA in aqueous solution.....	79

Chapter 1

1 Introduction

1.1 Background

Continuing processes of industrialization and urbanization due to population growth, deforestation, and pollution are exerting pressure on the depleting freshwater resources in many parts of the world. A recent UN report (Reuters, 2010) mentions that the world's "freshwater is not being used sustainably" and calls for a "radical rethink" of policies to manage competing claims. The long-term sustainability of clean water supply is dictated by source water protection, management of water resources, and the efficiency of water reclamation from various effluents. Trace concentrations of numerous organic compounds (emerging contaminants (EC), and endocrine disrupting compounds (EDCs)) such as pharmaceuticals and personal care products (PPCP), including prescription drugs and biologics, "nutraceuticals," fragrances, sunscreen agents, and numerous others are reported in various wastewater effluents and aquatic systems. In addition to these, increasing levels of naturally occurring organic materials (NOM) directly linked to societal nutrient management practices are of serious consequence for managing water resources (Caliman & Gavrilescu, 2009; Onesios et al., 2009; Li et al., 2010). These compounds and their bioactive metabolites are continually being introduced to the aquatic environment as complex mixtures via a number of routes but primarily through both untreated and inadequately treated sewage. Growing health and environmental concerns have made PPCPs of particular interest as long-term exposure to low levels of PPCPs could have adverse effects on aquatic and terrestrial ecosystems and/or human health (Environment Canada, 2009). For example, chronic exposure to small levels (2-6 ng/L) of the synthetic estrogen used in birth control pills (ethynylestradiol-EE2) has been shown to feminize wild fish populations in Canadian lake systems (Kidd et al., 2007).

In the past, many countries including Canada have relied on "dilution being the solution" for discharging of micropollutants, but with increasing populations along major waterways, increasingly high loads of micropollutants, and higher water demands,

dilution is proving to be no longer a cheap, viable solution. The occurrence of micropollutants, therefore, poses problems for two major water management aspects, protection of source water, and reuse potential of a vast majority of municipal and industrial wastewater effluents. The traditional treatment methods such as secondary biodegradation cannot appreciably remove many of these contaminants of emerging concern. While advanced treatment technologies such as activated carbon and reverse osmosis can produce high quality water, they only transfer and concentrate the pollutants from one phase to another, requiring further processing to render the compounds inert.

Advanced oxidation processes (AOPs), which produce reactive species like hydroxyl radicals in-situ, are identified as one of the potential technologies for the removal of trace concentrations of organics from various water streams (Abdelmelek et al., 2011).

Traditional water disinfection treatment processes such as ozonation and UV disinfection can easily be retrofitted to accomplish advanced oxidation in both water and wastewater treatment plants. There has been over three decades of intense research into many different types of AOPs as well as wide adoption of some of these processes. Of the many AOPs tested, ozonation, UV/ozone, UV/hydrogen peroxide, and UV/photocatalysis are most commonly studied and used for many applications. Unfortunately, the common disadvantage shared between all AOPs is the high operating cost, which has somewhat limited large-scale application of this otherwise very powerful technology. However, with the advent of higher efficiency UV lamps, visible light catalysts, and improved reactor design, with the help of computational fluid dynamics and energy modeling, both UV and solar-based photocatalysis have great potential for large-scale application (Chong et al., 2010). However, further research is still needed in developing new immobilised photocatalysis reactors and to improve the performance, the immobilisation, and illumination in the reactor of the photocatalyst.

Although AOPs are perceived to be expensive for complete mineralization of the organic compounds, *partial oxidation* of the initial compounds to less stable intermediates is a viable option, if the intermediates readily degrade in the environment and are harmless to the aquatic environment and human health. However, partial oxidation of organic contaminants can in some cases result in the formation of intermediates more toxic than

the parent compound (Rizzo, 2011), and the nature and number of the degradation products will depend on the employed oxidation process, reaction time, and water quality metrics. Quantifying the accumulated effects of the resulting mixture of compounds on living systems rather than on the precise quantification of their chemical compositions, which is costly and time consuming, and can be futile without the prior knowledge of dose and effect relationship of an intermediate, can be beneficial to assess the performance of a specific AOP. Application of various bioassays to characterize the effluent quality from different AOPs could be a useful tool to optimize the performance of AOPs. Although bioassays have been used in determining toxicity of individual chemicals, they have never been used in determining efficacy and comparative performance of various AOPs.

Objectives of the Present Study

Based on the above, further research and development are needed in both upstream process optimization and downstream water quality evaluation in order to implement AOPs in large-scale water treatment. The objective of this work is to address both the upstream and downstream issues, specifically to (i) determine an effective immobilization technique and catalyst support for a proprietary photocatalyst and compare its performance with the industry standard P25 TiO₂ using methylene blue as a model compound, and (ii) to evaluate the effectiveness of three commonly used AOPs namely ozonation, UV/H₂O₂, and UV photocatalysis for the removal of bisphenol A using two different bioassays, the Ames Test and yeast estrogen screen (YES).

Overview of Dissertation

This thesis is divided into the following chapters:

Chapter 1 provides the background and the objectives of the research.

Chapter 2 presents a literature review of the relevant theories for both stages in the research project.

Chapter 3 describes the first stage of the research, in which a proprietary catalyst was evaluated for the use in an immobilised photocatalytic reactor, and was characterised and compared to the performance of the reference catalyst P25.

Chapter 4 discusses the secondary stage of the research where the toxicity using two bioassays is compared for the degradation of bisphenol A in three commonly studied advanced oxidation processes.

Chapter 5 reports the conclusions and recommendations for future work.

Chapter 2

2 Literature Review

2.1 Background

The widespread occurrence of organic micropollutants such as pesticides, pharmaceuticals and personal care products, flame retardants, and endocrine disrupting compounds (EDCs) in receiving bodies and drinking water influents has been a global issue of concern for academia and environmental agencies for over two decades, and more recently in the general public. In many cases, these pollutants can be traced back to their incomplete removal and discharge from wastewater treatment facilities. Although the direct effect of these compounds on human health is not yet fully understood the detrimental effect on organisms in these receiving bodies from EDCs has already been demonstrated (Routledge & Sumpter, 2005), such as the feminization of male fish due to the release of natural hormones (Rodgers-Gray et al., 2000). Research on organic micropollutants in relation to the point of wastewater discharge can be divided into two major areas: upstream treatment and downstream monitoring. Developing advanced technologies and improved operation of wastewater treatment plants results in higher quality effluents. At the same time, in the downstream analysis, improved techniques to detect pollutants at lower concentrations and tools to evaluate the toxicity of the contaminated stream, feed back to the upstream process in order to optimize plant operation. With looming water scarcity in many parts of the world, providing clean drinking water and sustainable development will require the use of water recycling in the future and it will be imperative that recycled water will not impact both environmental and human health (Falconer et al., 2006). Consequently, extensive research and development in both upstream processing and downstream monitoring are needed.

2.2 Advanced Oxidation Processes

For the treatment of drinking water and tertiary wastewater, a group of chemical oxidative technologies classified as advanced oxidation processes (AOPs) has garnered a significant level of interest academically and industrially over the last three decades. All

AOPs are characterized by the production of highly reactive and non-selective hydroxyl radicals, which are the strongest oxidants in an aqueous medium (Staelin & Hoigne, 1985). Hydroxyl radicals are capable of oxidizing nearly all organic compounds to water, carbon dioxide, and mineral salts through a process termed *mineralization* (Chen et al. 2000b). The technologies that can be classified as AOPs fall under two general categories. The first utilizes UV in conjunction with other chemical additives, examples of this are: UV/H₂O₂, UV/O₃, UV/TiO₂, and UV/Fenton. When no UV source is used the technology can be termed as a *dark oxidative process*, such as: ozonation (O₃), Fenton's reagent, ultrasound, and microwaves to name a few. Of the many AOPs developed three have garnered the most study and use industrially: ozonation, UV/H₂O₂, and photocatalysis utilizing either ultraviolet (UV) or solar irradiation with titanium dioxide (TiO₂). There has been significant research done on each of these AOPs with respect to reactor design, optimization, and modeling. In-depth reaction kinetics of many pollutants have also been investigated, which are essential for large-scale application.

2.2.1 Ozonation

The use of ozonation in water treatment has seen the most application compared to all other AOPs and has been used for disinfection, odor control, and colour removal (Rice et al., 1981). The degradation of pollutants in water using ozonation occurs through two mechanisms. The first is the direct oxidation by ozone, which is a highly selective process with low reaction rates (Hoigne, 1998). The other is an indirect mechanism to produce hydroxyl radicals. The first step of this process is the decomposition of ozone by hydroxide ions (Eq. 2.1). The formed hydroperoxyl radical is in an equilibrium state (Eq. 2.2). The superoxide anion radical and ozone then react to form ozonide anion radical (Eq. 2.3), which then immediately decomposes into oxygen and a hydroxyl radical (Eq. 2.5) (Gottschalk et al., 2010). Overall, three ozone molecules theoretically produce two hydroxyl radicals as shown in Eq. 2.6.



Overall:



A major limitation of ozonation is the formation of potentially harmful by-products reacting with background compounds in water, one of which, bromate, is regulated and is considered a possible human carcinogen (Gunten & Hoigne, 1994; Boorman et al., 1999). It is then important to optimize both the disinfection and oxidation processes of ozonation to minimize toxic by-product formation.

2.2.2 UV/H₂O₂

UV irradiation of tertiary wastewater for disinfection is common practice, but photolysis alone does not appreciably degrade the vast majority of organic micropollutants of increasing concern. The addition of hydrogen peroxide (H₂O₂) in conjunction with UV radiation at 254 nm cleaves apart the O-O bond to generate hydroxyl radicals (Eq. 2.7) (Legrini et al., 1993). Due to the low molar extinction coefficient (19.6 M⁻¹s⁻¹) of hydrogen peroxide at 254 nm (Andreozzi et al., 1999), a high concentration of H₂O₂ is needed for adequate radical formation, but it is essential not to add too much of the peroxide as it can act as a scavenger (Eq. 2.8). Therefore, it is important to determine the optimal peroxide concentration necessary based on the parameters of the polluted water.



The advantages of UV/H₂O₂ are that it has high reaction rates and a modular reactor design, leading to a smaller footprint in the treatment plant. Since UV-254 nm lamps are used, the system also provides disinfection. Unlike ozonation and chlorination there are no toxic disinfection by-products formed after treatment that require expensive removal units. On the other hand, UV/H₂O₂ requires water with a very high UV transmittance. A pre-treatment filtration unit is required to lower the turbidity before the water enters the reactor, especially in wastewater applications. Energy for the UV lamps and the addition and removal stages of hydrogen peroxide result in a high operating cost.

2.3 Semi-Conductor Photocatalysis

Unlike the previously mentioned AOP methods, photocatalysis up to this point has seen limited full-scale application either in drinking or wastewater treatment, but has garnered a significant amount of research interest in academia over the last three decades. The one major advantage of this process is the potential to use natural sunlight. Combined with a highly active catalyst, this technology could be applied worldwide not only for water treatment, but for hydrogen production, self-cleaning coatings, and many other uses. This explains the fact that even though it has the least industrial application to date compared to ozonation and UV/H₂O₂, it has received the majority of the academic research, with >1000 papers published per year over the last decade, mostly with P25 TiO₂, an inexpensive and non-toxic photocatalyst.

2.3.1 Photocatalytic Mechanism

Titanium dioxide in either the anatase or rutile phase has a band-gap of 3.2 or 3.0 eV, respectively (Carp et al., 2004). When the energy of a photon from the light source exceeds this gap, $\lambda < 388$ nm, a photoexcited electron will be promoted to the conduction band, leaving a positive hole in the valence band, this is termed as the *electron – hole pair* ($e^- - h^+$), where *cb* and *vb* denotes conduction band and valence band respectively (Eq. 2.9). The charged particles can then; recombine to produce heat (Eq. 2.10), become trapped, where *tr* is the trapped charge (Eq. 2.11-2.12), or migrate to the surface to participate in a series of redox reactions. The overall scheme is shown in Fig 2.1.

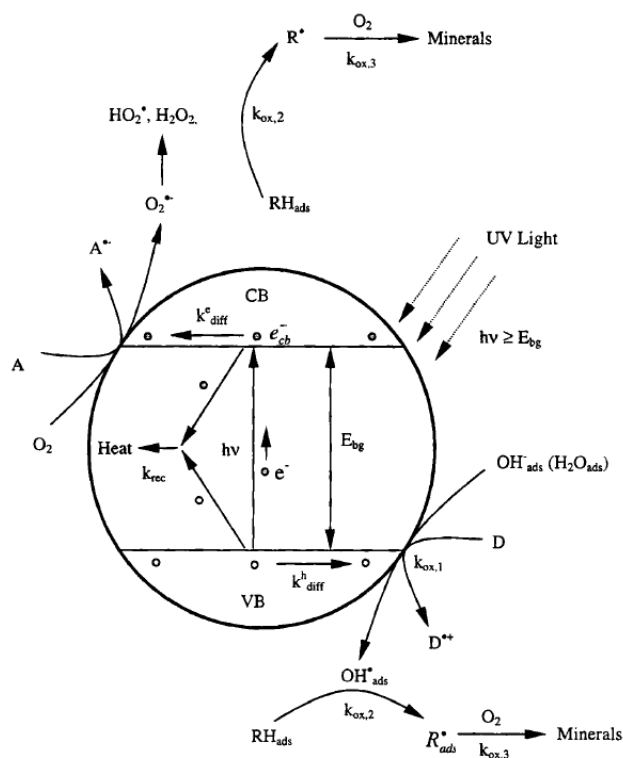


Figure 2.1: Photo-induced formation of electron–hole pair and corresponding reactions pathways in a spherical TiO₂ particle (Chen et al., 2000b).



In the aqueous solution under irradiation the catalyst remains in an electrostatic equilibrium, where at steady-state there is an equal rate of electron and hole migration to the surface (Pruden Childs & Ollis, 1981). Surface trapped holes are responsible for the mineralization of organic micropollutants by either direct oxidation between the pollutant

and hole, where *ads* is the adsorbed species (Eq. 2.13) or by reacting with surface adsorbed molecular water and hydroxide ions to produce hydroxyl radicals, Eq. 2.14-2.15.



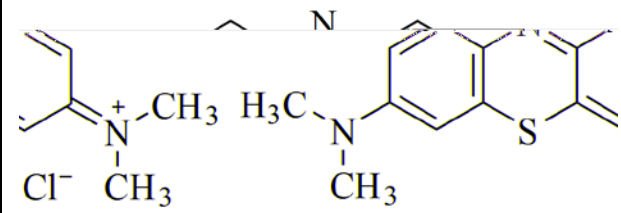
As the holes are involved in the oxidative reactions, the surface electrons must also react to maintain the charge equilibrium and to minimize recombination. Oxygen is used as an electron scavenger due to the minimal processing cost of sparging the solution with air. Dissolved oxygen will adsorb onto the catalyst surface and be reduced by the surface trapped electron (Eq. 2.16). From there, a series of further reactions occur as shown in Eq. 2.17–2.20. Even though hydrogen peroxide is produced, its contribution to the reactive hydroxyl radicals towards mineralisation is deemed minimal.

2.3.2 Photocatalysis Model Compound – Methylene Blue

Textile dyes and industrial dyestuffs represent an important class of aqueous pollutant found in industrial wastewater discharge. A large amount of industrial dyes are lost in the dyeing process. In the textile industry, this loss can be 4% of the dye used (Martínez-Huitle & Brillas, 2009). If released directly into the aqueous environment, this can cause an aesthetic effect by changing the visible colour of the water. These dyes are highly stable and are not completely removed in conventional wastewater treatment processes. The dyes and their by-products formed from the transformation during treatment and in the receiving body, can have a toxic effect on organisms in the environment (Platzek et al., 1999; Sharma et al., 2007). For photocatalytic research, dyes are one of the most common model compounds tested not only because they represent a persistent water pollutant, but when dissolved in water the bleaching of the dye during the reaction

provides a quick and simple qualitative response. As well dyes have characteristic absorption properties in the UV/visible spectrum, allowing UV-spectrophotometers to be used to determine kinetic data. Methylene blue (MB) is a cationic dye and the chemical structure and basic properties are shown in Table 2.1. In terms of use as a model compound: kinetic data in terms of parameters (Lakshmi et al., 1995), photocatalytic degradation mechanisms with intermediate analysis (Houas et al., 2001), and tests on reactor configurations (Guillard et al., 2003; Ling et al., 2004) provide a framework for catalytic evaluation. MB also has a high extinction coefficient in the visible range, allowing for lower concentrations to be used in the reaction. MB is relatively transparent to UV radiation, which is used by the TiO₂ catalyst (Fretwell & Douglas, 2001).

Table 2.1: Properties of methylene blue.

Properties	
Structure	
Formula	C ₁₆ H ₁₈ N ₃ SCl
Molecular Mass (g/mol)	319.85

2.3.3 Immobilisation of Titanium Dioxide

Laboratory studies on photocatalysis are typically performed using nano-sized catalyst suspended in the reactor. In these designs the catalyst is evenly dispersed in the solution as it passes through the reactor. The uniform catalyst distribution provides very high surface area to volume ratios with low mass transfer limitations. Even though there have been several patents pertaining to the catalyst in suspension, there has been very little application at a larger scale for water treatment (Mukherjee & Ray, 1999; Chong et al., 2010). Since the catalyst is dispersed as very small particles, energy intensive post-treatment filtration and recycling units are required, which are cost prohibitive (Pozzo et al., 1997). It is essential to provide efficient exposure of light to the catalyst, and due to scattering and small penetration depths, scale-up of suspension reactors is very limited

(Mukherjee & Ray, 1999). The second reactor configuration is immobilisation of the catalyst onto a support. The supports can range from macro particles, such as glass beads and sand (Serpone et al., 1986), to the glass tubes that surround the light source in the reactor (Ray & Beenackers, 1998). Coating the catalyst reduces the active surface area and mass transfer limitations can occur, reducing pollutant degradation in the reactor. Since the catalyst is in a continuous operation, fouling of the active sites on the coated support can reduce the rate over time. Reactor designs that have been developed involving immobilised catalysts include: fluidized bed (Pozzo et al., 2000), supported membrane (Kim et al., 2003), and coated optical fibre (Peill & Hoffmann, 1996) to name a few.

2.3.4 Immobilisation Procedures

One of the standard ways of coating a support with catalyst is to simply create a dispersed solution of commercial catalyst, typically Aeroxide P25. Coating techniques such as dip coating (Fretwell & Douglas, 2001; Rodriguez et al., 2009), spin-coating (Fretwell & Douglas, 2001), electrophoretic coating (Byrne et al., 1998), and spray coating (Byrne et al., 1998) have been used. The coating cycle is followed by high temperature treatment to better bond the commercial catalyst to the support. Dip coating is the easiest of all the coating methods and produces non-uniform films that require several dipping cycles (Byrne et al., 1998; Fretwell & Douglas, 2001). As well, these films are not typically mechanically robust and can be easily wiped off or damaged in the reactor (Mills et al., 2005). The other coating solutions are relatively stable, but could be difficult to produce at larger scales. The other procedure for immobilisation is to synthesize a nano-crystalline thin film of TiO_2 onto the support. Thin films can be synthesized from a solution-route or gas phase deposition (Carp et al., 2004). Sol-gel is the most common solution technique; others include reverse micelles, solvo-thermal, and electrochemical deposition. Common gas phase methods include chemical vapor deposition, electron beam evaporation, spray pyrolysis deposition, and DC-sputtering. As mentioned previously, it is essential to choose a synthesis and coating technique compatible with the support and required film configuration in the reactor, this limits the practical use of many techniques discussed above.

2.3.5 Titanium Dioxide Thin Films from Sol-Gel

Titanium dioxide can be produced from sol-gel using two methods based on the precursor employed. The first is a non-alkoxide route using inorganic titanium salts such as nitrates, chlorides, and sulfates (Sivakumar et al., 2002). Further processing to remove the inorganic anion is required and application for inorganic TiO₂ films is limited. TiO₂ can also be made using alkoxide precursors, most commonly metal alkoxides, such as titanium isopropoxide (Xagas et al., 1999) and titanium propoxide (Kwon et al., 2004). Upon making a stable sol, which is a colloidal suspension of titanium oxide particles formed from the hydrolysis and condensation of the alkoxide, the support is then coated with this solution. The coated film is dried further, condensing to form a gel of amorphous TiO₂ (Brinker et al., 1991). Final heat treatment, typically >400°C, crystallizes the amorphous TiO₂ into the anatase phase, which is usually the desirable crystal phase for photocatalysis. The overall reaction is shown in Eq. 2.21 (Su et al., 2004), where R is the alkyl group. The sol-gel method is advantageous for making TiO₂ thin films, because these films are prepared from highly pure and stable solutions, which require relatively inexpensive reagents and simple batch processing, typically just mixing and a high temperature treatment. The solutions are adaptable to many different coating techniques which further allows for the coating of complex supports. Composition control allows for the addition of dopants to modify optical properties and other additives to better improve film quality towards photocatalytic activity by simply adding the desired reagent (Kim et al., 2002). Scale-up production would still require extensive research and investment, but once an economically feasible reactor design, support, and sol-gel recipe are achieved this would be one of the most viable options available for large-scale application of photocatalysis.



2.4 Bioassays for AOP Water Quality Analysis

Emerging contaminants in wastewater effluents and drinking water influents have become a cause for concern in terms of potential impact on human health. The application of advanced oxidation processes (AOPs) to improve water quality has been

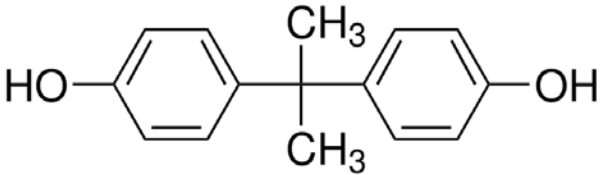
effectively demonstrated with ever-increasing applications worldwide. Although these technologies have potential for complete mineralization of organic compounds to CO₂ and H₂O, cost-optimized technologies for water treatment will lead to the partial oxidation of organic micropollutants. This leads to concern over the formation of potentially more toxic degradation intermediates relative to the starting compounds (Rizzo, 2011). For treated water samples, chemical analysis can determine the existence of specific chemical species but does not provide any information on the adverse effects in absence of prior knowledge about compound and concentration specific toxicity. Also the synergetic and additive toxic effects of the complex chemical mixtures may not be determined by chemical compositional analysis alone. Bioassays measure the acute or chronic response of the test organism relative to the water matrix, based on a specific endpoint for analysis such as: mortality, growth rate, enzymatic activity, and luminescence (Rizzo, 2011). A toxic response is determined by comparing the sample to a positive control and the background, where based on statistical analysis, a confidence of toxicity can be made. The three classes of organisms used in bioassays are: microorganisms, plants and algae, invertebrates and fish for a water sample. The most common assays that have been applied for AOP analysis are: *Daphnia magna*, yeast estrogen screen, salmonella mutagenicity, and *Vibrio fischeri* (Rizzo, 2011). The major advantages of bacterial assays are that they require a comparatively short time for analysis, have simple operation, are relatively inexpensive, and can be used on demand as the bacteria can be stored long-term. The combination of a battery of tests may be implemented as a continuous monitoring technique to confirm the safety of water treated by advanced oxidation processes, both for discharge into the environment and for human consumption.

2.5 Model Compound - BPA

One of the most studied aqueous pollutants has been bisphenol A (BPA) due to its widespread use as an intermediate in the production of mainly polycarbonate and epoxy resins which represent ~94% of the total produced BPA (The Dow Chemical Company, 2012). In 2008, the total global production capacity of BPA was estimated at 5.2 million metric tons (Burridge, 2008). The basic properties of BPA are shown in Table 2.2. As a

result of its use in plastics production, BPA ends up in a variety of consumer goods such as plastic bottles and canned food liners. Major routes for BPA to enter the aqueous environment are through wastewater effluent (Nakada et al., 2004; Hing-Biu & Peart, 2000) and land-fill leachate (Yamamoto et al., 2001; Asakura et al., 2004). Hing-Biu and Peart (2000) studied the occurrence of BPA in both municipal and selected industrial wastewater effluents and found the concentration to range from 0.01-1.08 $\mu\text{g/L}$ to 0.23-149.2 $\mu\text{g/L}$, respectively. The higher range of the industrial effluents was attributed to the chemical and chemical products sector, commercial dry cleaning and paper products (Hing-Biu & Peart, 2000). Consequently as so many commercial products contain BPA, eventually they end up in landfills and can leach from the products into the wastewater stream. Yamamoto et al. (2001) found BPA at a range of 1.3-17,200 $\mu\text{g/L}$ in land-fill leachate in Japan.

Table 2.2: General properties of bisphenol A.

Property	
Structure	
Chemical Formula	$\text{C}_{15}\text{H}_{16}\text{O}_2$
Molecular Mass	228 g/mol
Water Solubility ^a	120-300 mg/L

^a(Ali et al., 2006)

BPA is considered as a weak synthetic endocrine disrupting compound (EDC), which as defined by the U.S. Environmental Protection Agency (EPA) is: “*an exogenous agent that interferes with synthesis, secretion, transport, metabolism, binding action, or elimination of natural blood-borne hormones that are present in the body and are responsible for homeostasis, reproduction, and developmental process*” (United States Environmental Protection Agency, 2011). The discharge of EDCs into receiving bodies from wastewater treatment plants has been shown to cause a detrimental impact on organisms in the environment (Snyder et al., 2003). Due to its high water solubility,

ubiquitous use, proven toxicity, and occurrence in a variety of aqueous pathways, BPA is a very good representative compound for use in environmental engineering research.

2.6 Application of AOPs for BPA Degradation

BPA has gained increased attention from the scientific community for its potential impact on human health, and has gained general public awareness due to its potential to leach from baby bottles and food containers (Diamanti-Kandarakis et al., 2009). This has resulted in a large amount of research focused on its removal from water using advanced oxidation processes such as: UV/H₂O₂ (Rosenfeldt & Linden, 2004), O₃ (Deborde et al., 2005), O₃/UV (Irmak et al., 2005), UV/TiO₂ (Ohko et al., 2001), UV/Fenton (Katsumata et al., 2004), sono-Fenton (Ioan et al., 2007), and ultrasound (Torres et al., 2008). The intermediate analysis below focuses on the three most common AOPs which are relevant to this study: UV/H₂O₂, O₃, and UV/TiO₂. All three AOPs produce hydroxyl radicals and it would be expected that there would be similar intermediate formation in these AOPs. On the other hand, photocatalysis can also oxidize pollutants using photogenerated holes and superoxide radicals (Guo et al., 2010). Ozone can also directly react with the pollutant. This, along with changes in reaction conditions such as pH, can result in the formation of a variety of intermediates, with each compound having potential toxic effects. For intermediates formed from ozonation of BPA, Deborde et al. (2008) found five primary intermediates and proposed the following reaction pathway shown in Fig 2.2. All experiments were run with tert-butanol as a hydroxyl radical scavenger (Deborde et al., 2008) in order to determine the reaction products formed from direct oxidation of ozone. Resorcinol and acetone have also been identified as intermediates of BPA ozonation (Garoma et al., 2010). Further ozonation transformed these primary intermediates to organic acids such as acetic, formic, maleic, and oxalic acids (Garoma et al., 2010). Deborde et al. (2008) also noted the formation of higher molecular weight intermediates formed from the secondary reaction between BPA and smaller intermediates. For the removal of BPA by TiO₂ photocatalysis, Fukahori et al. (2003) proposed a mechanism for the formation of quinone derivatives from two initial reactions (Fig 2.3). BPA hydroxylation results in the formation of water by the abstraction of a hydrogen atom from the phenolic hydroxyl groups of BPA. The phenoxy radicals

further reacted to form quinone derivatives (p-HMS, p-BQ and p-HBA) (Fukahori et al., 2003). The continued photocatalytic degradation resulted in acetaldehyde, formic acid, and acetic acid (Watanabe et al., 2003).

A non-exhaustive list of the different intermediates that have been found for the degradation of BPA by ozonation and photocatalysis is presented in Table 2.3.

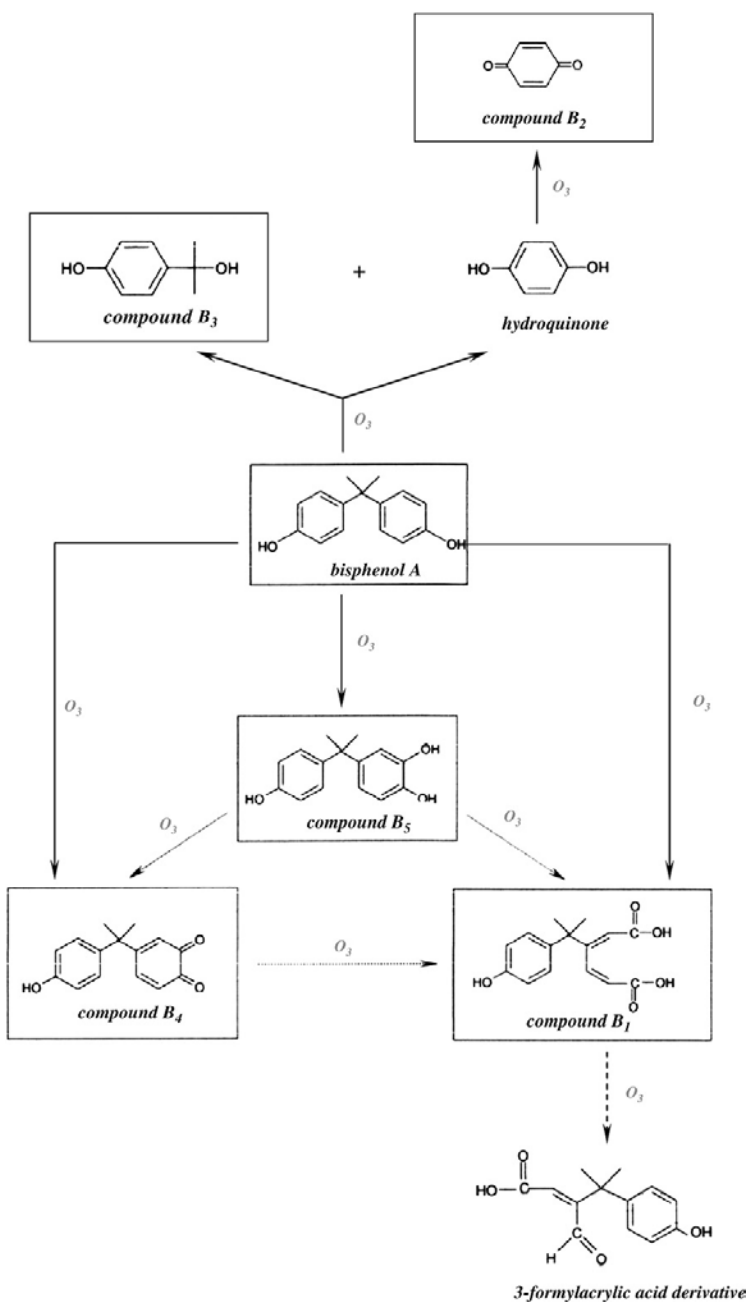


Figure 2.2: Ozonation degradation mechanism of BPA (Deborde et al., 2008).

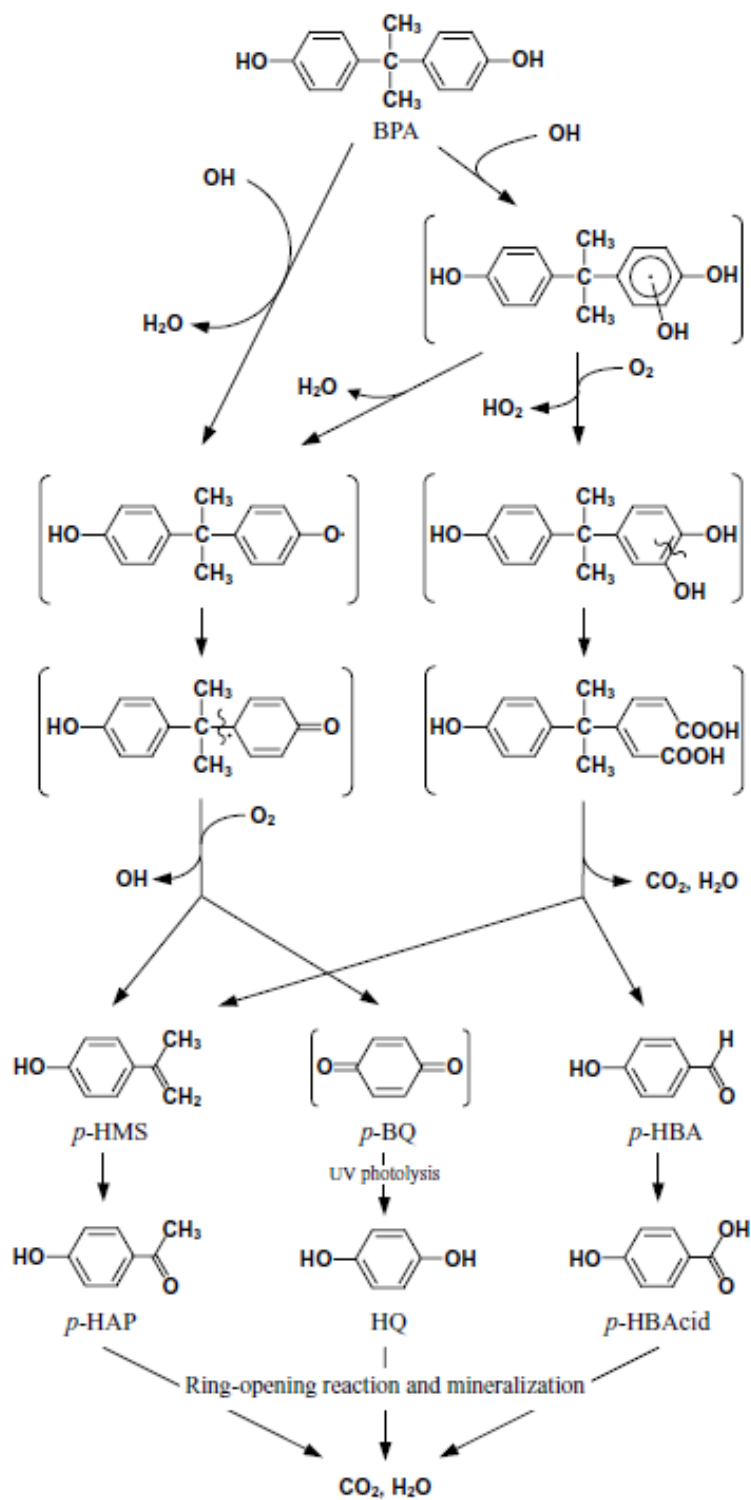
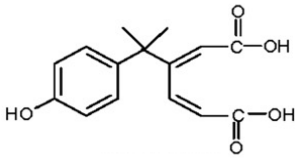
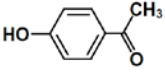
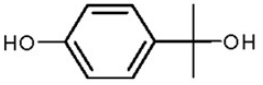
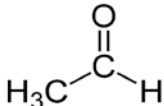
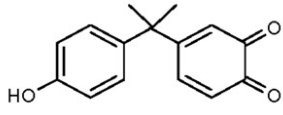
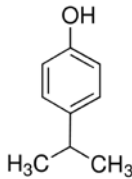
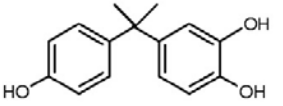


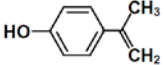
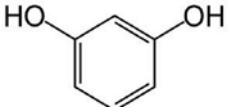
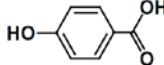
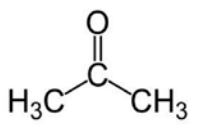
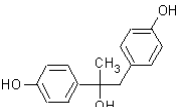
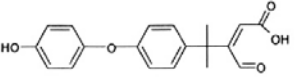
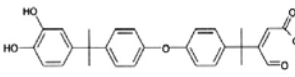


Figure 2.3: UV/TiO₂ degradation mechanism BPA (Fukahori et al., 2003).

Table 2.3: Detected primary intermediates for BPA degradation by AOPs.

O ₃		UV/TiO ₂	
Name (if given)	Structure ^{a,b}	Name (if given)	Structure ^{c,d}
		4-hydroxyacetophenone	
2-(4-hydroxyphenyl)propanol-2-ol		acetaldehyde	
		4-isopropylphenol	
		hydroquinone	
1,4-benzoquinone		p-isopropenylphenol	
resorcinol		p-hydroxybenzaldehyde	
acetone		4-hydroxyphenyl-2-propanol	
			
			

^a(Deborde et al., 2008)

^b(Garoma et al., 2010)

^c(Fukahori et al., 2003)

^d(Ohko et al., 2001)

2.7 Mutagenicity Analysis of Water

A *mutagenic substance* is one that can cause permanent and transmittable changes to the genetic material of cells in an organism. These mutations can cause alterations in the expression of genes or changes in the structure of gene products (Höfer et al., 2004). The major use of in-vitro mutagenic bioassays is as an initial screening for genotoxic carcinogens, as there is a high degree of correlation between the carcinogenicity of a compound and its mutagenicity (McCann et al., 1975; Ashby & Tennant, 1988). Upon obtaining a positive mutagenic response from several assays, compound-specific analysis to determine the occurrence of known carcinogens, or further investigation of the suspect compounds' carcinogenicity using the long-term rodent test, can then be conducted (Zeiger, 1987). One of the most important areas for the screening of mutagenicity is in drinking water post-treatment for disinfection by-products (DBPs) (Richardson et al., 2007). There are many established bioassays developed to determine specific mutagenic mechanisms, but a limited number have been applied to water quality analysis (Ohe et al., 2004). The most commonly used assays are: the Salmonella mutagenicity, micronucleus, comet, and alkaline elution (Ohe et al., 2004), with by far the most used test (>60%) being the Salmonella assay which is discussed in following section. The mutagenicity of BPA has been tested using several in-vitro assays: the Ames Test, the mouse lymphoma mutagenesis assay (MOLY), sister chromatid exchange (SCE) induction, chromosomal aberration (ABS) analysis, and mammalian gene mutation assay (V79/HPRT) with no mutagenic response found (Schweikl et al., 1998; Schrader et al., 2002; Tennant et al., 1987). The use of mutagenic bioassays in water quality analysis can help screen for compounds that can produce genetic damage without specific information on the physical and chemical properties of the water. Bioassays using bacteria are quick, inexpensive, reliable, and sensitive. These tests can be run as a battery of tests to identify various classes of mutagens in water samples.

2.7.1 The Ames Test

The Ames Test (Salmonella typhimurium/microsome assay) is a widely used and standardized bio-assay for determining substances that can cause mutations from specific damage to the genes. The test is considered a reversion assay as it utilizes Salmonella

strains each with specific pre-existing mutations that render the bacteria unable to synthesize an essential amino acid (histidine) for their growth. Each of these strains tests for a point mutation; a positive mutagen will cause a reversion of the gene and the *Salmonella* bacteria will be able to grow independent of histidine (Mortelmans & Zeiger, 2000). Specific *Salmonella* tester strains have been developed and standardized to test for different mutagenic mechanisms. The two strains used in this study are TA97a and TA100. TA97a responds to a frame-shift mutation which occurs when there is an addition or deletion of nucleotides, (Fig 2.4) shifting the reading frame of the codon, which can severely alter the amino acid sequencing (Davis & Weller, 1998). TA100 responds to a base-pair substitution, where a nucleotide is replaced with another (Fig 2.5). This can result in a silent mutation which causes no change in the gene expression, a nonsense mutation which results in the stopping of protein synthesis, or in the case of TA100 a missense mutation. A missense mutation occurs when there is a change in the codon from the substitution codes for a different amino acid (Davis & Weller, 1999).

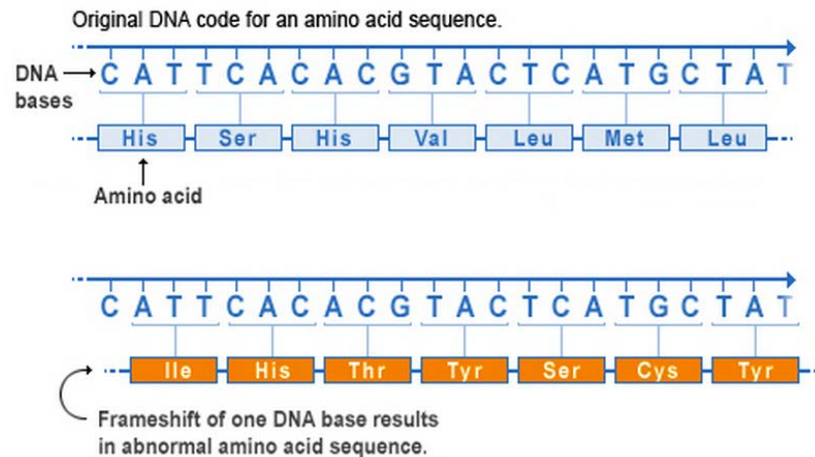


Figure 2.4: Frameshift mutation mechanism (U.S. National Library of Medicine, Genetics Home Reference, 2010).

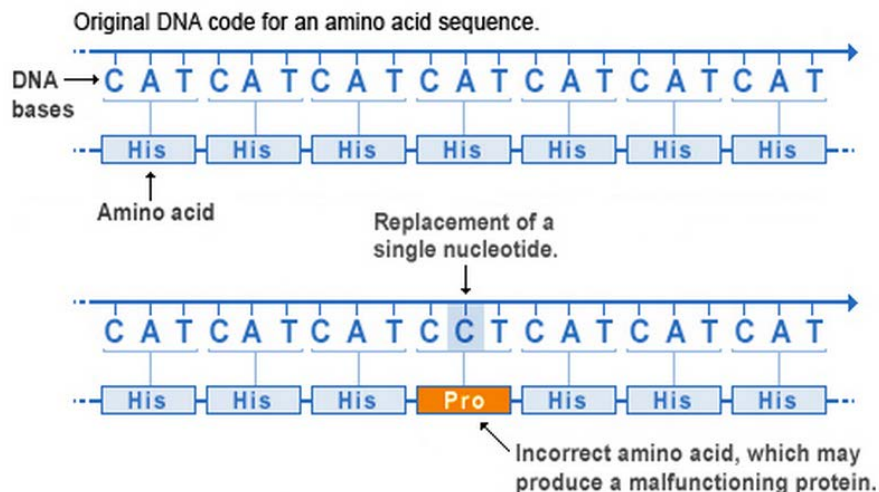


Figure 2.5: Base pair substitution resulting in a missense mutation (U.S. National Library of Medicine, Genetics Home Reference, 2010).

2.8 Yeast Estrogen Screen

Developed by Routledge and Sumptar (1996), the yeast estrogen screen (YES) is a cellular bioassay for measuring the total estrogen response of the water matrix, without prior knowledge of the specific pollutants and their concentrations in the sample. The assay uses genetically modified yeast cells (*Saccharomyces cerevisiae*) in which the chromosome in the cells has the gene sequence for the human estrogen receptor (hER), and the reporter gene lac-Z are integrated into it. When the receptor is activated by the EDC, this causes the expression of lac-Z, which produces the enzyme β -galactosidase. This enzyme is released into the growth medium and metabolizes a chromogenic substrate, turning the solution colour from yellow to red. Based on the change in absorption of the solution, the estrogenicity can be determined relative to a reference, 17β -estradiol. The assay is commonly applied to monitor the change in estrogenicity in AOP treatment studies of EDCs (Klavarioti et al., 2009). The assay has been used to monitor the removal of estrogenicity following treatment using AOPs for several EDCs such as: 17β -estradiol and 17α -ethinylestradiol by ozonation (Maniero et al., 2008), and mixtures of EDCs by UV/H₂O₂ (Chen et al., 2007). Chen et al. (2006) investigated the removal of BPA using UV/H₂O₂ and also monitored the decrease in estrogenicity using

the YES assay found BPA transformed into intermediates which retained some estrogenic activity.

2.9 Summary of Literature Review and Literature Gaps

The extensive literature review indicates that although exhaustive scientific studies have been conducted on kinetics and mechanisms of oxidation, various oxidants and catalysts, limited studies have been conducted on large-scale application of AOPs. Specifically, for photocatalysis, the issues of suitable catalyst precursor formation for a durable catalyst film on inexpensive, mechanically strong, and high surface area supports can be explored in further detail. On the other hand, bioassays have been used for determining toxicity of drinking water after treatment, estrogenicity of selective compounds in water, and mutagenicity of intermediates of AOPs. However, no studies were found where bioassays were conducted to determine the comparative performance of the various AOPs and correlate that with parent compound degradation, as well as relate to intermediate and TOC degradation. These are the objectives of this study, which are elaborated in Chapters 3 & 4. In this chapter, a broad literature review with respect to various aspects of AOPs has been presented. A short background on prevailing literature pertinent to the specific objectives of this work is presented in Chapters 3 and 4.

Chapter 3

3 Photocatalytic Performance of Titanium Dioxide Thin Films from Polymer Encapsulated Titania

3.1 Introduction

Among various semiconductor photocatalysts, titanium dioxide (TiO_2) in nanocrystalline form has been demonstrated extensively to be highly effective for water and air treatment (Herrmann, 1999). The majority of research for this application is focused on utilizing titanium dioxide in a suspended form, whereby the catalyst is dispersed in water to be treated (Herrmann, 1999). So far, detailed investigations into the degradation of a vast number of pollutants (Konstantinou & Albanis, 2004; Pera-Titus et al., 2004; Klavarioti et al., 2009) have provided essential information on the kinetics and degradation pathways critical for reactor design and modeling (Chong et al., 2010). However, the design of large-scale suspension reactors has critical limitations. Post-treatment separation and recycling of the suspended nano-catalysts are very energy intensive, and the light penetration in suspension is limited (Mukherjee & Ray, 1999). The focus on reactors utilizing the catalyst in an immobilized form has been very attractive to alleviate these issues, but immobilized catalysts also have disadvantages, such as: reduced surface area to volume ratio, difficulty in light penetration to the entire thickness of catalyst, as well as increased mass transfer limitations reducing the overall rate of pollutant removal (Pozzo et al., 1997). The development of both reactors and immobilization techniques to overcome these issues is still on-going.

By far the most studied immobilised system has been the development of titanium dioxide thin films from a tailored sol-gel route (Shan et al., 2010), where, in most cases, the film is formed on the chosen substrate through a simple dip coating and sintering technique (Carp et al., 2004). This technique allows for a highly controllable preparation route utilizing inexpensive reagents and simple operations. Modifying the sol-gel formulation allows for control over the characteristics of the film and when combined with pore-directing agents such as polyethylene glycol (Yu et al., 2000) and surfactants

(Choi et al., 2007), researchers have demonstrated, in some cases, greatly enhanced photocatalytic activity when compared to similar unmodified sols.

Even though there have been a number of sol-gel recipes developed by a variety of researchers globally with a variety of relevant substrates tested such as glass (Lee et al., 2002), stainless steel (Byrne et al., 1998), and inorganic fibres (Horikoshi et al., 2002), the development and testing of larger scale immobilized photocatalytic reactors are still limited (Mukherjee & Ray, 1999; Chong et al., 2010). For the implementation of large-scale immobilized photocatalytic reactors, major challenges include (i) production of specific catalyst precursors in bulk to be adopted for supports with high surface area, (ii) production of uniform and stable thin coating of catalyst on various supports, (iii) an efficient light and catalyst coated support assembly, and (iv) a flow regime free of mass transfer limitations with sufficient contact time. Of all the above factors, (iii) and (iv) are independent of the nature of catalyst precursors and immobilization techniques. Large-scale photocatalytic processes are significantly affected by factors (i) and (ii), where there is a lack of cost-effective and simple methods to synthesize suitable precursors, such as sol-gel, suspension, etc. to produce titanium dioxide thin films on suitable supports that can be easily scaled up. The objective of the work presented in this chapter is to characterize a cost effective proprietary catalyst precursor that can be easily used to create titanium dioxide thin films for the use in immobilized photocatalytic reactors at a pilot scale. In this chapter, experimental results for the application of a proprietary solution-based precursor ideally suited for making thin films of titanium dioxide on various supports are presented. The catalyst precursor is a suspension of polymer encapsulated titanium dioxide. Experiments were performed to determine the most appropriate coating technique as well as suitable supports. Subsequently, photocatalytic performance of the catalyst films was evaluated in a semi-batch swirl flow reactor. The films' surface morphology and characteristics, mechanical stability, and re-use potential were also investigated. The performance of a hybrid catalyst (proprietary and commercial catalyst, Aeroxide P25) was also tested.

3.2 Experimental

3.2.1 Preparation of Support Mediums and Coating Procedures

The polymer encapsulated titanium dioxide was received as a yellowish solution from Vive Crop Protection Inc. (Toronto, ON, Canada), a partner company in this project. The solution had a solids concentration of 20 g/L of which 20% (w/w) was titanium dioxide. It was stored in polypropylene containers at room temperature where the solution remained stable for several months.

Fibreglass insulation papers (McMaster-Carr, Atlanta, GA, USA) with a thickness of 0.32 cm were cut into 11.43 cm diameter disks to support the catalyst (Fig. 3.1). These disks had a 0.5 cm hole punched through the centre for flow to exit from the reactor. The disks were first heated in an oven for 1 h at 500°C to remove the organic binding agent. Following heat treatment and cooling, the disks were dipped into the catalyst solution and dried at 100°C for 1 h. The dipping and drying was repeated to increase the catalyst loading on the disks, if required. Finally, the coated disks were calcined at 500°C at a ramp rate of 10°C/min and held for 3 hours and then allowed to cool down naturally.

For the hybrid catalyst coatings the same disk preparation method as above was used, but the dipping solution was modified by the addition of Aeroxide P25 from Sigma–Aldrich (Oakville, Ontario, Canada). Based on the titanium dioxide content (400 mg in 100 mL) of the VN-TiO₂ stock solution, P25 was added accordingly to obtain different ratios of VN-TiO₂ and Aeroxide TiO₂. The powder was added to the solution under vigorous stirring followed by 30 min of sonication to disperse the P25 catalyst. The fibreglass disk was then dipped and dried at 100°C twice followed by calcination at 500°C for 3 hours.

For the investigation of higher calcination temperature, quartz wool mat (Fig. 3.1) (Technical Glass Products, Inc.) was used, as the fibreglass mat was not stable above 600°C. This mat consisted of quartz fibres of similar size and configuration to the fibreglass, but was stable up to 1200°C. A dip coating procedure similar to fibreglass was followed for the quartz mat, but it was held for 1h at the selected temperature for calcination.

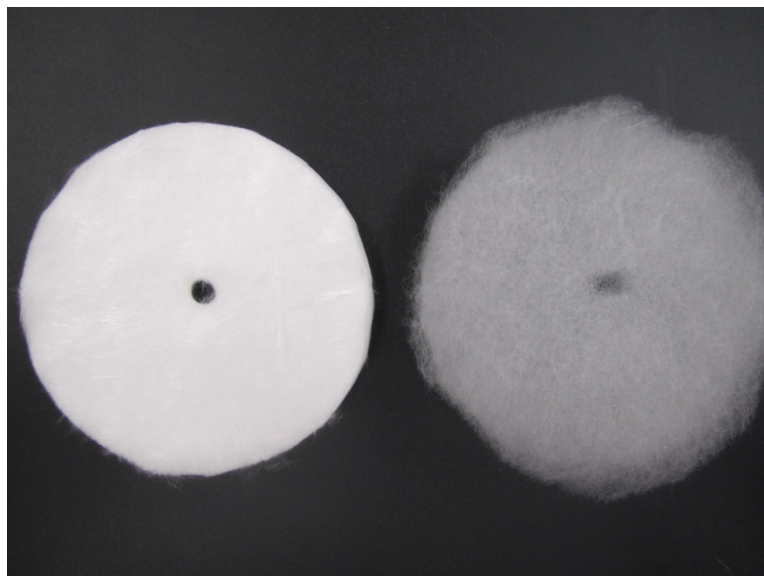


Figure 3.1: Blank fibreglass (left) and quartz wool disks (right).

3.2.2 Characterization of Titanium Dioxide Films

Determining the characteristics of titanium dioxide thin film directly on the fibreglass surface is very difficult due to low surface area of the fibreglass and the small amount of catalyst material on the support. Thus, thin film characterization for the various samples was conducted with scraped-off titanium dioxide films produced on borosilicate glass disks. Since both the glass fibres and borosilicate glass disks are of very similar chemical composition, this technique provided a good representation of the characteristics of the films formed on the fibres. This characterization technique has been previously demonstrated to be effective for immobilised thin films (Choi et al., 2007; Yu et al., 2004). Thin films of catalyst were obtained by depositing 50 ml of catalyst solution with or without hybridization with powder TiO_2 (Aeroxide P25) onto cleaned borosilicate glass disks and drying the disks at 100°C until a transparent polymer film was formed. Following this process, the disks were calcined for 3 hours at 500°C to remove the polymer matrix. The films were then scraped off the glass disk for characterization.

For determination of the crystal size and phase, X-ray diffraction (XRD) analysis using a Rigaku – MiniFlex II (Japan) powder diffractometer with $\text{CuK}\alpha$ (λ for $\text{K}\alpha = 1.54059 \text{ \AA}$) over the desired 2θ range with step width of 0.05° was used. The morphology of the

films was analysed using the S4500 Hitachi field-emission scanning electron microscope (SEM) equipped with a 6460 EDAX energy dispersive X-ray spectrometer. Differential scanning calorimetry and thermogravimetric analysis were carried out using SDT Q600, TA instruments (USA) at a heating ramp rate of 5°C /min in air. Surface properties, such as surface area, pore volume, and pore size distribution, were measured using a Micromeritics TriStar 3000 Gas Absorption Analyzer. Samples were de-gassed at 90°C for 120 min followed by 180 min at 170°C before analysis.

3.2.3 Photocatalytic Activity Measurement

The photocatalysis experiments were performed in a semi-batch swirl flow reactor developed by Ray and Beenackers (1997). The reactor has been demonstrated to be very effective for the study of pollutant degradation using immobilised TiO₂ as swirl flow inside the reactor induces good mixing and eliminates mass transfer limitations (Chen & Ray, 1999; Chen et al., 2000a). For this study, a slight modification to the reactor was made: two inlets instead of one were used, which further enhanced mixing in the reactor (Fig 3.2).

The reactor shown in Fig. 3.2 consists of a stainless steel central housing with a stainless steel top plate and a borosilicate glass window at the bottom of the reactor. The plate cuts off UV light <300 nm, eliminating any effect of photolysis. The coated fibreglass disk was placed at the top of the reactor and two small stainless steel meshes at each inlet were used to keep the disk in place and to allow for uninhibited flow (Fig. 3.3). The reaction solution enters from two opposing inlets of the housing resulting in a swirling effect over the surface of the fibreglass disk. The flow exits through the top of the reactor into a well-mixed buffer tank from which it is recirculated back to the reactor. The reactor was placed on top of a wooden box which contained a 175 W medium pressure mercury vapor lamp (Osram Sylvania Ltd.) that was 2.0 cm from the bottom plate of the reactor. The average UV-A intensity at the peak wavelength of 365 nm was 3.6 mW/cm² measured using a radiometer (UVX-36, UVP, LLC). The total volume of the reaction solution was 500 mL, with methylene blue (MB), (Aldrich) as the model compound. The initial concentration of MB in all experiments was 10 ppm (mg/L) and was prepared using deionized water. The natural initial pH of the reaction solution was 6.8. A digital

peristaltic pump, using a recirculation rate of 2 LPM and a stirring rate of 400 RPM, was used to induce mixing in the buffer tank. The buffer tank also allowed the reaction mixture to cool, with an equilibrium temperature of $30^{\circ}\text{C} \pm 1.5^{\circ}\text{C}$. All reactions were performed in an oxygen saturated solution by sparging the solution with air. The degradation experiments consisted of an initial 60 min dark adsorption followed by the UV-A photocatalysis. The concentration of methylene blue was measured using a 96-well microplate reader (Infinite 200 PRO, Tecan Group Ltd., USA) by monitoring the change in absorption at 664 nm.

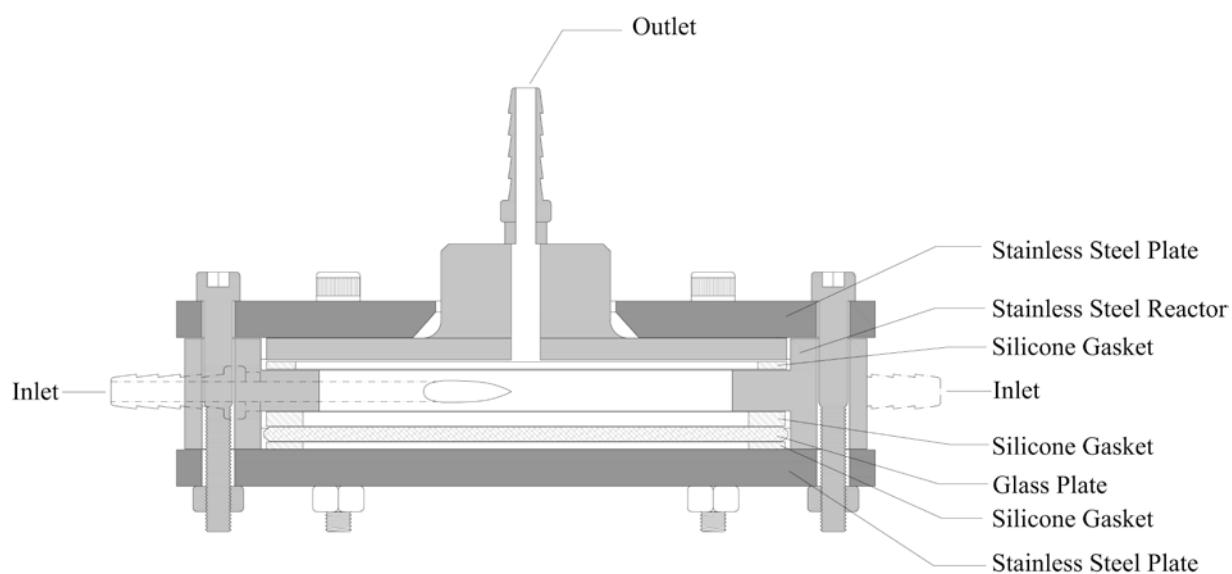


Figure 3.2: Cross-sectional diagram of swirl flow reactor.

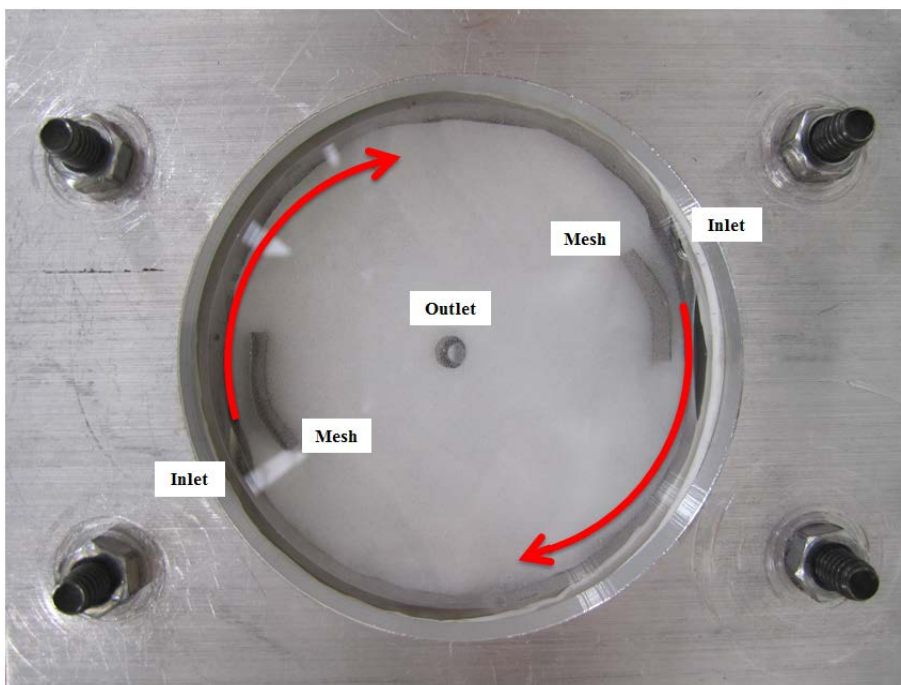


Figure 3.3: Photograph of coated fibreglass disk in swirl flow reactor.

3.3 Results and Discussion

3.3.1 Proprietary Titanium Dioxide Catalyst

The titanium dioxide catalyst is produced by Vive Crop Protection Inc., the partnering company and is referred to as VN-TiO₂. Further information about the product and method of production is given in the following patents: (Goh et al., 2009; Anderson et al., 2008).

A brief description of the synthesis process is provided below with a schematic diagram shown in Figure 3.4. A titanium-containing complex, which acts as a counter ion to an extended form polyelectrolyte in solution, bonds to the electrolyte due to attractive forces. The polyelectrolyte then collapses into a globular form. Subsequent treatment (a proprietary method practiced at Vive Crop Protection Inc.) results in polymer-encapsulated nano-particles, whereby titanium has been converted into an amorphous titanium dioxide form. Due to the surface charge of the particles, they do not agglomerate and remain dispersed in solution with an average size of ~10 nm. The transmission electron microscope (TEM) images of the encapsulated particles in solution, and particle

size distribution of the particles, are shown in Fig 3.6. For the specific batch used in this work the polymer electrolyte was poly (diallyldimethylammonium chloride) (PDDA), and titanium complex was titanium (IV) bis(ammonium lactato)dihydroxide (Fig 3.5). The solution remains stable for months and is stored at room temperature in opaque polypropylene containers.

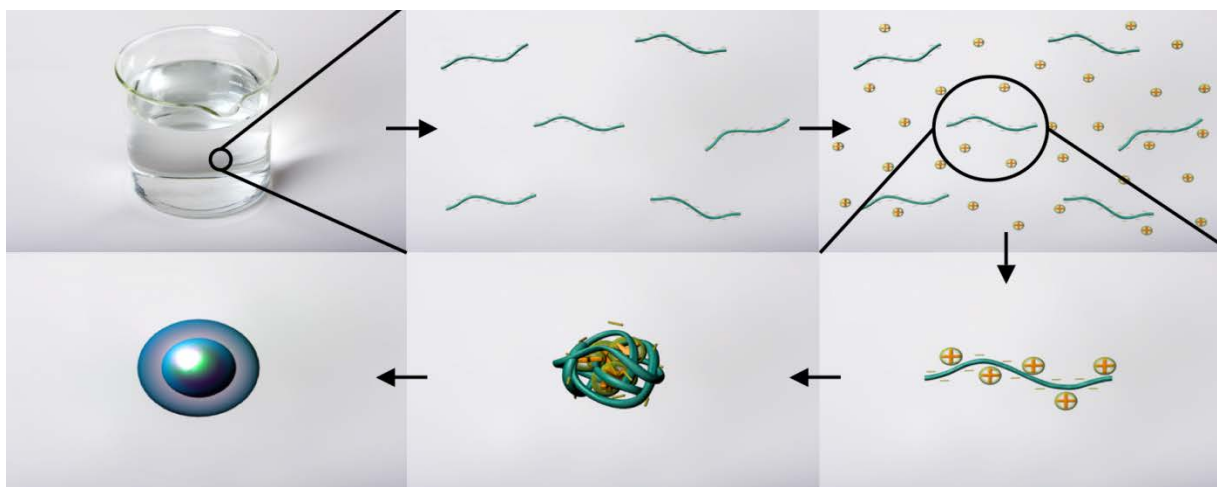


Figure 3.4: General scheme of VN-TiO₂ synthesis procedure.

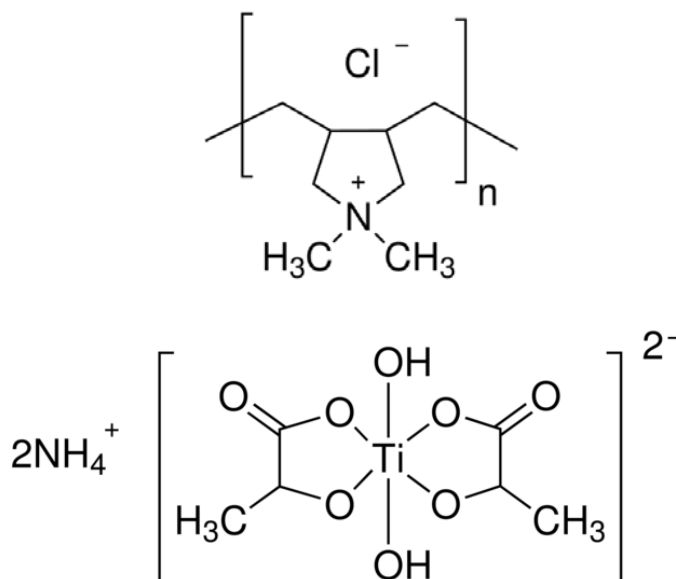


Figure 3.5: PDDA (top) and titanium precursor (bottom) chemical structure.

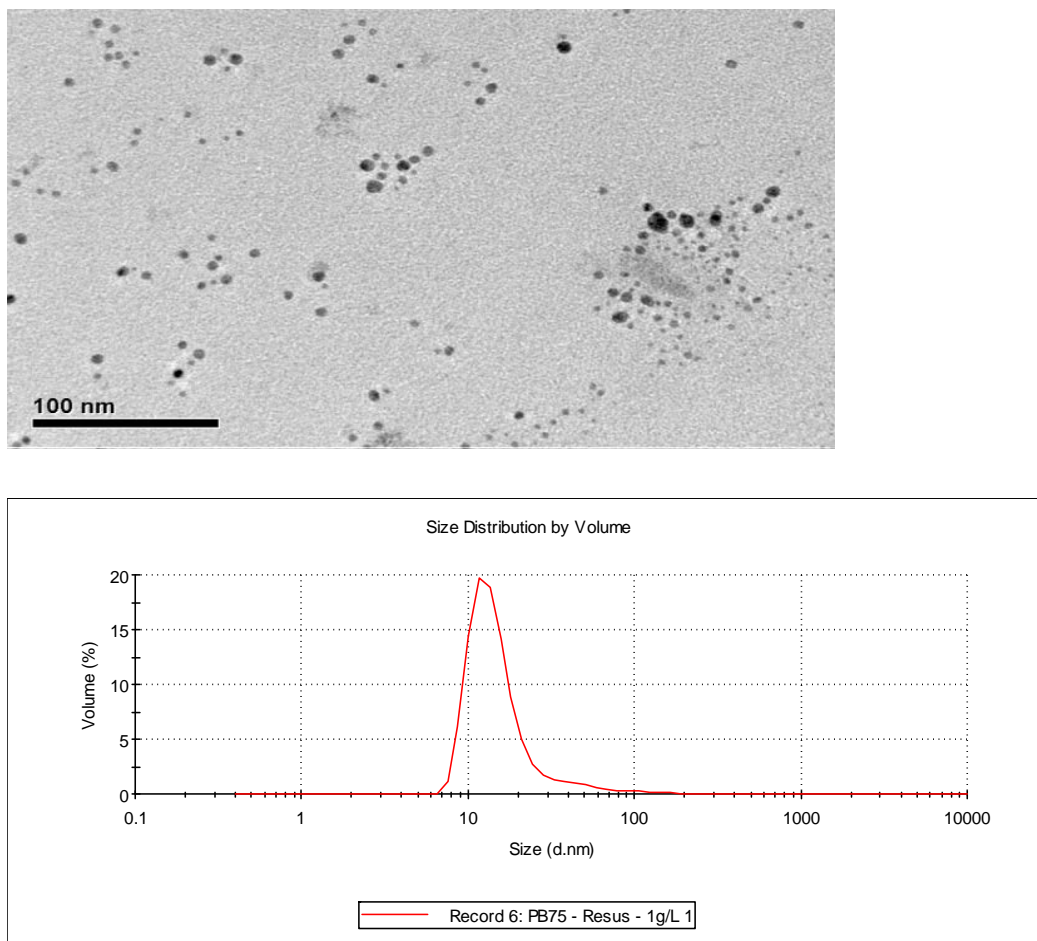


Figure 3.6: TEM image (top) and size distribution (bottom) of VN-TiO₂ encapsulated nano-particles in solution.

3.3.2 Support Material and Coating Procedure

For immobilization of photocatalysts for diverse reactor configurations, selection of an appropriate support medium and coating procedure is necessary for successful large-scale application. The support must meet the following requirements, (i) good thermal resistance and mechanical stability, (ii) inexpensive, (iii) conformable to reactor configuration, and (iv) suitable for coating process. As the intended application of the VN-TiO₂ catalyst is for large-scale photocatalytic reactors, in addition to the cost of the support, other considerations such as material cost, bulk preparation and coating, and ease of reuse and replacement were taken into account. Two commonly found supports with two different coating methods were evaluated: borosilicate glass plates with spray

coating, and glass fibres coated with dip coating. Based on the preliminary experiments, a support and a coating procedure were then selected for the complete evaluation of the VN-TiO₂ catalyst.

3.3.2.1 Glass Plate with Spray Coatings

The first support selected was borosilicate glass in the form of a disk which conformed to the design of the reactor. Glass has been one of the most common materials used for testing catalyst efficiency in immobilised state and for larger-scale system designs (Ray & Beenackers, 1998). Initial attempts to coat the VN-TiO₂ on glass disks using dip coating resulted in uneven layers as well as a very low loading rate per dipping cycle. Thereafter, a spraying apparatus at the Vive Crop Protection Inc. laboratories which used a pneumatic paint spray gun, controlled by a computer numerical control (CNC) system, was used for coating glass disks. The 11.43 cm diameter glass disks were cleaned by soaking for 24 h in a base bath followed by subsequent acid and distilled water washes. The cleaned disks were dried and stored at 100°C before use. The disks were placed on a heating block set at 50°C for coating; this was done to completely dry the deposited layers between each coating cycle. The un-calcined coating shown in Fig. 3.7a indicated that a smooth polymer layer had formed on the surface. EDX confirmed the presence of titanium and chlorine in the film (Fig. 3.8b); chlorine came from the PDDA polymer. The cavities that formed on the surface were most likely caused by the evaporation of water. The calcined films in all cases resulted in cracking and delamination of the titanium dioxide film (Fig. 3.7b). A maximum stable loading of 10 mg of TiO₂ per disk (0.097 mg/cm²) was consistently found after rinsing the disks and is seen as a dispersion of evenly sized particles within the stable film (Fig. 3.7c). Based on the density of pure anatase TiO₂ of 3.84 g/cm³ (Bischoff & Anderson, 1995) and assuming a 100% dense film, the thickness of the films was calculated to be 254 nm. Thicker films can be achieved by this method, but this is done by repeated coating and heat treatment cycles to layer films, sometimes up to 10 cycles (Mills et al., 2003). This would greatly increase cost due to longer processing time and more consumables. The EDX confirmed that these films were TiO₂ (Fig. 3.8c-d). The photocatalytic activity of P25 coated on the glass plate and fibreglass is compared and discussed in section 3.3.3. The surface of the

cleaned disk shows an evenly distributed coating of nano-particles, ~30 nm in diameter (Fig. 3.7c). The P25 coatings showed a thick layer of agglomerated particles of even distribution (Fig. 3.7d).

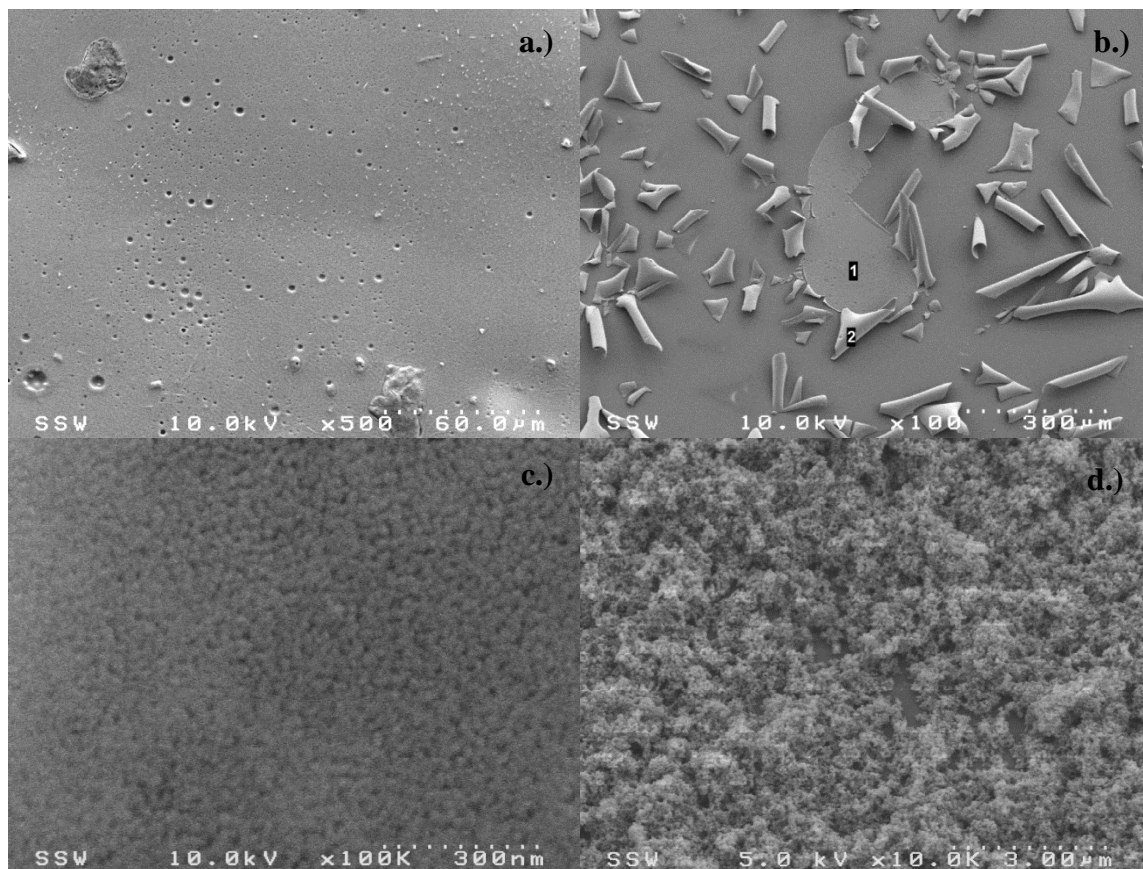


Figure 3.7: SEM of coatings on borosilicate glass disks - a.) uncalcined coating, b.) calcined VN-TiO₂ (Area 1 & 2 labeled for EDX analysis), c.) stable and remaining TiO₂ film on glass, and d.) P25.

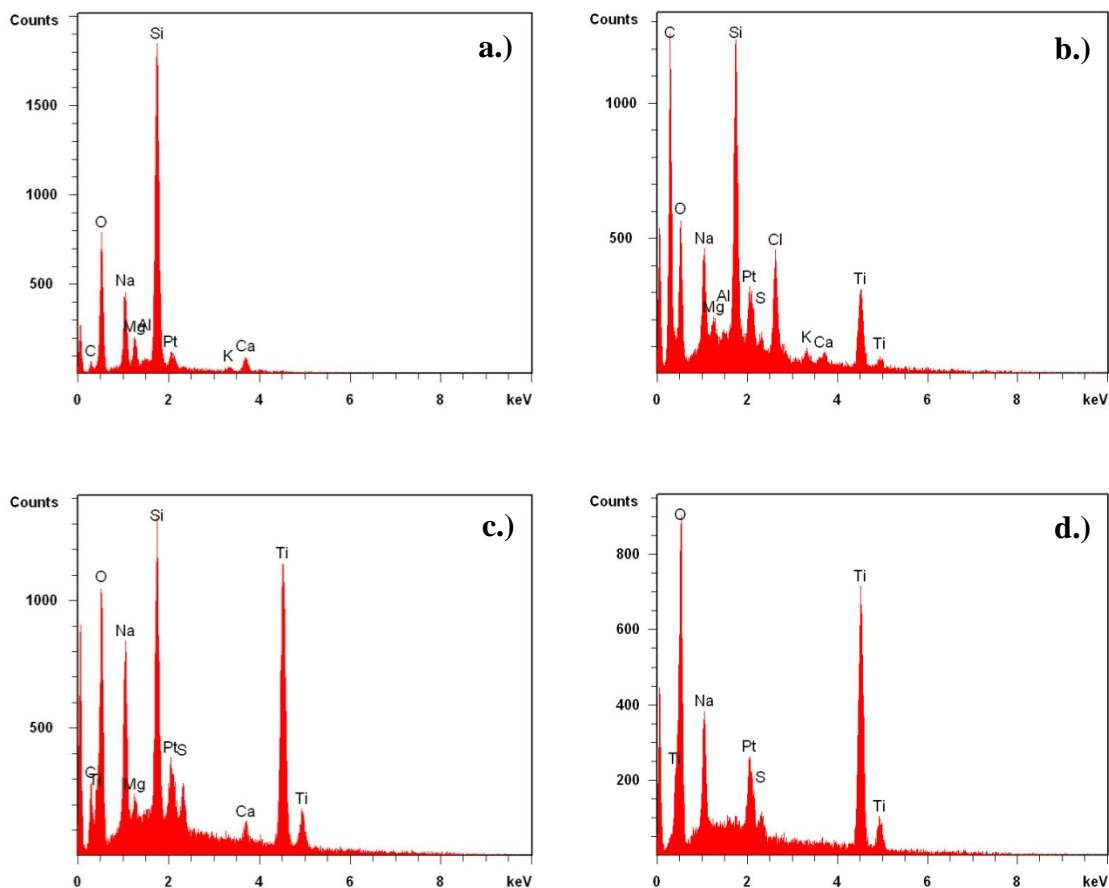


Figure 3.8: EDX results - a.) blank glass, b.) uncalcined coating, c.) area 1, and d.) area 2 from Figure 3.7 image b.).

It was clearly demonstrated that the VN-TiO₂ could be coated on glass supports at similar loadings achieved by other groups (Gelover et al., 2004; Sonawane et al., 2003), but preliminary degradation reactions of methylene blue conducted with the coated glass disks showed low rates (results are shown below) and were not deemed adequate for a comprehensive study. For pilot-scale reactor testing and evaluation, the availability of a simple, fast, and economical process to produce uniformly coated supports in greater quantity is necessary. The cost of the disks and the extensive processing to spray coat them did not meet this requirement and therefore, an alternative support material, such as inorganic fibres, was tested as described below.

3.3.2.2 Inorganic Fibres with Dip Coating

In evaluating other substrates for immobilisation, the limitations of the glass supports were taken into consideration. The smooth support greatly reduced the surface area, which affects number of active sites and flow characteristics in the reactor. Stacking of numerous glass disks in the photoreactor may not be feasible for space limitation. Therefore, it was required that another support with high surface area was tested. Several types of inorganic fibres that have been tested for immobilised photocatalysis include fibreglass (Horikoshi et al., 2002), cotton (Liuxuea et al., 2007), and activated carbon (Fu et al., 2004). The fibreglass paper was selected because it was very inexpensive and easy to manipulate for coating. Fibreglass insulation paper consists of 7 μ m glass fibres of random length and orientation within the paper. The starch binder of the paper was removed before coating, but the disk remained robust during the coating procedure. The glass in the fibres was of a similar composition to borosilicate glass described above and provided a good basis for comparison.

3.3.2.2.1 TGA & DSC

The thermal behaviour of VN-TiO₂ was investigated using differential scanning calorimetry (DSC) and thermogravimetric analysis (TGA) and is presented in Fig. 3.10. A sample of the catalyst in a dried form (polymer and metal) was used for analysis. The thermal behaviour was analysed in air from room temperature to 1000°C at a rate of 5°C/min. The loss of mass from the TGA curve can be broken down into three stages. For the first stage up to 200°C, there is a broad endothermic peak attributed to the removal of absorbed water and VOCs (Ohtani et al., 1999), which corresponded to a weight loss of ~15%. The second stage represents the initial point of polymer degradation occurring over a broad temperature range from 200-400°C. This may have been due to the dissociation of the quaternary ammonium salt under heat to form methyl chloride (Francis et al., 2007) (Fig. 3.9). This represents a further removal of ~30% of mass.

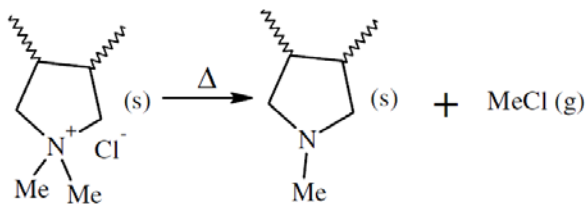


Figure 3.9: Dissociation of PDDA monomer (Francis et al., 2007).

In the final stage there is a dramatic release of heat which can be attributed to two events as seen in the two peaks at 438°C and 485°C. The first corresponds to the decomposition of the intermediate products formed in the second stage, this occurs over a narrow range of 400-500°C, and represents a significant loss of mass ~30% (Francis et al., 2007).

There is no further decrease in mass beyond 500°C, indicating the secondary exothermic peak is independent of the removal of any organic residue; this therefore represents the crystallization of amorphous titanium dioxide to the anatase phase (Ohtani et al., 1999).

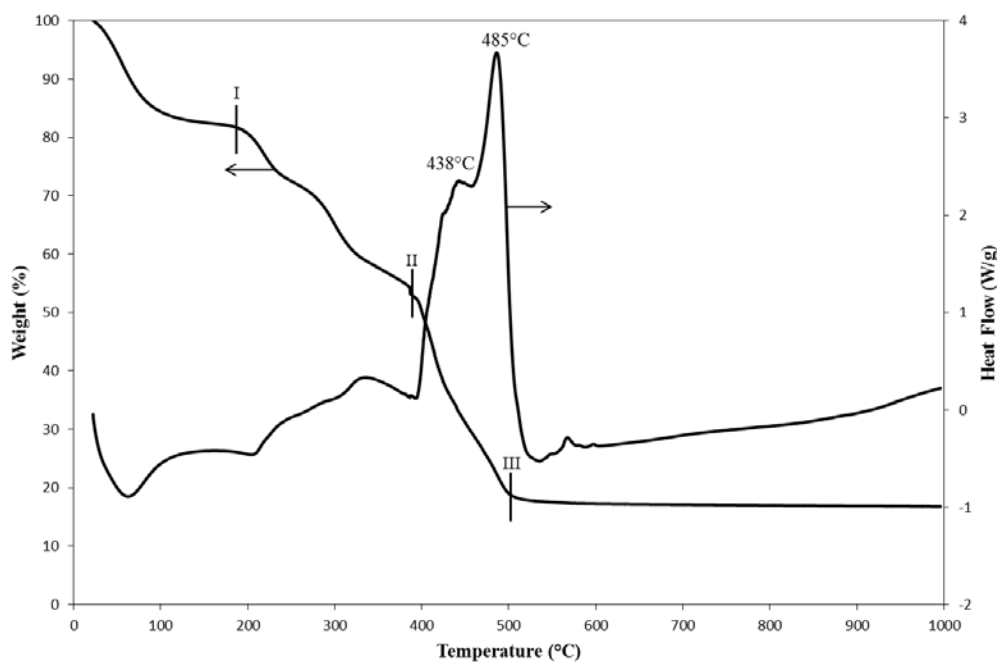


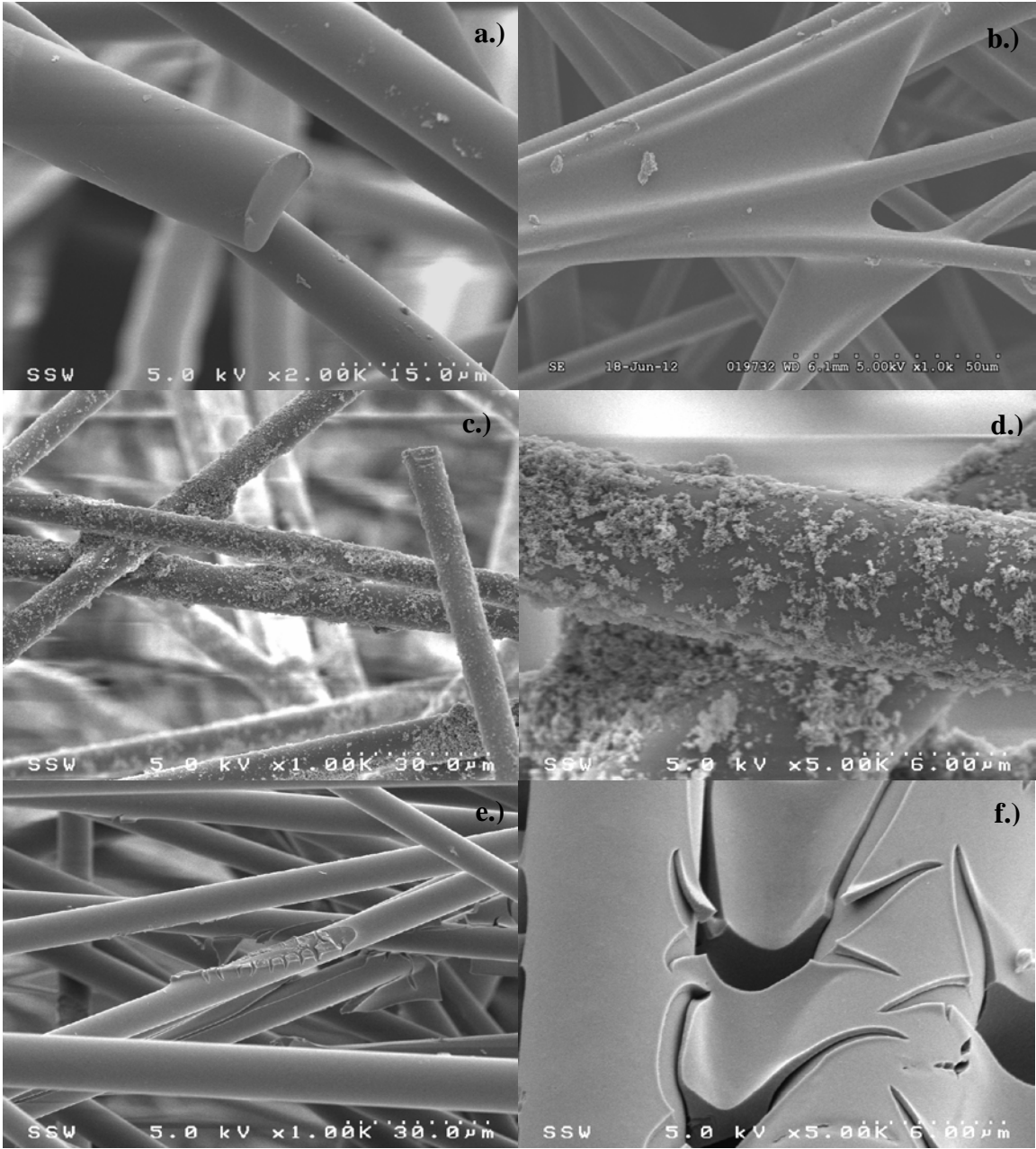
Figure 3.10: TGA and DSC curve for VN-TiO₂ dried powder sample.

TGA/DSC confirms that the original product consisted of 80% non-metal solids as indicated by Vive Crop Protection Inc., and demonstrates the importance of selecting a

calcination temperature of 500°C to achieve complete removal of the polymer and to form a highly crystallized film.

3.3.2.2.2 Surface Morphology

The film morphologies of the various coatings on the fibreglass were investigated using SEM analysis. As can be seen in Fig. 3.11a, the blank fibreglass consisted of fibres approximately 7 μm in diameter with a very smooth surface with some minimal distribution of impurities on the fibres. The coating of VN-TiO₂ before calcination resulted in a polymer film that not only completely covered all of the fibre, but resulted in the polymer forming a sheet between closely located fibres (Fig. 3.11b). This cross-linking of fibres was very important for the mechanical properties of the coatings (Fig. 3.11f). Similar to the coatings of P25 on glass disks, P25 coated as evenly distributed agglomerates on the fibres (Fig. 3.11c-d). When fibres were located very close together, there was a build-up of P25 between them. However, this would not be expected to have any significant impact on the mechanical properties of the film, and most likely contributed to the loss of some catalyst after rinsing. Calcining the VN-TiO₂ films resulted in a very smooth crack-free film. Fig. 3.11e-f shows that the films had an approximate thickness of 1 μm , the film cracking only occurred between fibres and was not typical. The addition of P25 into the VN-TiO₂ resulted in the even distribution of aggregates in the film (Fig. 3.11g-j). Increasing the loading from 15% to 50% did not significantly change the amount of particles in the film and the excess P25 built up as either large clumps on the fibre or at the joining of the fibres. This demonstrates that the polymer solution only allowed a certain maximum amount of P25. The surface of the film remained smooth with the P25 agglomerates covered with a VN-TiO₂ cage to better bind the particles to the fibre. Again, cross-linking of the closely located fibres occurred as a continuous film. There was no micro-crack formation on the surface of the fibre; films formed from sol-gel solutions modified with P25 have been shown to result in the formation of micro-cracks due to internal stress resulting from the increased concentration of P25 (Balasubramanian et al., 2003). These micro-cracks may affect the long-term mechanical stability of the films (Chen & Dionysiou, 2008).



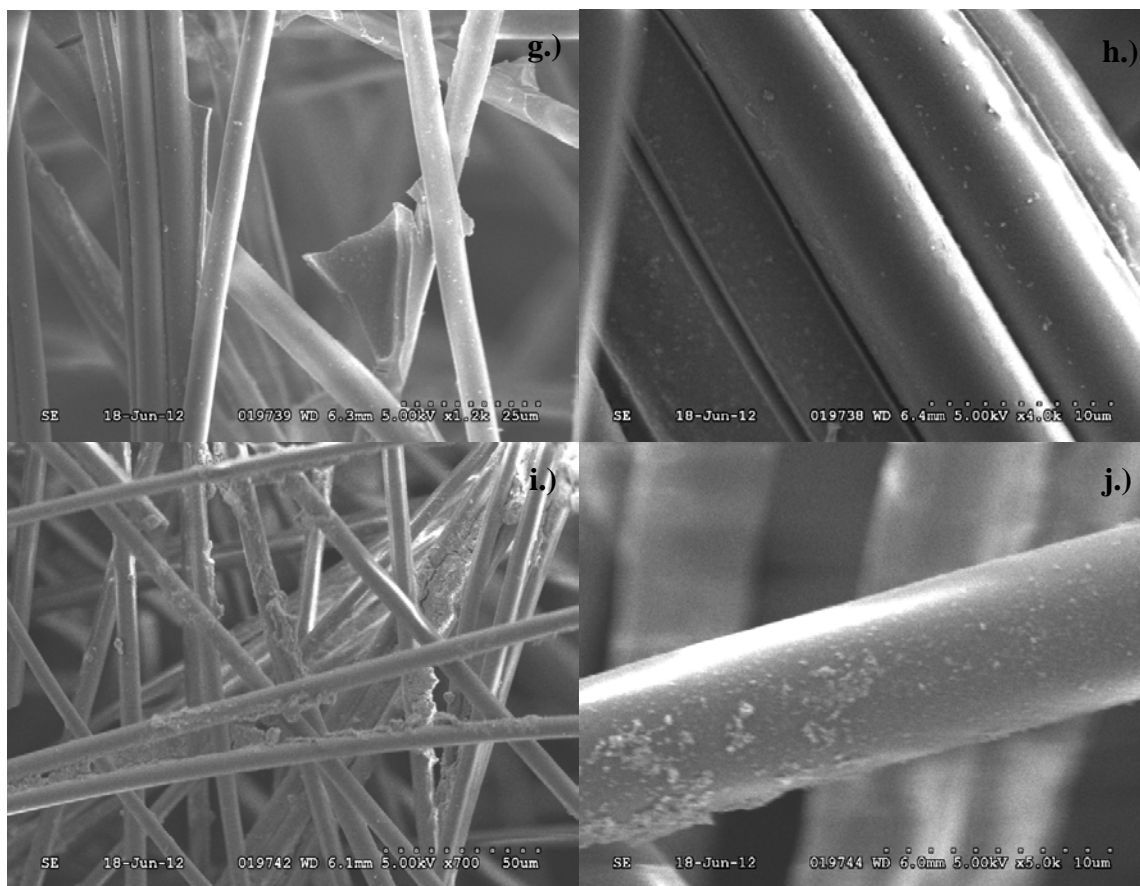


Figure 3.11: SEM of a.) blank fibreglass, b.) VN-TiO₂ uncalcined, c.) & d.) P25, e.) & f.) VN-TiO₂ calcined, g.) & h.) hybrid-15%, and i.) & j.) hybrid-50%.

Figures 3.12a and b show the composition of the blank and coated fibres from EDX analysis. Since the fibres are electrical grade glass (E-glass), they can contain no more than 1% Na₂O (Saint-Gobain Vetrotex, 2002). As a result, the coated fibres showed no significant concentration of Na⁺ and there would be no expected effect from ion diffusion on the crystallization of the films and their photocatalytic activity as described earlier.

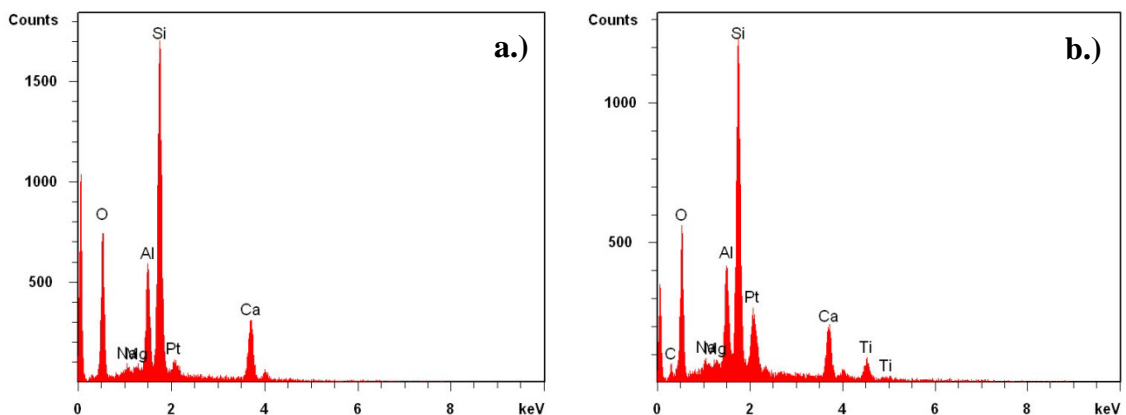


Figure 3.12: EDX of a.) blank fibreglass, and b.) VN-TiO₂ on fibreglass.

3.3.2.2.3 XRD

Figure 3.13 shows the XRD results for the various coatings on fibreglass; after coating and heat treatment the samples were ground up into a powder for analysis. The main peak is ascribed to anatase (101) crystal phase at a two-theta angle of 25.4°. The addition of P25 greatly increases the intensity of this main anatase peak as well as other secondary anatase peaks at (004), (200), (105), and (211). Due to the small amount of crystalline material, characteristic peaks for rutile were not detected. This analysis confirmed that for the coating conditions applied on fibreglass, VN-TiO₂ formed an anatase thin film on the surface.

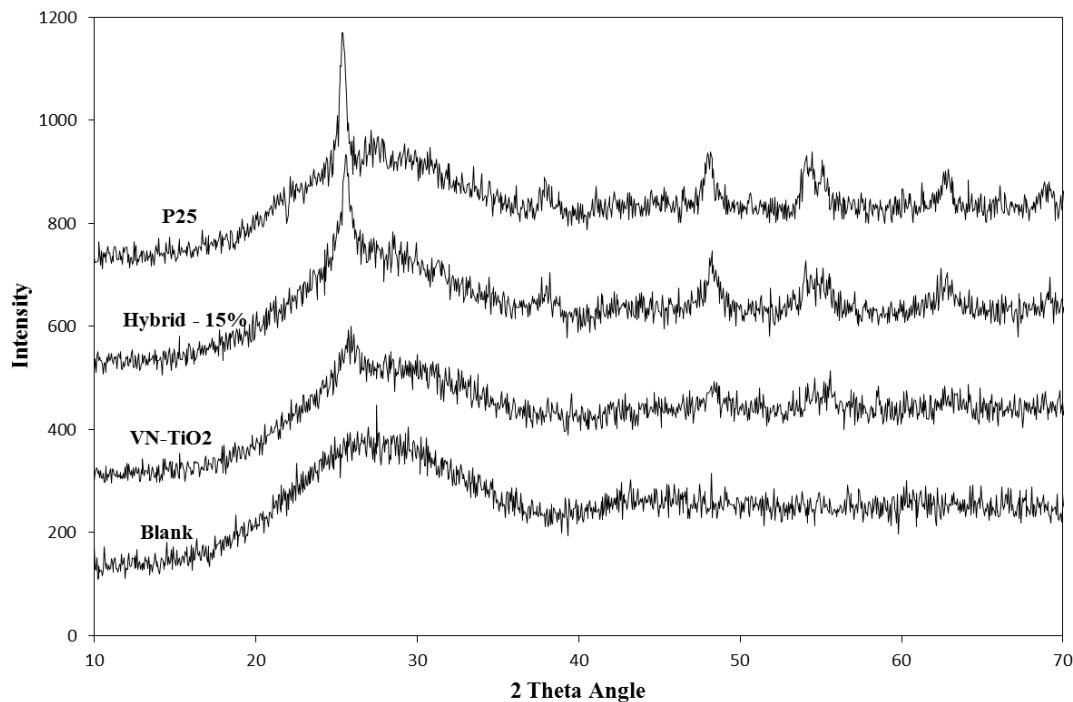


Figure 3.13: X-ray diffraction spectra of different types of films prepared on fibreglass disks.

Thick films formed on borosilicate glass disks at 500°C were scraped off and analysed using XRD. Increasing P25 loading enhances the peak height due to the increased amount of crystalline material. The crystal size is calculated from the Scherer equation using the half peak widths of VN-TiO₂, Hybrid 15% & 50% at the (101) peak (Table 3.1). The peaks indicate that the crystallites of the coatings are of similar size, but by increasing the P25 loading there is a small increase in the crystal size due to the contribution of the larger P25 particles (mean size > 30 nm) (Chen & Dionysiou, 2007). For both the 15% and 50% hybrid catalyst, a small sharp peak is visible for the main (110) peak of rutile, the crystal size was calculated to be 42.5 nm and is in agreement with the primary rutile particle size in P25 (Bakardjieva et al., 2005). At higher loading of 50% a secondary rutile peak at (101) is also visible further showing the impact of the P25 addition.

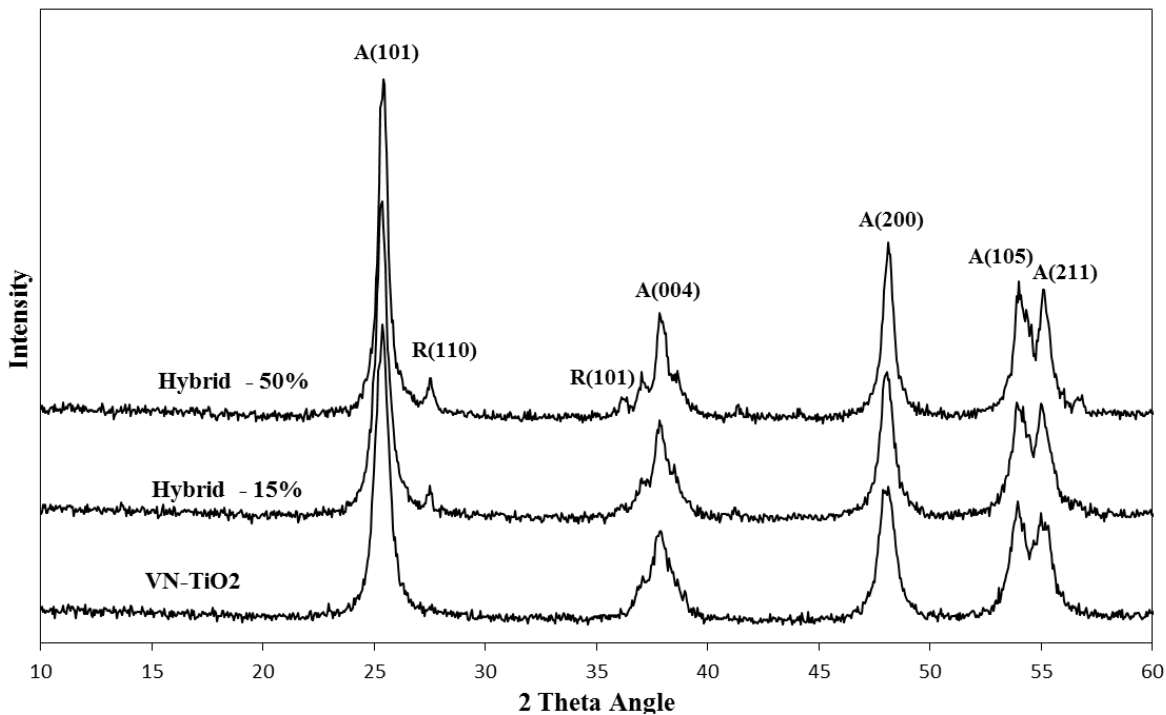


Figure 3.14: X-ray diffraction spectra of VN-TiO₂ and hybrid films removed from glass disks.

3.3.2.2.4 Surface Area and Pore size Distribution

Figures 3.15 and 3.16 show respectively the pore size distribution curves and adsorption/desorption isotherms for P25, VN-TiO₂, and hybrid films. VN-TiO₂ shows a type IV isotherm indicating that the film had a mesoporous structure (Rouquerol et al., 1999). The hysteresis loop is of type H₂, indicated by the dissimilar shape between the adsorption/desorption branches, which correspond to an ink-bottle type pore (Rouquerol et al., 1999). The film has a mono-modal pore size distribution with a narrow range; the average pore diameter was 4.8 nm and 4.1 nm for the adsorption/desorption isotherms, which indicated homogeneity of the pores. The addition of P25 into the VN-TiO₂ solution changes the hysteresis loop from an H₂ to H₃ shape gradually with increasing P25 concentration; this would be associated with the formation of slit shape pores (Rouquerol et al., 1999). As well, with increasing P25 loading in the hybrid coatings, there is a widening of the pore size distribution. Since the only change is the addition of P25, it can be concluded that the increased concentration of P25 results in the formation of secondary particles between crystallites formed from VN-TiO₂ and P25 (Chen &

Dionysiou, 2006a). The secondary particles can form inter-aggregate pores, which result in an increase in average pore size as presented in Table 3.1. P25 has a type H3 hysteresis loop with a wide pore size distribution from 2 – 100 nm; the pore structure of P25 is due to the aggregation of crystals and not the individual crystallites (Yu et al., 2006). The high surface area and porosity of VN-TiO₂ is as a result of the decomposition of the polymer shell which leaves a stable cavity. The pore formation during the calcination stage is similar to that of pore directing agents, such as non-ionic surfactants: Tween 20, Tween 80, and Triton X-100. When used in sol-gel films, these surfactants resulted in high surface area and porosity films with a narrow pore distribution (Choi et al., 2007). Chen and Dionysiou (2007) found an increase in the surface area with the addition of P25 at the calcination temperature of 500°C and attributed this increase to the relatively high surface area of P25 and formation of the stable inter-particle pores.

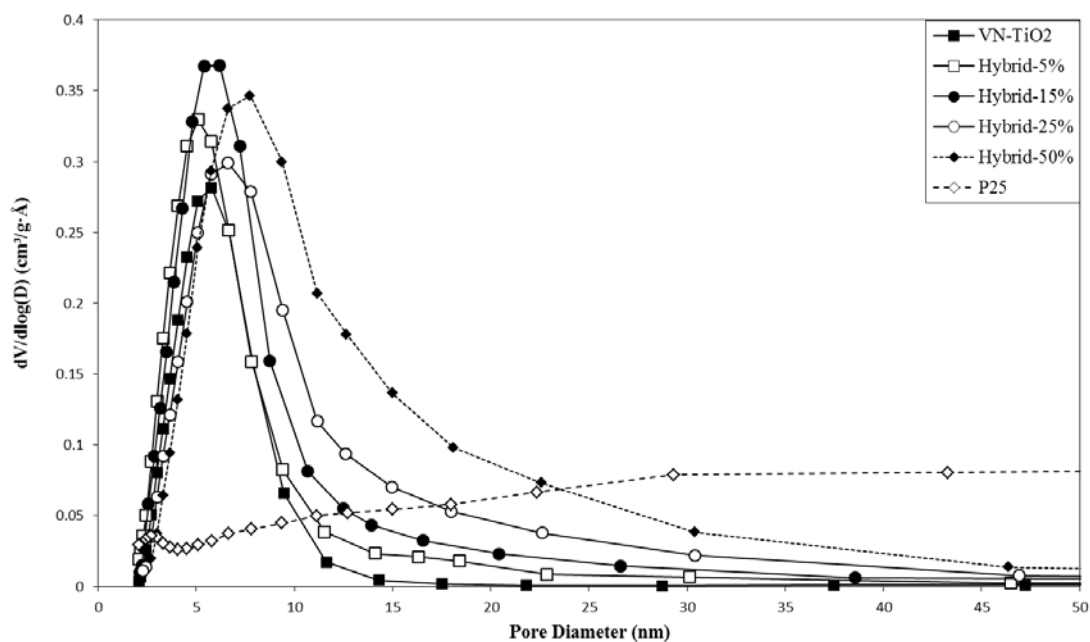


Figure 3.15: Pore size distribution of each thin film coating, P25 as powder.

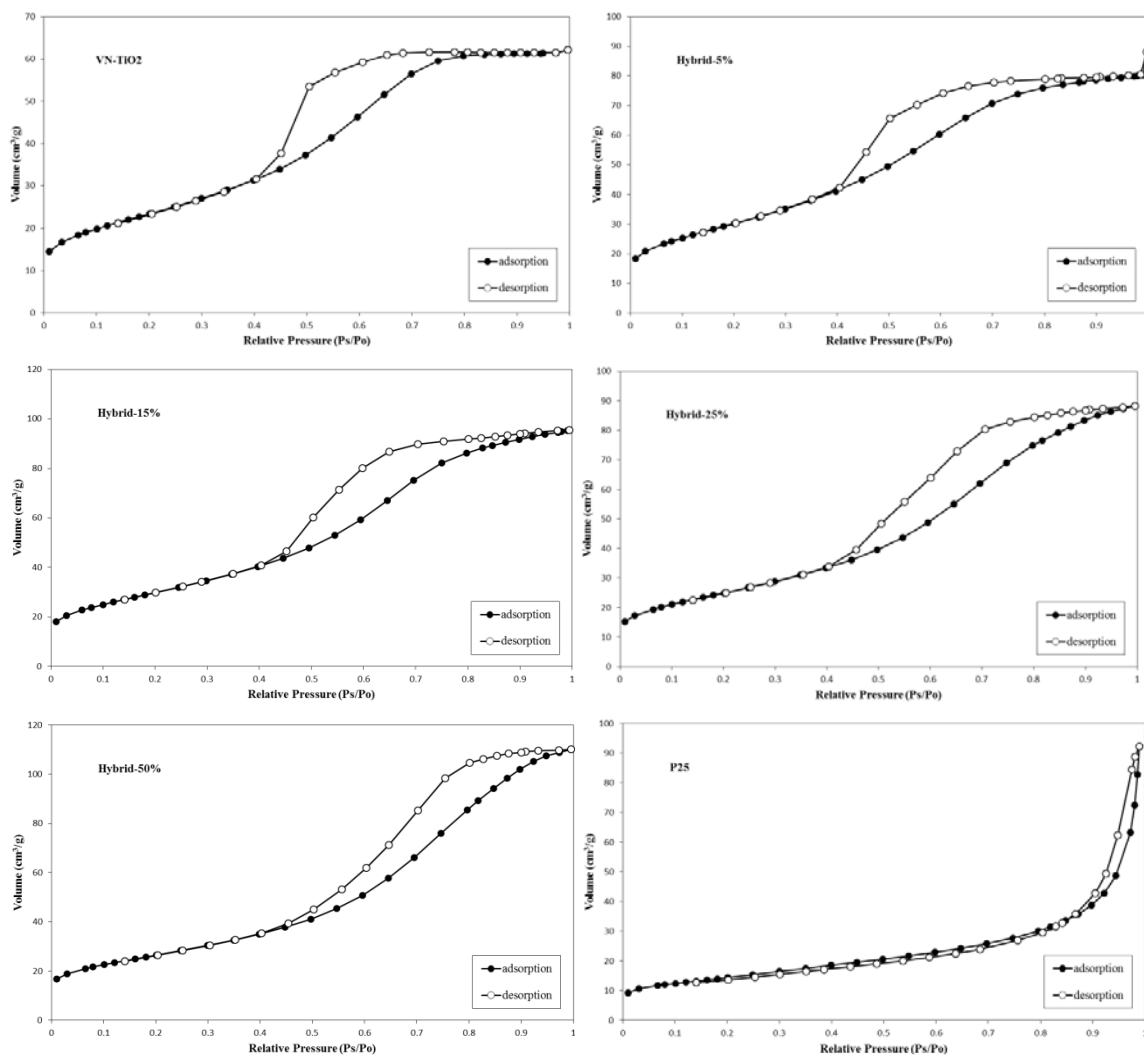


Figure 3.16: Adsorption/desorption isotherms for each coating, scraped from glass and P25 as powder.

It was difficult to determine the surface properties of thin films as the surface area of the support and total amount of TiO_2 was below the detection limit of the analyser. As well the systems for surface analysis are designed for powdered samples making preparation of coated supports either very difficult or not possible in the case of glass disks. In Fig. 3.17, the variation in surface area between two independent scraped-off films of VN- TiO_2 from glass fibres is shown. Although the surface area changes between batches slightly, there is no variation in the shape of the pore size distribution or that of the adsorption/desorption isotherm, which indicates the pore structure was not affected by scraping off the film from the surface. Typically films formed from standard sol-gel

methods have been found to have a very low surface area and to be non-porous, $\sim 9 \text{ m}^2/\text{g}$, (Yu et al., 2004). The coating method adopted in this work still demonstrates high surface area and mesoporous structure of the VN-TiO₂ which would hold true to the films on the fibreglass.

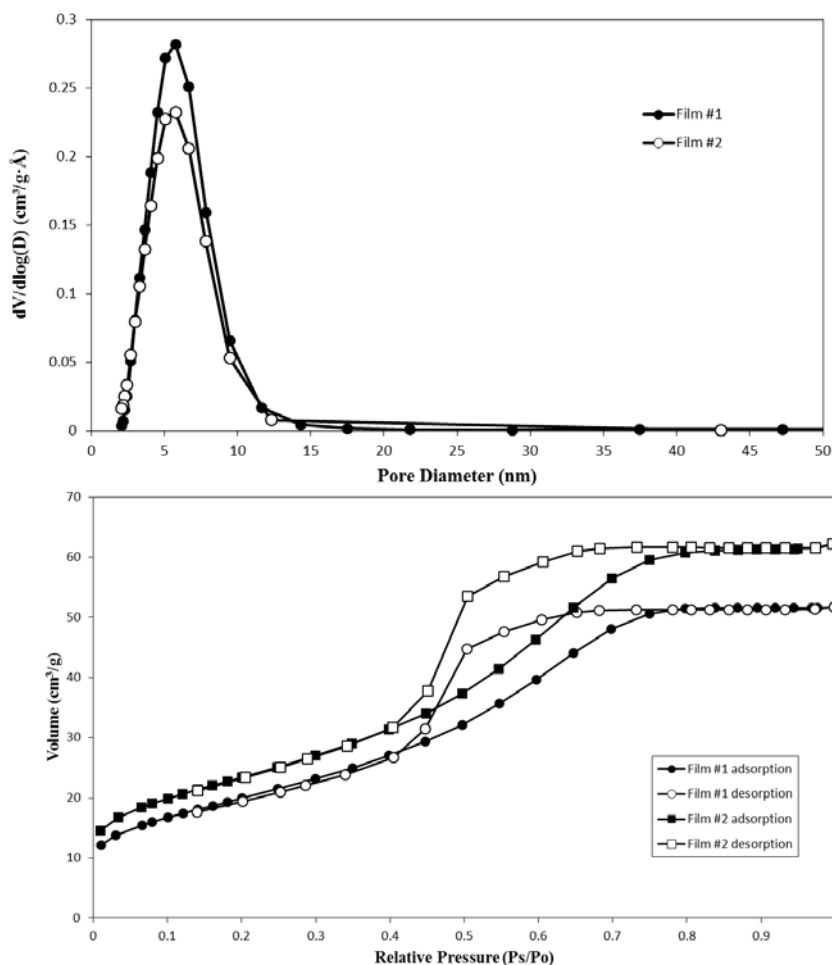


Figure 3.17: Film characteristics of two separately prepared VN-TiO₂ films, pore size distribution curve (top) and absorption/desorption isotherm (bottom).

Table 3.1: Surface characteristics and crystal properties of VN-TiO₂ and hybrid films.

	VN-TiO ₂ ^a	Hybrid -5%	Hybrid -15%	Hybrid -25%	Hybrid – 50%	P25
S _{BET} (m ² /g)	78.4±6.0	109.4	107.9	90.0	94.8	51.3
V _{pore} (cm ³ /g) ^b	0.096±0.008	0.148	0.162	0.148	0.184	-
Porosity ^c (%)	27.3±1.7	36.7	38.8	36.7	41.8	-
Pore Size (nm) ^d	4.7±0.1	5.1	5.5	6.1	7.1	-
Crystal Size ^e (nm)	12.0	-	13.1	-	16.5 (A)/ 42.5 (R)	20.8 (A)/ 30.5 (R) ^f

^a Two independent films of VN-TiO₂ to show variations in method, XRD analyzed once.

^b BJH adsorption cumulative volume of pores.

^c Porosity (%) = (pore volume / (pore volume + volume without pores))x100%, volume without pores = 1/density of anatase, anatase density = 3.9 g/cm³.

^d BJH adsorption average pore size.

^e Determined using Scherer equation for anatase (101) peak from XRD analysis.

^f From literature, for the anatase (A) and rutile (R) crystal size (Bakardjieva et al., 2005).

3.3.3 Photocatalytic Performance

The photocatalytic performances of the coatings were evaluated by the degradation of methylene blue (MB) in a swirl flow reactor. Since this is a semi-batch operation the reaction time was determined by multiplying the total time by the residence volume, which is the ratio of the reactor volume to the total reaction solution. The comparison of the two supports is shown in Fig. 3.18, where both were coated with enough P25 to exceed the optimal loadings >0.3 mg/cm² for the glass plate (Ray & Beenackers, 1998) and ~70 mg/g fibreglass from one dipping cycle in a 0.5 wt % solution of P25. Both coatings provided appreciable MB removal and displayed first-order kinetics. Unlike the smooth surface of the glass disk, fibreglass provides a three dimensional titanium film which results in much higher surface area and better light absorption because adjacent fibres can capture scattered light. The solution was able to flow through the fibreglass disk and the random orientation of the fibres may have resulted in better mixing over the active surface. Mikula et al. (1995) compared the degradation of phenol, for P25 loaded onto fibreglass and in slurry, and found that the supported catalyst had comparable rates of removal for the same reactor configuration. As previously mentioned, coating VN-

TiO₂ onto the glass disks resulted in very low catalyst loadings and would be expected to show lower rates of MB removal on the glass disk. Therefore, the fibreglass mat was selected as the support for further investigation due to the rapid removal of MB (in less than 30 min of reaction time), simpler coating technique, and significantly less expensive material costs.

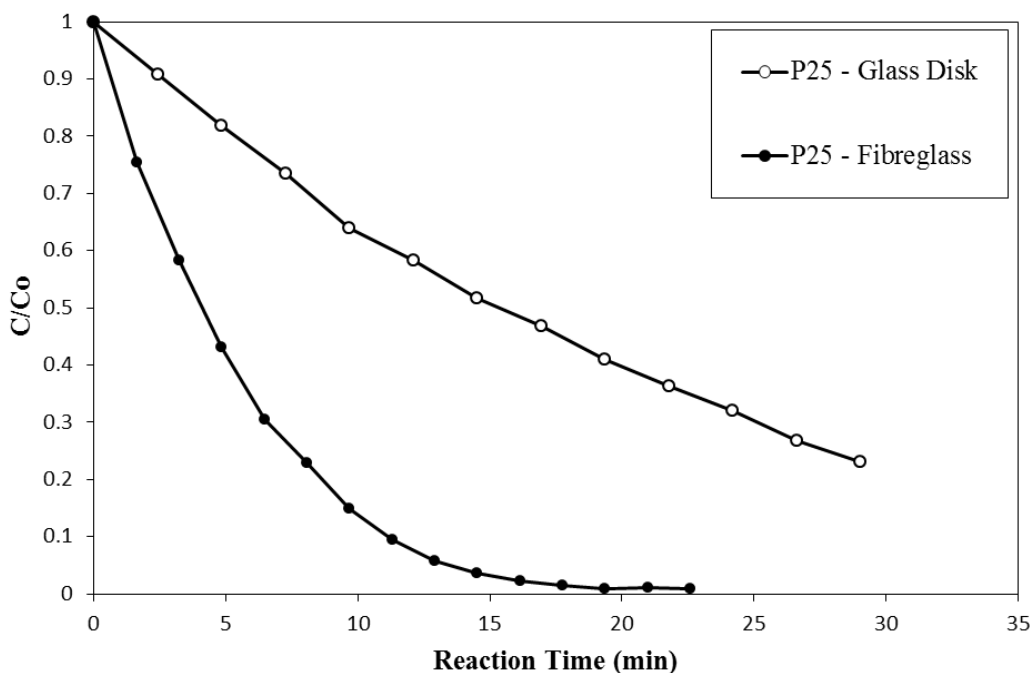


Figure 3.18: Removal of MB for immobilised P25.

The optimal loading of catalyst was determined for VN-TiO₂ by the number of dipping cycles into the stock solution, and comparing photocatalytic activity. The fibreglass could be coated by simply dipping the disk into the solution and drying at 100°C for less than 1 h, then repeating the procedure. This is in sharp contrast to coating onto the glass disks, which requires many intermediate high-temperature calcination stages each followed by overnight cooling. Optimal loading was achieved after two dip cycles (Fig. 3.19) with an average of 62 mg TiO₂/g fibre.

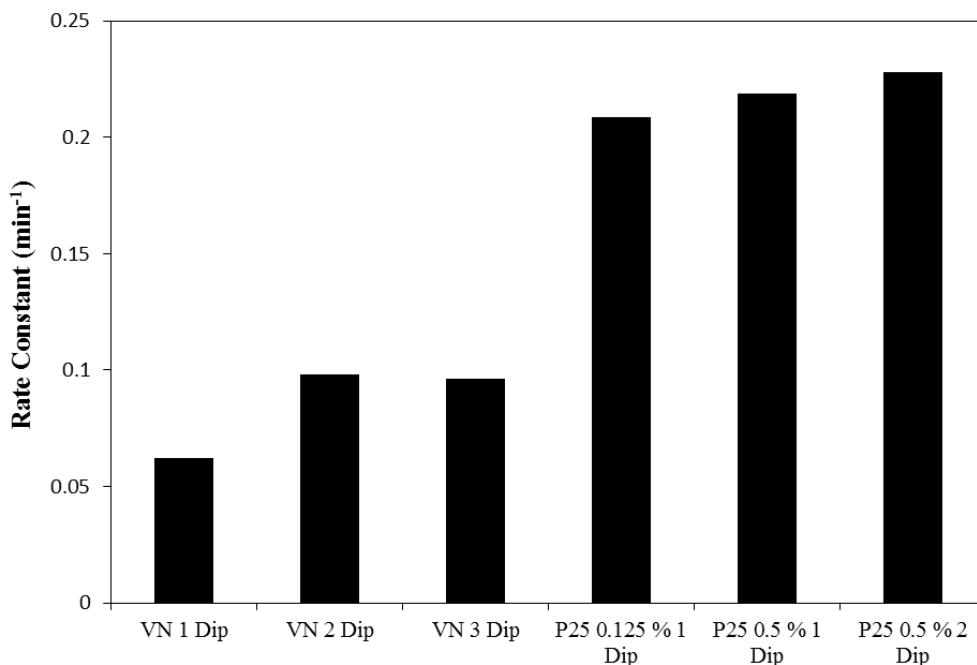


Figure 3.19: Optimal loadings for VN-TiO₂ and P25 on fibreglass disks.

The photocatalytic activity for the optimal coatings is shown in Fig. 3.20. There was no degradation of MB due to photolysis in the absence of TiO₂ under UV irradiation. VN-TiO₂ had a rate 50% that of P25, but was considered highly active as it achieved a 1-log reduction in under 30 min reaction time. For films formed from standard sol-gel routes, Choi and Ryu (2006) showed that there was insignificant degradation of MB due to the nonporous properties of the film. However, with the addition of a pore directing agent, Tween 80, the removal increased dramatically due to the increase in surface area and porosity. Similarly, the films formed from VN-TiO₂ are mesoporous due to the decomposition of the polymer shell during calcination, but unlike modified sol-gel techniques, no processing or optimization of a pore-directing agent is required for VN-TiO₂. The addition of P25 into the films increased the reaction rate by 40%. The increased degradation can be partially attributed to the increased BET surface area and pore volume, and also probably due to the better electronic property of P25. The interaction of MB with the P25 would account for most of the increased reaction rate. This could occur by direct exposure to P25 particles not completely covered by the film. Also the interaggregate pores between P25 and the crystallites formed from VN-TiO₂ could act as channels for the MB to further contact P25 (Chen & Dionysiou, 2007). A

maximum rate of reaction was achieved with the addition of only 15% P25 to VN-TiO₂. The surface morphology of these films shows an even distribution of particles on the film up to 15% loading and increasing this to 50% only resulted in a build-up of particles in between the fibres (Fig. 3.11h and j). Other researchers have found results in line with this study for hybrid films prepared from sol-gel on fibreglass, where the optimal P25 loading was 15% relative to the theoretical amount of TiO₂ in the solution (Medina-Valtierra et al., 2006).

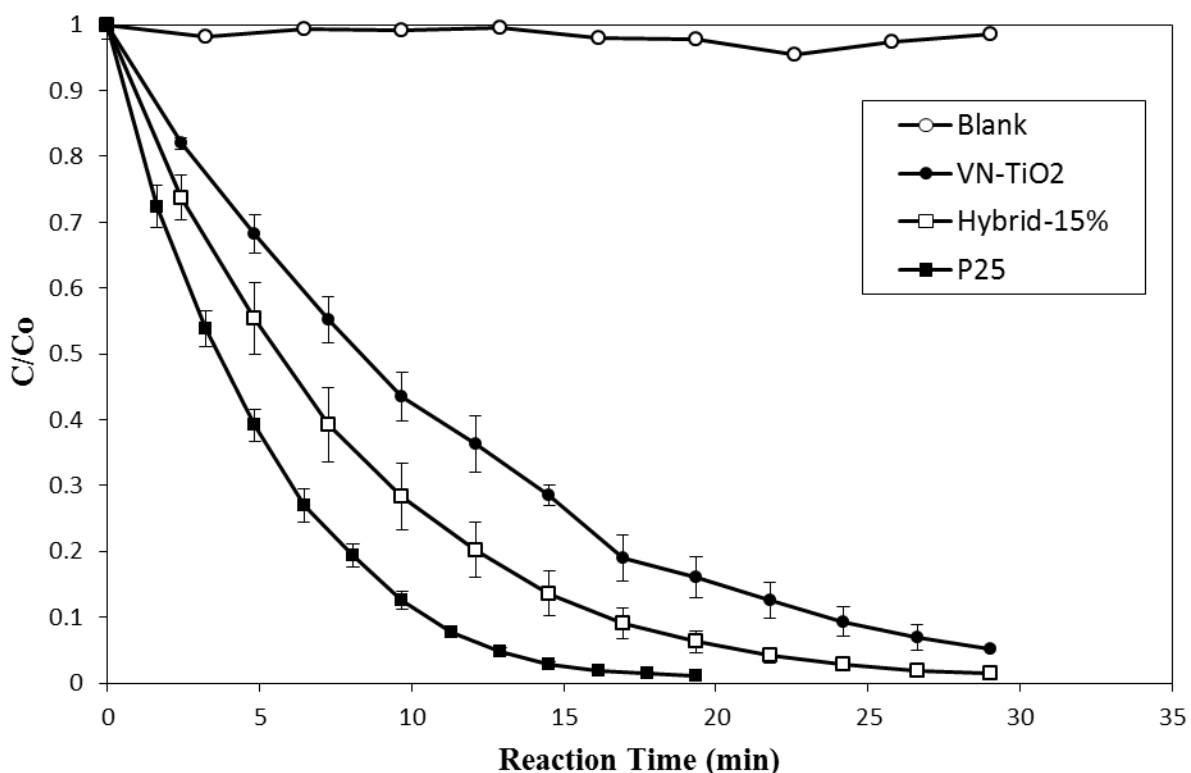


Figure 3.20: MB degradation curve for various coatings on fibreglass: VN-TiO₂ (62.2 mg TiO₂/g fibre), Hybrid-15% (65.0 mg TiO₂/g fibre), P25 (69.4 mg TiO₂/g fibre).

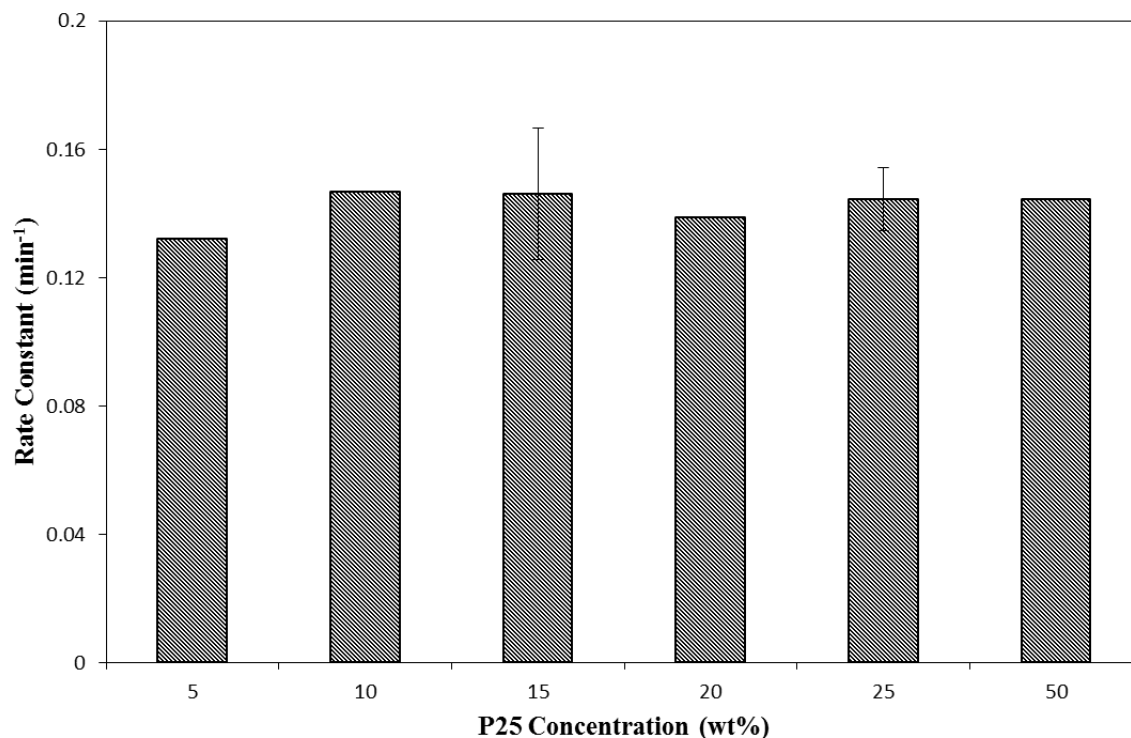


Figure 3.21: Effect of P25 mass loading in hybrid VN-TiO₂ coated fibreglass disks.

3.3.4 Mechanical Stability of the Films

Coated fibreglass disks were thoroughly rinsed by repeatedly dipping and firmly pressing the disk in pure water before each reaction. A consistent average mass loss of 8% relative to the amount of catalyst loaded was found for all types of coatings. This demonstrated that both the film and the powdered catalyst bonded very well to individual fibres as a result of the heat treatment. VN-TiO₂ was able to form a film around the fibre and this contributed to the stability as shown in Fig. 3.11e-f. To assess long-term stability, a coated VN-TiO₂ disk was tested in a five-day only water recirculation test. There was no change in the mass and no material was visible in the buffer tank. ICP analysis did not detect Ti in water, indicating non-detectable TiO₂ leaching out of the support.

While photoactivity is the most important aspect of the supported catalyst in the reactor, the support must be able to conform to the reactor design. In the case of an annular reactor, the support would have to surround the lamp in a cylindrical shape and the

support itself must be stable over time. In all cases the disks were completely opaque with no visible light passing through. Fibreglass disks coated with VN-TiO₂ were rigid after calcination (Fig. 3.22a); they maintained their shape and structural integrity after the reaction (Fig. 3.22b), whereas the P25 disks started to fray and fibre layers started to separate (Fig. 3.22b). As a consequence P25 coated fibreglass disks would not be suitable for long-term use in a reactor, especially at a larger scale.

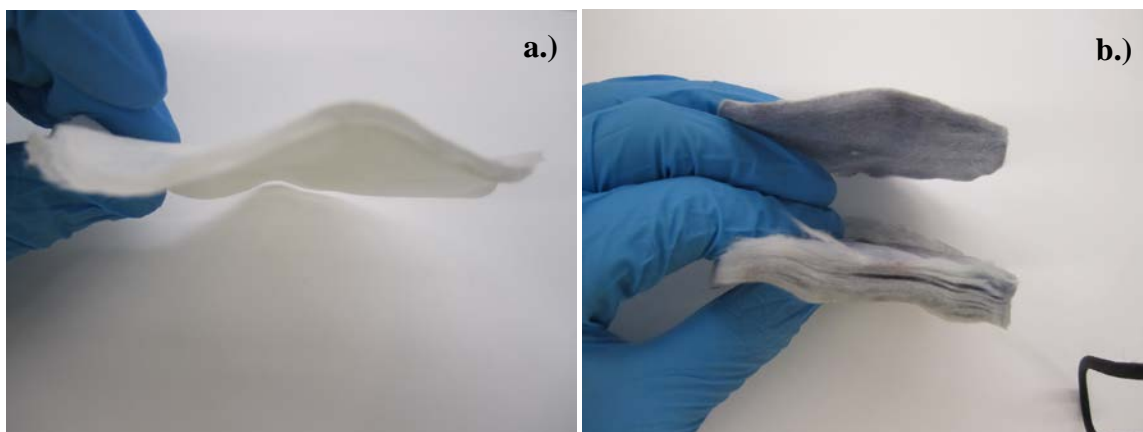


Figure 3.22: Image of coated fibreglass disks (a) VN-TiO₂ fibreglass disk post-calcination, (b) coated fibreglass disks post-reaction: VN-TiO₂ (top) and P25 (bottom).

3.3.5 Long-Term Photocatalytic Performance

Since the catalysts in the immobilised reactors are operated in a continuous environment, fouling and catalyst poisoning will eventually reduce the removal rate enough that either the catalyst must be regenerated or a new one is installed. To assess the effect of continuous operation on the coated fibreglass disks the reaction was repeated several times for both P25 and VN-TiO₂. After each reaction the reactor was flushed with water and a fresh 500 mL solution of MB at 10 ppm was added. It was necessary to limit the extent of degradation, in order to be more representative of realistic operation conditions, which was set at 30 min for VN-TiO₂ and 20 min for P25 and in both cases for the first test, a greater than 90% removal of MB was achieved. For both types of catalyst a similar trend was found in that the rate decreased steadily after each reaction. For P25 coated on fibreglass, Brezova et al. (1994) found a similar steady decrease in rate of

phenol degradation over the course of 16 repeating 90 min experiments. The major factor for the reduction in reaction rate was fouling, caused by the adsorption of degradation intermediates. Specifically, the increased concentration of Cl^- ions on the surface has been shown to contribute to inhibiting the rate of reaction for repeated use of TiO_2 catalyst (Al-Sayyed et al., 1991). Further indication of intermediate adsorption was a drastic change in colour of the disks after the five repeat reactions (Fig. 3.25). The colour of the disks was a dark bluish-purple indicating a build-up of any of the several demethylated intermediates of MB which are also blue. The change to purple would be caused by thionine which is somewhat water insoluble, and consequently would have build-up on the TiO_2 surface (Zhang et al., 2001). The colour change for VN- TiO_2 was much greater than that of P25, this could be explained by the greater degree of degradation for the P25 and the mesoporous structure of the VN- TiO_2 film where both MB and its degradation products could diffuse and become trapped in the pores of the film. After being dried both disks had a mass greater than that of their respective initial mass, this indicated a significant amount of adsorbed material as shown in Table 3.2. In a study performed by Rao et al. (2004), the loss of catalyst was considered a significant reason for the decrease in the rate for TiO_2 , loaded on polymer fibres and pumice stones after multiple reactions. For VN- TiO_2 and P25 loaded on fibreglass the change in mass between the first and fifth reaction was very small (Table 3.2), and as a result was not considered to be a factor that contributed towards the reduction in rate.

Table 3.2: Change in mass for coated fibreglass disks after reusability testing.

	VN- TiO_2	P25
Disk Before Experiment #1	2.4105 g	2.5208 g
Disk After Experiment #5	2.4212 g	2.5262 g
Regenerated Disk	2.4080 g	2.5052 g

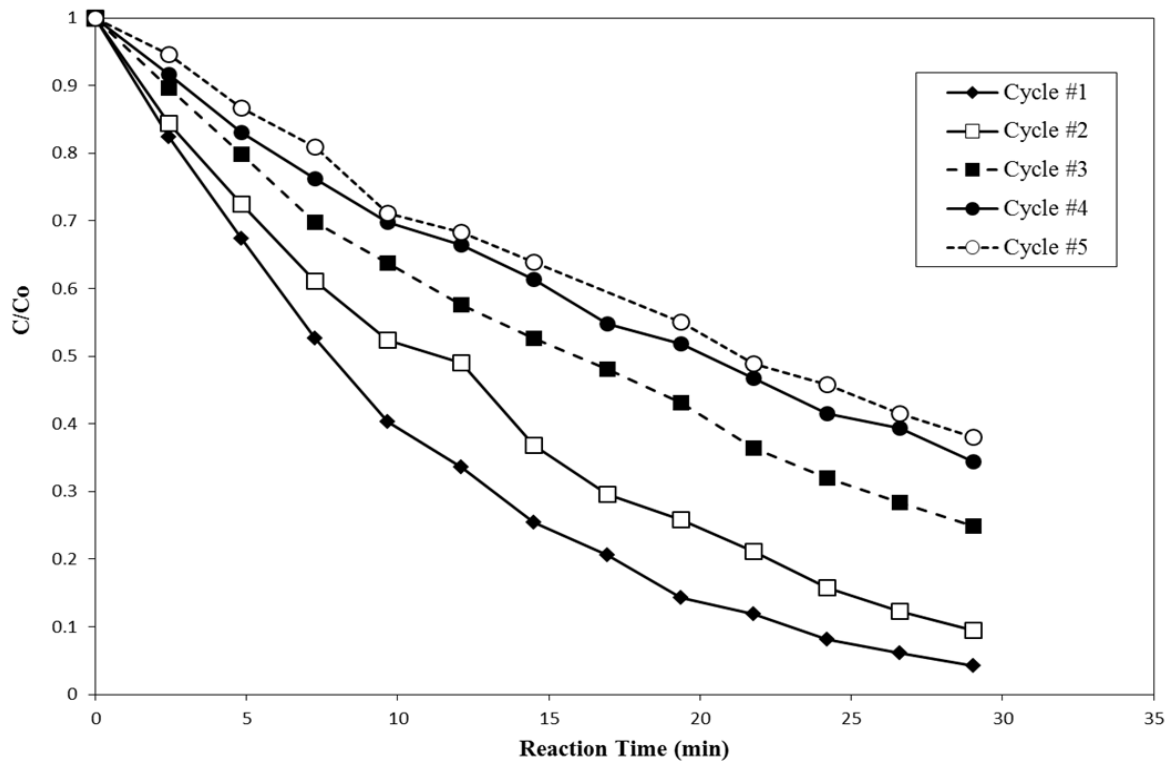


Figure 3.23: Reusability tests for VN-TiO₂ coated fibreglass.

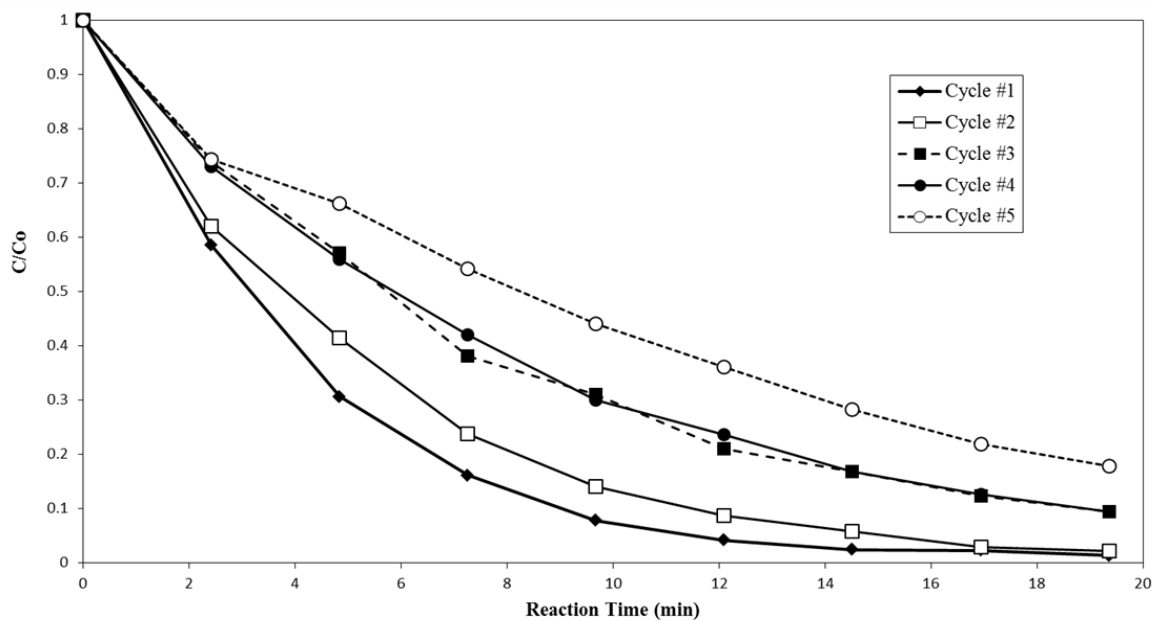


Figure 3.24: Reusability tests for P25 coated fibreglass.

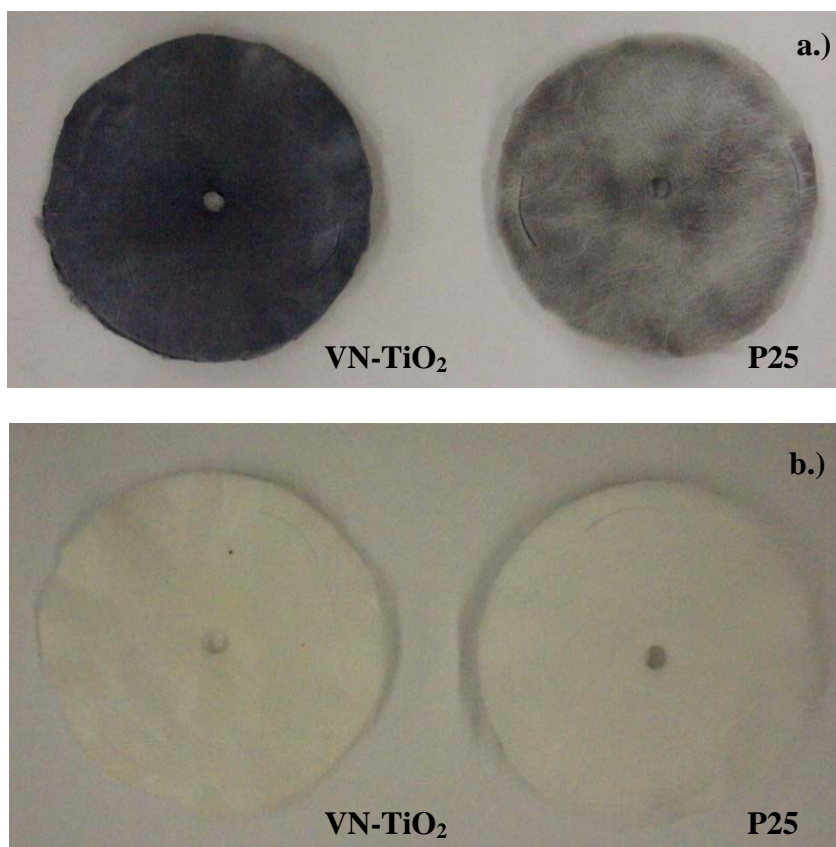


Figure 3.25: Images of the effect of long-term testing and regeneration on the apparent colour on coated fibreglass disks - a.) dried after 5 repeat cycles, and b.) regenerated.

To test the potential for re-use, the disks were regenerated by calcining them at 500°C for 3 hours. Both disks returned to a near pure white colour with no soot visible on the disks from organic compound decomposition (Fig. 3.25b). The mass of the disk also decreased for both, indicating the removal of adsorbed organic matter. The disks returned to a mass similar to the initial reliability test (Table 3.2). Regenerating the disks only resulted in a recovery of rate by 50% for VN-TiO₂ and 60% for P25 relative to the initial testing. A study on regeneration of P25 in slurry showed the same result after heating the catalyst at 450°C, this was attributed to the heat treatment damage of the catalyst (Rao et al., 2004). Further for VN-TiO₂ because of its mesoporous structure the heat treatment could have also reduced the surface area and porosity of the VN-TiO₂ by collapsing the pores.

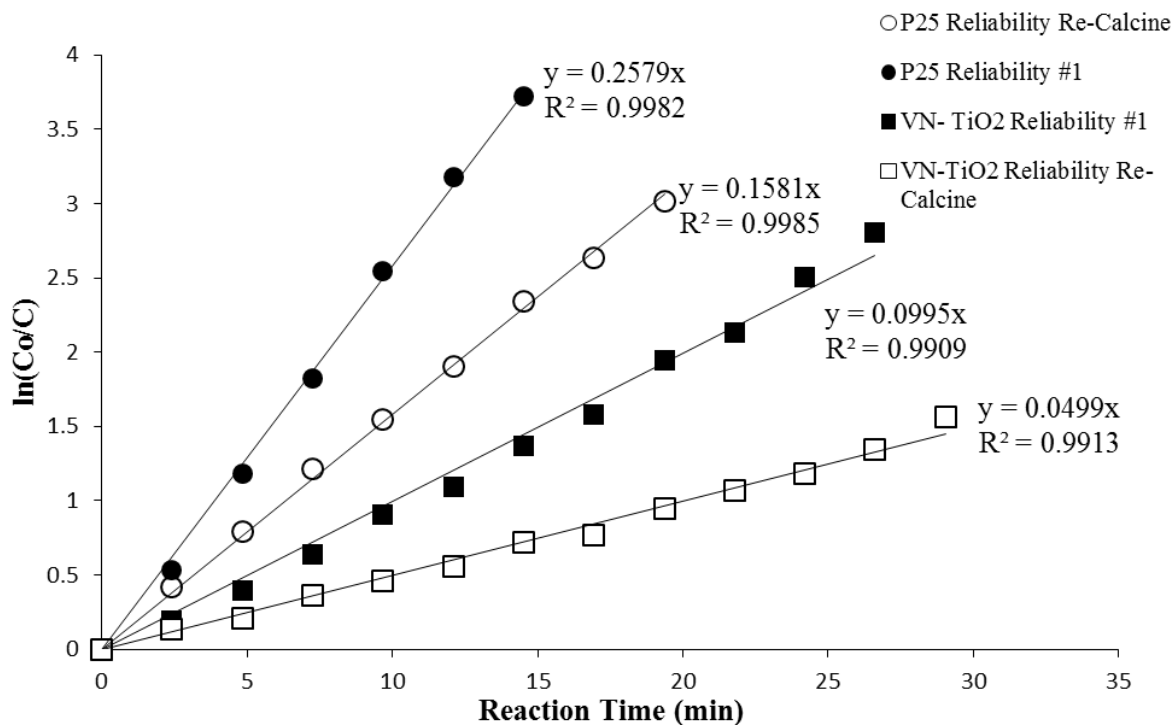


Figure 3.26: First order rate constants for regenerated fibreglass disks compared to initial rate of degradation.

3.3.6 Photocatalytic Degradation Mechanism of Methylene Blue

For the degradation of methylene blue using Degussa P25 under UV, Zhang et al. (2001) investigated the N-demethylation of the dye. Methylene blue contains methyl groups, which are weak electron donors which can be removed by hydroxyl radicals. This degradation pathway occurs stepwise with one methyl group removed at a time resulting in the formation of coloured intermediates (Fig. 3.28). This results in a blue shift in the peak absorption band of MB. Choi and Ryu (2008) studied this effect using various commercial catalysts and showed that the type of titanium dioxide catalyst can greatly affect the extent of the demethylation mechanism. The catalyst with minimal to no spectral shift, Hombikat UV100, would degrade MB through the breakage of the aromatic ring skeleton (Fig 3.29). Anatase from Sigma had the greatest peak shift, which indicated that degradation proceeded predominately through demethylation. P25 had a moderate shift indicating both mechanisms were significant (Choi & Ryu, 2008). In comparing this effect for the VN-TiO₂ film it can be seen in Fig. 3.27 that there is no

difference between any of the systems tested and that the extent of demethylation is the same for all the catalysts. There is a gradual change in the wavelength shift over the conversion range of MB. This could be explained by the fact that the shift is moderate up to that point of conversion, where the primary mechanism is from ring opening, but the intermediates formed from this would continue to react, seemingly with the radical species involved in the ring opening, which would force the remaining MB to be degraded through demethylation. While conducting tests with reused catalysts, there was no change in wavelength shift for both VN-TiO₂ and P25 over the same conversions which indicates that the same mechanisms were still prevalent, but to a lesser extent, due to catalyst inactivation.

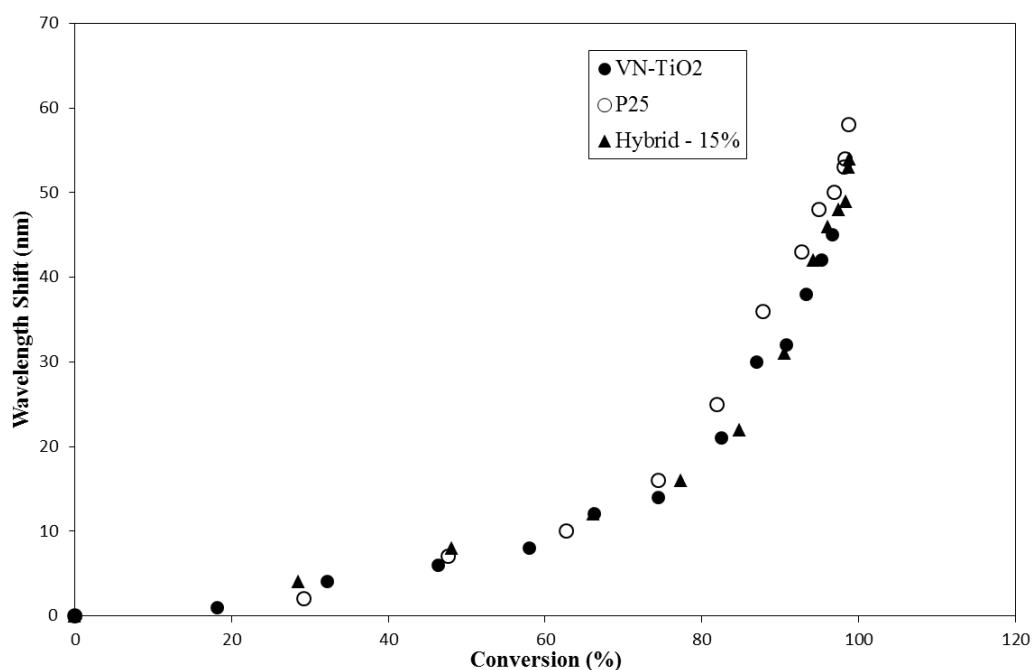


Figure 3.27: Comparison in the degree of blue shifting relative to MB conversion for different catalysts on fibreglass.

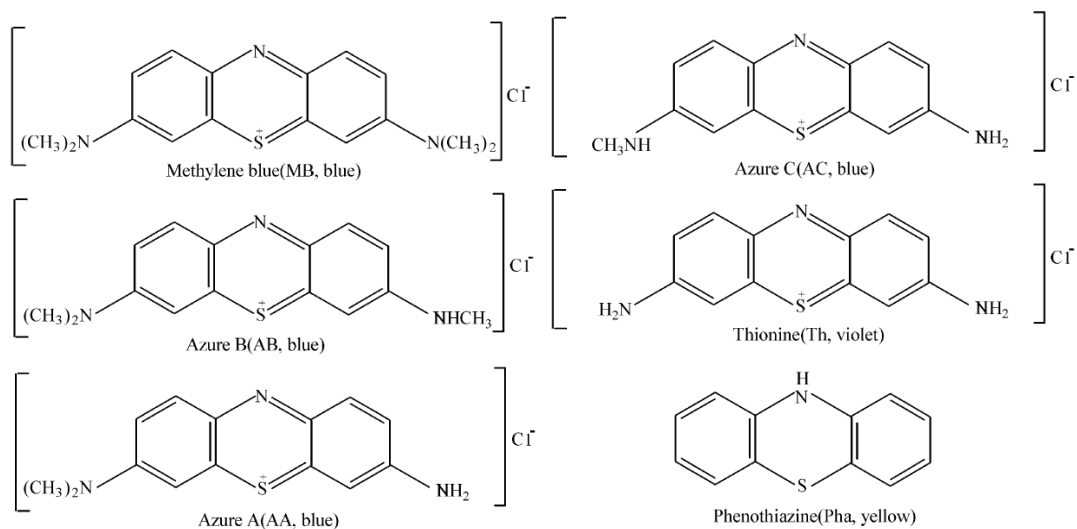


Figure 3.28: N-demethylation products of methylene blue with corresponding colour, proposed by (Zhang et al., 2001).

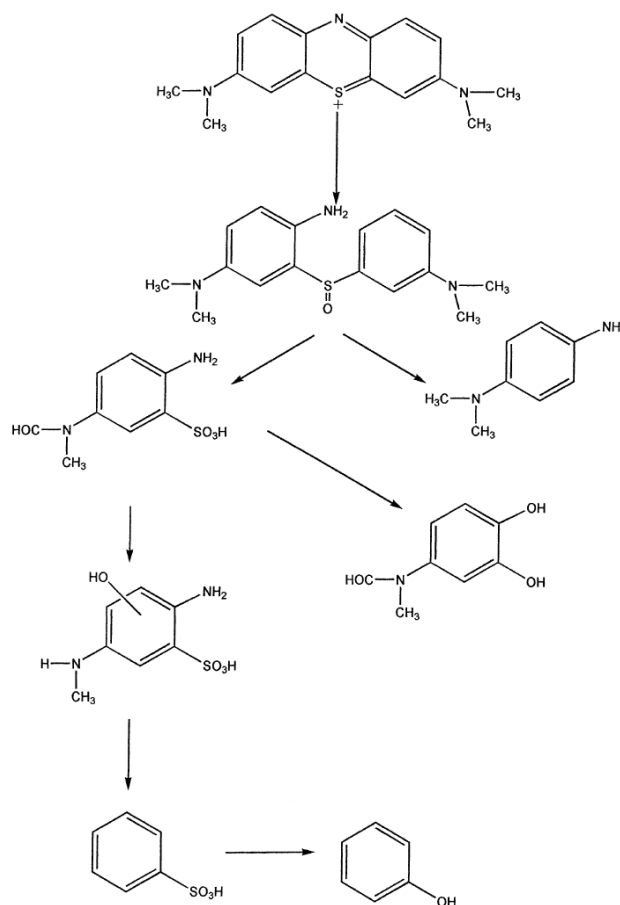


Figure 3.29: Degradation mechanism of methylene blue through breakage of aromatic ring, proposed by (Houas et al., 2001).

3.3.7 Effect of Calcination Temperature

One of the most important preparation parameters is the calcination temperature for making highly crystalline and photoactive thin films. The TGA analysis demonstrated the importance of selecting a temperature of 500°C to completely remove the organic contaminants. Higher calcination temperatures can result in a phase change of the TiO₂ from anatase to the more stable rutile phase. The mixture of 75% anatase and 25% rutile in P25 is considered essential to its overall high catalytic activity, potentially due to the interface between the phases reducing the recombination rate (Hurum et al., 2003). The exact mechanism is still unknown but nevertheless the mixture of phases is essential for its activity (Henderson, 2011).

In this study, quartz wool was cut into disks to fit into the reactor, which had very similar fibre size and orientation to the fibreglass support. The major difference was in terms of cost; the cost per quartz disk was 10 times more expensive than that of the fibreglass. The effect of calcination temperature from 500°C – 700°C was investigated (Fig. 3.30). Up to 650°C there was a steady drop in the reaction rate which would be due to the decrease in surface and porosity caused by the sintering and growth of TiO₂ crystallites (Yu et al., 2003). At 700°C there is a dramatic drop in the apparent rate, this is as a result of the TiO₂ in the film nearly converting completely to the rutile phase (Tanaka & Suganuma, 2001). The synthesis technique can affect the phase transition temperature, but other studies have shown this dramatic drop in the rate at certain elevated temperatures, and attributed this to the majority of the film's crystal phase changing from anatase to rutile (Yu et al., 2003). On the impact of calcination temperature for hybrid films, Chen and Dionysiou (2006b) showed the same decrease in rate with increasing temperature due to the lower surface area and porosity. By simply changing the thermal treatment procedure in the preparation of TiO₂ films an improvement in the photocatalytic rate was not found, indicating either no synergetic effect of anatase and rutile or that the detrimental impact of the loss in surface area or porosity outweighed any benefit in a mixed phase film. Therefore, 500°C was the optimum calcination temperature for VN-TiO₂ where all of the polymer film was removed.

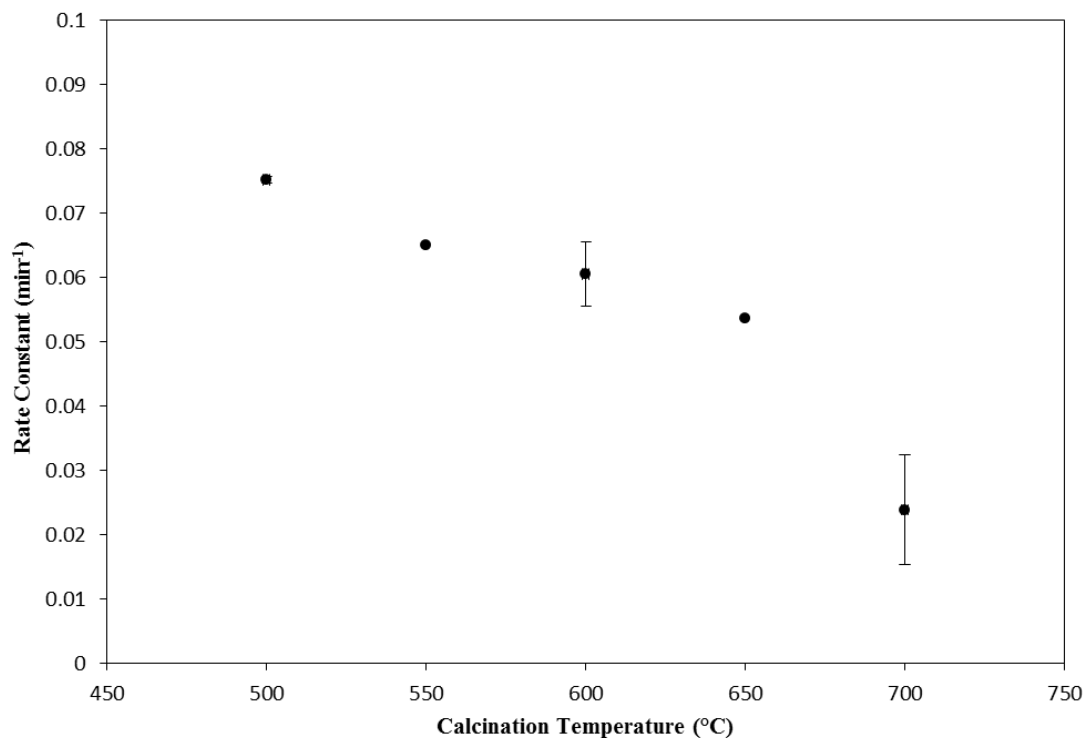


Figure 3.30: Effect of calcination temperature VN-TiO₂ films on quartz wool disk.

3.4 Summary and Economic Considerations for Proposed Application

The conclusions from the experimental results presented in this chapter are summarized in this section. Initially the research indicated that the VN-TiO₂ catalyst was not suitable for coating onto a glass support as high catalyst loadings could not be achieved quickly and simply; catalyst cracking and loss were significant. When comparing the maximum degradation rates achieved for P25 on the glass disk versus the fibreglass support, a much higher overall rate was found for the fibreglass due to its surface morphology.

Thereafter, fibreglass was used as support material for all the catalysts. The thermal behaviour and loss of mass during calcination of VN-TiO₂ indicated that to synthesize highly crystalline anatase films a temperature of 500°C was necessary to remove all organic material. From XRD analysis it was found that the films were of the titanium dioxide phase anatase with a primary crystal size of 12 nm. The films formed on the surface of the fibreglass were smooth and crack free with the film acting as a binding agent between the fibres indicated by the SEM analysis. The VN-TiO₂ and P25 hybrid

films showed the same result with P25 particles distributed evenly throughout the film. Heat treatment caused the removal of the polymer which resulted in the films having a mesoporous structure at an average pore size of 5 nm and surface area of $78\text{m}^2/\text{g}$. The hybrid coatings had a higher surface area and porosity due to the formation of inter-particle pores between the film and P25 particles. The maximum photocatalytic activity of each coating on the fibreglass support showed that the VN-TiO₂ had a rate 50% that of P25, but the addition of a small amount of P25 into it increased the rate by 40%, which was attributed to MB degrading on P25 directly exposed on the film or inside the inter-particle pores. An optimal amount of P25 in the hybrid coating was found to be 15%, where the SEM also showed that increasing the loading above the concentration did not increase the amount of P25 particles in the film. The P25 coated disks on the other hand had poor mechanical stability in the reactor, while due to the film bonding the fibres together the VN-TiO₂ coated fibreglass disks were mechanically robust and able to maintain their shape throughout a reaction; the same was true for the hybrid coatings. Both the P25 and VN-TiO₂ coatings suffered from fouling in long term tests, and regeneration of the disks only retained 50% of the original reaction rate. This indicated that long term use of the fibreglass may not be possible, but for short term analysis under a testing environment the low cost and simplicity of the coating made the fibreglass with the VN-TiO₂ solution ideal as discussed below.

The evaluation of the VN-TiO₂ catalyst was not based on the goal of making the highest photoactive catalyst for use in water treatment, which seemingly is the shared goal among many research groups globally. This work proposes that this catalyst can be used for the design, testing, and optimization of photocatalytic reactors for water treatment at pilot or larger scales, which to date have not been conducted comprehensively. The fibreglass paper can be coated by simply dipping it in the stock solution, and once dried the polymer holds the shape necessary to meet the optimal placement in the reactor. Heat treatment produces a stable, highly photoactive support that is ideal for reactor testing. Table 3.3 compares the important measures for the use of the support (fibreglass paper and glass) in photocatalytic reactors. The fact that the coated fibreglass can be made quickly and at a very low cost is ideal for a testing environment where modifications and a vast variety of experiments would require the continuous production of new catalysts

for testing. This work demonstrates that VN-TiO₂, which is a commercially available product that could be used to coat the fibreglass to obtain a highly active TiO₂ film, eliminating the very expensive and time consuming processing to produce an “in-house” immobilised synthesis procedure. It is available globally making it ideal for use as a reference thin-film catalyst. Use of fibreglass as a support can make it easier to develop photoreactors for large-scale application.

Table 3.3: Fibreglass versus Glass for use in an immobilised photocatalysis reactor.

Measure	Fibreglass Paper	Glass
Cost ^a	\$0.15 per disk	\$20 per disk
Catalyst loading	Simple multi-dip coating, no high temperature calcination in between, multiple supports made quickly	Spray or spin coating for consistent film, dipping produces uneven coatings, multiple high temperature coating cycles required
Conforming to optimal reactor design	Simple, post drying polymer maintains shape	Possible, but expensive as custom product may be required
Replacement	Inexpensive	Expensive
Re-use	Limited, fouling permanently inactivates catalyst	Less prone to fouling, but still significant limitation, reactivation possible
Photocatalytic Rate	Very high due to surface area, mixing, and effective usage of light	Low, due to low surface area and utilization of light

^acost per disk that met the reactor requirements in this study, the relative difference in price would still hold true at a larger scale.

Chapter 4

4 Assessment of the Mutagenicity and Estrogenicity of BPA Following Advanced Oxidation Treatment

4.1 Introduction

The use of bioassays in water quality monitoring has increased significantly due to concern over the occurrence of a large number of chemical substances found in wastewater effluents, surface water, and even drinking water influents. The assays can be used to screen for various types of toxicity by monitoring end-points such as mortality, growth rate, and luminescence in test organisms without knowledge of the specific compounds and their concentrations within the solution. Short-term bioassays are relatively inexpensive with limited processing and can be combined as a battery of tests to evaluate a wide range of toxic responses, making them an ideal tool for continuous water quality analysis. A very important toxicity measure is to monitor mutagenicity of a substance, which is characterized by the ability of the pollutant to cause mutations in an organism's DNA (Ohe et al., 2004). The most widely used assay for testing mutagenicity is the Ames Test which uses a variety of modified *Salmonella typhimurium* strains that respond to different mutagenic mechanisms. The strains are genetically modified to require a specific enzyme (histidine) for survival; when the test substance causes a reversion in this mutation the bacteria can then grow without the enzyme. Based on the statistical deviation of the sample relative to the background, determination of the probabilistic mutagenicity of the pollutant can be made (Ashby & Tennant, 1988). The importance of testing for mutagenicity is in the strong correlation between mutagenicity and rodent carcinogenicity; a positive mutagenic response warrants further investigation using human carcinogenic tests (Kirkland et al., 2011).

The mutagenicity of surface water has been extensively evaluated as it is a main influent source to drinking water treatment facilities all over the world. In a review article, it was indicated that about 3-5% of the tested sources were classified as highly mutagenic (Ohe et al., 2004). This may be an indicator that the wastewater effluents are releasing mutagenic compounds into the environment either as non-degraded or transformed

pollutants. There has been a significant increase in use of advanced oxidation processes in the water treatment industry either for disinfection of drinking water, or for tertiary treatment of the secondary effluent from the wastewater plant. These processes lead to the partial degradation of organic pollutants resulting in the formation of intermediates, which may be more toxic than the parent compounds. Due to the vast number of chemicals entering water treatment plants, bioassays can provide information on the potential hazard of the treated water, including the synergetic toxic effect that can occur between compounds without time-consuming, expensive chemical identification and knowledge of the physical/chemical properties of specific compounds and complex intermediates (Ohe et al., 2004).

There have been several studies monitoring the mutagenicity of drinking/wastewater post AOP treatment, especially for ozonation (Martijn & Kruithof, 2012; Guzzella et al., 2002; Petala et al., 2008). Heringa et al. (2011) found an increase in the mutagenicity of the tester strain *Sal. TA98* following UV/H₂O₂ treatment of three hydrologically independent surface water samples, which indicated that the mutagenicity was formed from ubiquitous contaminants present in the water. On the other hand, very few studies were conducted on specific compound mutagenicity during and after AOP treatments.

The degradation products formed from the ozonation of naphthalenesulfonic compounds showed genotoxic activity for salmonella strain *Sal. TA100* (Rivera-Utrilla et al., 2002). Cantavenera et al. (2007) looked at the formation of mutagenic intermediates in the degradation of paraquat in photocatalysis; under optimal conditions, no toxicity was found, but reducing the concentration of the catalyst by one order of magnitude resulted in the formation of mutagenic intermediates. This shows that simple changes in the operation of the treatment process can result in different degradation mechanisms and potential toxic by-products. To the best of our knowledge, there has been no comparative toxicity study on compound-specific degradation using various AOPs. In addition to the traditional selection criteria such as cost, simplicity of operation, and process efficiency, the ability to render water safe based on simple bioassays, can also be used as a criterion in the selection of the most appropriate AOPs for a specific compound, which would eliminate expensive and time consuming chemical analysis.

The objective of this study was to determine the differences in toxicity, if any, of bisphenol A (BPA) intermediates using three of the most commonly used AOPs, namely: ozonation (O_3), UV-254nm/hydrogen peroxide (UV/ H_2O_2), and UV photocatalysis (UV/ TiO_2). Two bioassays were used: the Ames test for mutagenicity, and yeast estrogen screen (YES) to monitor estrogenic activity. These assays would account for the formation of different intermediates based on the different reaction mechanisms of each AOP without specific sophisticated chemical analysis such as GC-MS, LC-MS/MS, etc. The results would be used to determine the most effective AOP for removing BPA from water.

4.2 Experimental

4.2.1 Chemicals

BPA (MW: $C_{15}H_{16}O_2$, CAS: 80-05-7) was obtained from Sigma–Aldrich (Oakville, Ontario, Canada). Hydrogen peroxide (H_2O_2 , CAS: 7722-84-1) and catalase (CAS: 9001-05-2) were purchased from Sigma–Aldrich (Oakville, Ontario, Canada). HPLC grade acetonitrile and methanol were purchased from Caledon Laboratories (Georgetown, Ontario, Canada). All reagents were used as received without further purification. Laboratory-grade water (LGW, 18M Ω) was used from a Millipore purification system (model Integral 5, EMD Millipore Corporation, Billerica, MA, USA).

4.2.2 HPLC Analysis

BPA concentration was measured by HPLC (ICS 300, Dionex), which included a DP pump, an AS auto sampler, a DC column oven, and PDA UV detector, connected to Chromeleon software. Separations were carried out with an Acclaim 120 C18 reversed-phase column (150mm \times 4.6mm i.d., 5 μ m particle size, Dionex, USA). The injection volume was 100 μ L from 10 mL HPLC vials, capped and sealed with PTFE lids. Two mobile phases were prepared run in an isocratic mode. The first one was for the kinetic experiments with BPA, which was a mixture of acetonitrile and Milli-Q water (45:55, v/v) with BPA retention time of 3.90 min. The second mobile phase for intermediate analysis was a mixture of methanol and Milli-Q water (55:45, v/v), with a BPA retention

time of 45.0 min. Both were at a flow rate of 1mL/min by the HPLC pump. The column temperature was maintained at 30°C and detection wavelength was set at 228 nm.

4.2.3 Other Analyses

Total organic carbon (TOC) was measured using a Shimadzu TOC-V_{CPN} analyser with an ANSI-V auto sampler, and the pH and temperature were determined with a pH meter (model pHi 460, Beckman Coulter, Inc., Fullerton CA, USA).

4.2.4 Ozonation

The experimental set-up for ozonation of BPA is shown in Fig. 4.1. A stainless steel cylindrical reactor was used. Ozone was produced by an ozone generator (model TG-40, Ozone Solutions, Hull, Iowa, USA). Oxygen was fed to the generator from a compressed air tank set at a pressure of 15 psi. The produced ozone was at a concentration of 2500 ppm, measured using an ozone analyzer (model UV-100, Eco Sensors, Newark, California, USA). The ozone was fed into the reactor at 1.2 LPM. A total reaction volume of 1.45 L was used in all experiments with a BPA concentration of 11.6 ppm prepared in Milli-Q water. The solution had a temperature of 25°C with an initial pH of 5.8.

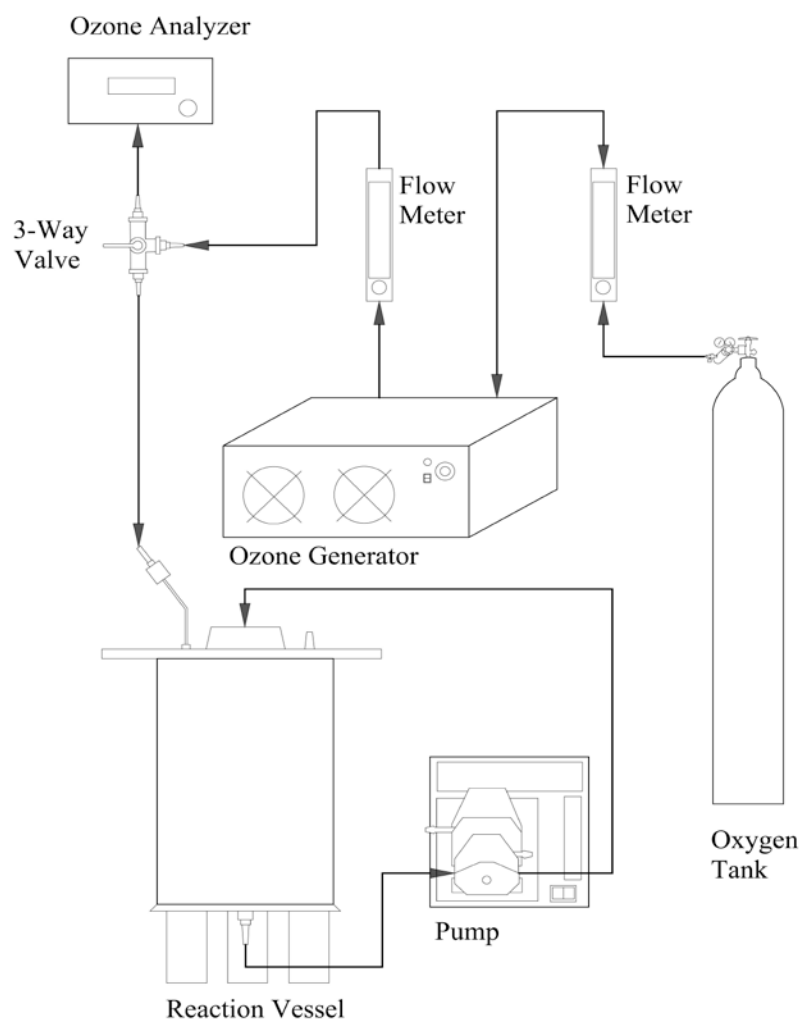


Figure 4.1: Experimental set-up for ozonation.

4.2.5 UV/H₂O₂

The experiments were performed in a bench-scale annular reactor (Fig. 4.2). A 13W low-pressure Hg lamp (model Philips TUV PL-S, 1000Bulbs.com, Texas, USA), with monochromatic light at 253.7 nm surrounded by a quartz protective sleeve, was used as the light source. The reaction volume was 750 mL with an initial concentration of BPA at 13 ppm prepared in Milli-Q water. A water cooling jacket was used to maintain the reaction temperature at 20°C; the initial pH of the solution was 5.2. Samples drawn from the reactor were immediately quenched with catalase to decompose H₂O₂; H₂O₂ is a

known mutagen and will interfere with the bioassays. However, catalase was not used for the TOC samples.

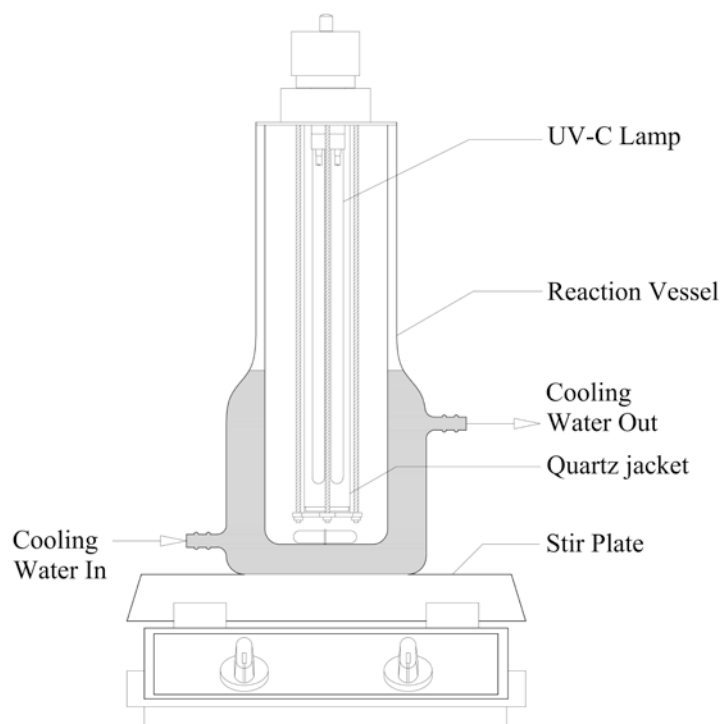


Figure 4.2: Experimental set-up for UV/H₂O₂.

4.2.6 Photocatalysis

The experiments were performed in a swirl flow reactor with Aeroxide P25 from Sigma-Aldrich (Oakville, Ontario, Canada) immobilized onto a fibreglass disk. The preparation method for the immobilised disk and the details of the experimental set up are described in Chapter 3, section 3.2.3. A BPA concentration of 10 ppm was prepared in Milli-Q water. The solution temperature was 30°C and had an initial pH of 5.8.

4.2.7 The Ames Test Protocol

The mutagenic activity was determined by using the Ames Test (Ames et al., 1975). The test employs two strains of *Salmonella typhimurium* TA97a and *S. typhimurium* TA100 (obtained from Environmental bio-detection product inc., Mississauga, ON, Canada), carrying mutation in the operon coding for histidine biosynthesis. Reverse-mutation

assays have been performed using the “Fluctuation test” originally devised by Luria and Delbrück (1943) and was modified by Hubbard et al. (1984). Standard mutagens of 9-*Aminoacridine* (0.4 mg/mL) were used for *S. typhimurium* TA97a and *Sodium azide* (0.1mg/mL) was used for *S. typhimurium* TA100.

A sample of 10 ml was filtered through 0.22 µm membrane PTFE filter, mixed with 2.5 mL of the reaction mixture (RxM) (D-M salt, glucose, bromocresol purple, biotine, and histidine), 7.5 mL of distilled water, and 10 µL of the bacteria grown overnight (18 hours at 37⁰C) with an optical density of 0.5 at 600 nm. The positive control was prepared by adding 0.1 mL of the standard mutagen to 2.5 mL of the (RxM), 17.4 mL distilled water, and 10 µl of the bacteria. The background was prepared by adding 17.5 mL distilled water to 2.5 mL of the (RxM), and 10 µl of the bacteria. The blank (the sterility check) was prepared by adding 17.5 mL distilled water to 2.5 mL of the (RxM) only. Afterwards, the mixtures were dispensed into 96-microtitre plates, (Corning Costar, USA) with each well having a volume of 200 µL of the mixtures. The plates were covered with a lid and put into a plastic bag to prevent evaporation, then transferred to a 37°C incubator for five days.

The response of the Ames Test to BPA samples after different oxidation times, using the two strains of *Salmonella* was determined visually by the color change from purple to yellow as a positive reaction. The “Background” showed the level of spontaneous mutation of the assay organism. The results for each treatment plate refer to positive responses in the sample plate vs. positive responses in the background plate, and the number of positive wells scored in a 96-microtitre plate leading to clear significance in the fluctuation test.

4.2.8 Yeast Estrogen Screen

Estrogenic activity was determined using the YES assay as described by Routledge and Sumpter (1996). A recombinant yeast strain (*Saccharomyces cerevisiae*) was obtained from Trojan UV (Ontario, Canada). A 250 µL concentrated yeast stock from cryogenic vial was added to the conical flask containing the growth medium. The flask was incubated at 28°C, 180 rpm for approximately 24 hours or until turbid with an optical

density of ≈ 1) on an orbital shaker. A standard solution ($50\mu\text{g/L}$) was prepared using 17- β estradiol (E2) and was diluted using a twofold serial dilution in absolute methanol; 12 dilutions in the range of 24.41-50,000 ng/L of E2 were prepared. For standard tests, 10 μL of the E2 standard dilutions were added to three rows of wells in a 96-microtitre plate (Corning Costar, USA) and allowed to dry completely. The blank was prepared by adding 10 μL of absolute methanol to 190 μL of the assay media (growth medium containing the dye, chlorophenol red- β -D-galactopyranosid (CPRG), and yeast) to two rows of the same 96-microtitre plate. Samples of 10 mL from each AOP reactor were collected and freeze-dried overnight and re-dissolved in 1 mL of methanol with a recovery of 87-100%. Thereafter, 60 μL of the concentrated samples were further two-fold serially diluted in two rows of the 96-microtitre plate using methanol, and were left to fully evaporate. Subsequently, 200 μL of the seeded assay medium was added to each well. The plates were sealed with sterile adhesive film and shaken vigorously for 2 min in a plate shaker (VWR). Subsequently, the plates were incubated at 30°C in a naturally ventilated heating cabinet for 3 days. After the incubation, the plates were shaken at 240 rpm for 2 min, and left for approximately 1 hour to allow the yeast to settle. The YES assay was done in duplicate for the samples and the blank, and in triplicate for E2 standard. A typical dose-response curve for E2 is shown in Fig. 4.3.

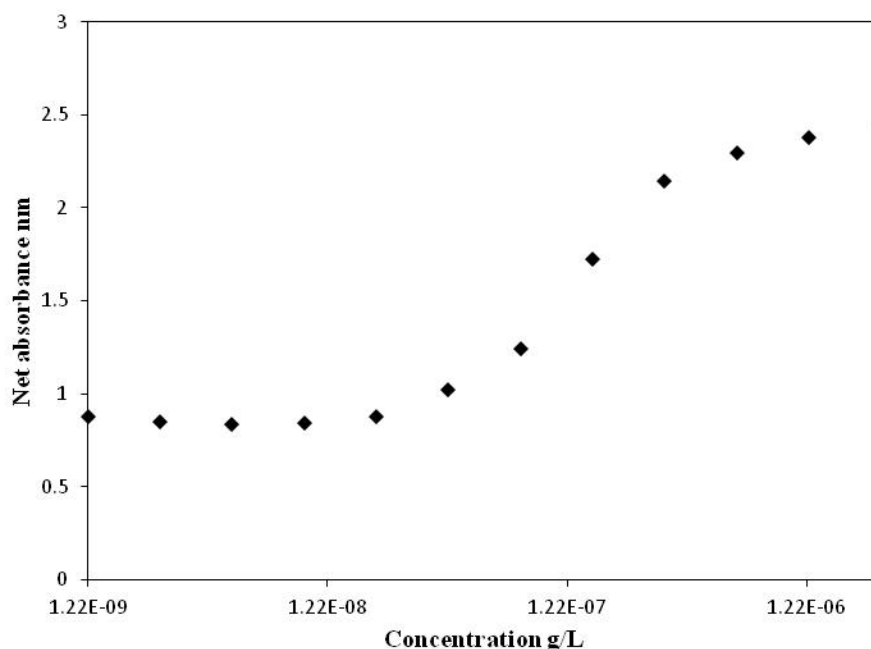


Figure 4.3: Estradiol $50\mu\text{g/L}$ dose-response curve using methanol.

4.2.8.1 Calculation of Sample Response

The estrogenicity of the sample was determined by measuring the absorbance of the sample at 540 nm, subtracting the value of absorbance at 620 nm for yeast in the medium and the absorbance of the blank (medium) at 620 nm using a plate reader (Tecan Infinite 200 PRO, Switzerland) as mentioned previously.

Calculations were performed using the following equation to correct for turbidity:

$$\text{Corrected value} = \text{chem. abs. (540 nm)} - [\text{chem. abs. (620 nm)} - \text{blank abs. (620 nm)}]$$

The data obtained for the standard was used to generate dose response curve. The curve was fitted to the Eq. 4.1, using Origin Labs (Northampton, USA).

$$\text{response} = a + \frac{b-a}{1+10^{(\log EC50 - \log c).m}} \quad (4.1)$$

where **a** is the baseline response (bottom), **b** is the maximum response (top), **c** is the concentration, **m** is the Hill slope, and **EC50** is the concentration corresponding to half-maximal response.

The data was processed as per the methodology explained by Huber (2004). The constants **a**, **b**, **EC50**, and **m** were obtained from the curve fitting for the standard. Thereupon, the constants were expressed as a percent with **a** and **b** varying between 0 and 100. The data for the standard was refitted by fixing values of **a** and **b** to get new EC50 and **m** values for the standard. The absorbance data for the sample was normalized in a similar manner and plotted with concentration factors by fixing the values of **a**, **b**, and **m** as derived from standard curve fitting. Estrogenic equivalents were calculated by dividing EC50 of the standard by EC50 of the sample.

4.3 Results and Discussion

4.3.1 BPA Degradation

Advanced oxidation studies of BPA have been conducted in literature. Since the objective of this study was to compare the mutagenicity of the intermediates formed from the oxidation of BPA in each AOP, the concentration range over which oxidation studies were conducted was selected based on the realistic concentration that may be available in standard water treatment system. It also should be noted that the experimental conditions and final removal of BPA for ozonation and UV/H₂O₂ were selected based on the studies (Garoma et al., 2010) and (Chen et al., 2006), respectively. This was done to avoid detailed intermediate analysis based on the assumption that identical intermediate compounds of BPA would form under identical experimental conditions.

The degradation curves for BPA in each process are shown in Fig. 4.4, the apparent rate constants are determined in Fig. 4.5. The contribution of photolysis from UVA (365 nm) and UVC (254 nm) towards the removal of BPA was considered insignificant as both have been demonstrated to be ineffective in other studies (Ohko et al., 2001; Rosenfeldt & Linden, 2004). Based on the experimental conditions, BPA degradation was slowest in ozonation, while the rate was fastest with UV/H₂O₂.

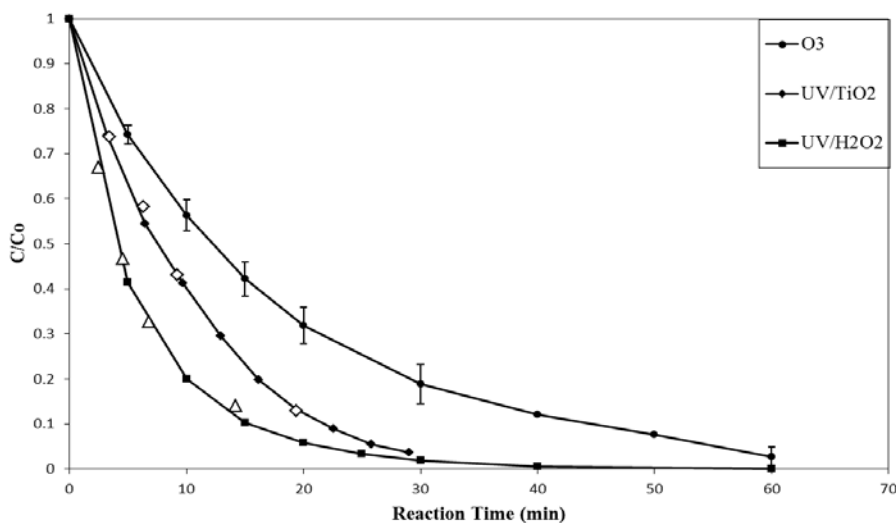


Figure 4.4: Degradation curves for BPA in each AOP tested. (Δ) & (\diamond) represent points sampled for Ames testing for UV/H₂O₂ and UV/TiO₂, respectively.

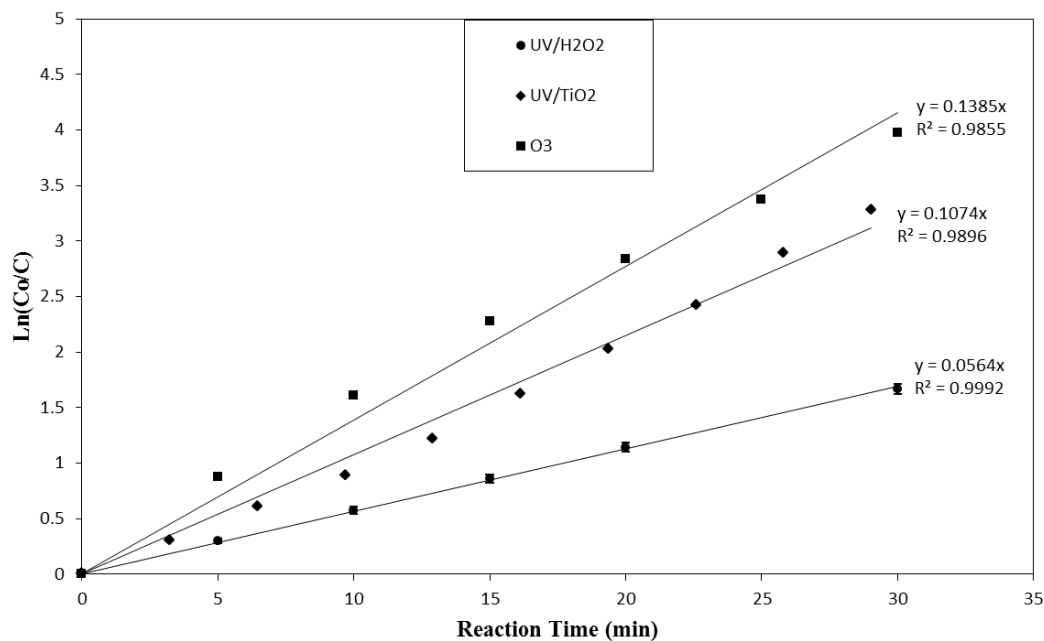


Figure 4.5: Determination of apparent first order rate constant, k (min^{-1}) for each AOP BPA degradation experiment.

For the bioassay tests, several samples up to 30 min or ~80% conversion of BPA were taken from the ozonation reaction. The corresponding sampling points for UV/TiO₂ and UV/H₂O₂ over a similar conversion range are shown by the open symbols in Fig. 4.4.

4.3.2 Degree of Mineralisation and Intermediate Formation

The degree of mineralisation is typically determined by measuring the relative change in total organic carbon (TOC). Typically, much longer degradation times are required after the removal of the parent compound to achieve complete mineralization (Comminellis et al., 2008). The TOC removal for each AOP was analysed within the 30 min treatment period as shown in Fig. 4.6. Both ozone and UV/H₂O₂ reduced the TOC only by 10%. Garoma et al. (2010) found similar results for ozonation; while BPA degraded below the detection limit within 10 min, it took 2 hours of treatment to reduce the TOC by 41%, and even after 6 hours TOC only decreased to 57% indicating that ozone resistant intermediates were formed. On the other hand, UV/TiO₂ had reduced the TOC content by 50% over the same treatment period. This result is in line with other studies on the photocatalytic mineralization of BPA where Chiang et al. (2004) achieved a similar

degree of BPA degradation in 45 min and had a TOC removal of 50%, complete mineralisation was obtained in 120 min using P25 under acidic conditions. The removal of TOC by UV/TiO₂ in our study can be explained by the adsorption capacity of the catalyst for BPA and the degradation intermediates, where in an acidic solution, as in our study, the surface of P25 is positively charged (Muneer et al., 2001). Further demonstrating the effect of pH on the TOC removal, Chiang et al. (2004) found a maximum TOC removal of only 20%, at pH = 10, over the same 120 min of treatment.

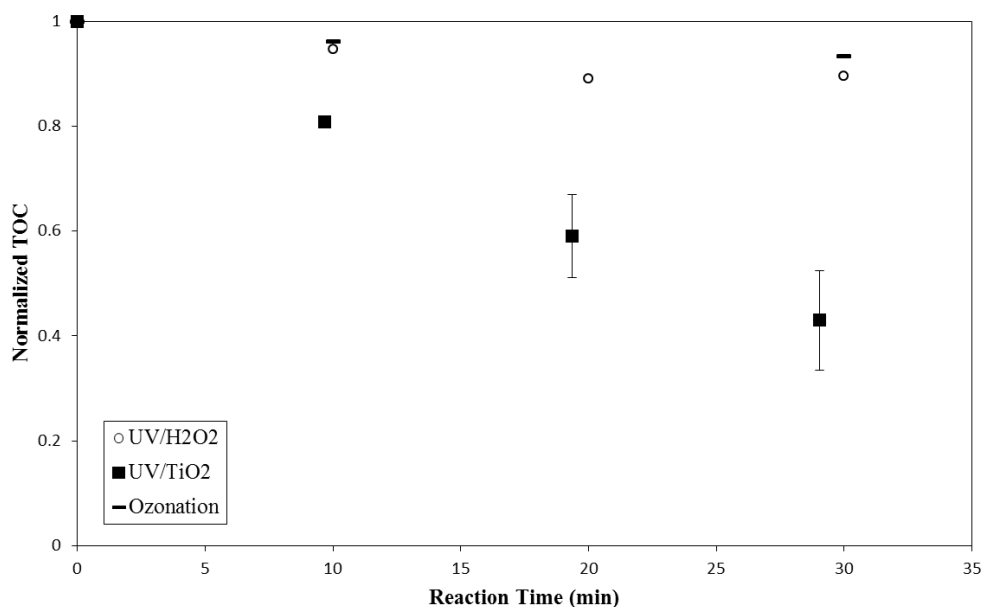
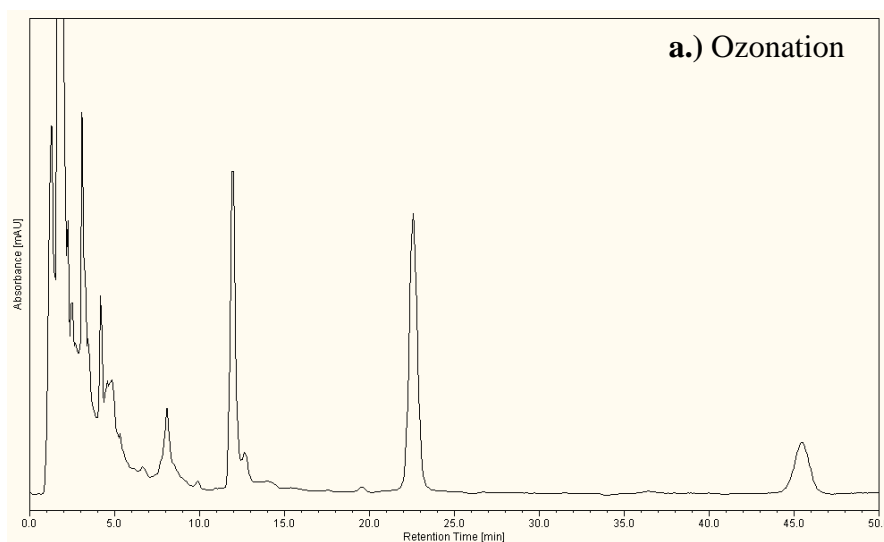


Figure 4.6: Degree of mineralization for BPA removal in each AOP.

The incomplete removal of TOC indicates the formation of several intermediates. The HPLC chromatogram for each AOP is shown in Fig. 4.7; BPA conversion was similar for all the experiments at >80%. For UV/H₂O₂ and ozonation reactions, there are several common peaks at the retention times of 8.0 min, 11.87 min, 12.53 min, and 22.27 min. For ozonation, there is a noticeable difference in size of the peak at 11.87 min and the overall size relative to the primary BPA peak. These differences are a result of the two reaction mechanisms in ozonation: hydroxyl radicals which are the reactive species, and direct reaction of BPA with ozone. Intermediate analysis has been performed for BPA degradation in UV/TiO₂ (Fukahori et al., 2003; Ohko et al., 2001) and for the direct oxidation by ozone, with the hydroxyl radicals scavenged by tert-butyl alcohol (Deborde

et al., 2008). The degradation mechanisms of BPA under various AOPs and a table of some of the intermediates that have been identified were previously discussed in section 3.2.3. Direct analysis of intermediates formed from UV/H₂O₂ has not been performed in literature, but it would be expected that similar intermediates (para-substituted phenolic compounds), found in BPA degradation in UV/TiO₂, would be formed (Chen et al., 2006) because hydroxyl radicals are the predominant oxidants in both UV/TiO₂ and UV/H₂O₂. The chromatogram for UV/TiO₂ is in agreement with the TOC results indicating most of the intermediates reacted quickly. There are very small peaks, some at the same position of the major peaks seen in the other AOPs, but no major intermediate formation occurred. This effect was seen in the removal of the industrial dye AO52, where both UV/H₂O₂ and UV/TiO₂ treatments were performed for BPA and it was found that a variety of toxic aromatic breakdown products for the UV/H₂O₂ process had formed, but they were not found in the UV/TiO₂ process; this was attributed to the fast adsorption and further degradation of the intermediates on the catalyst surface (Galindo et al., 2000).



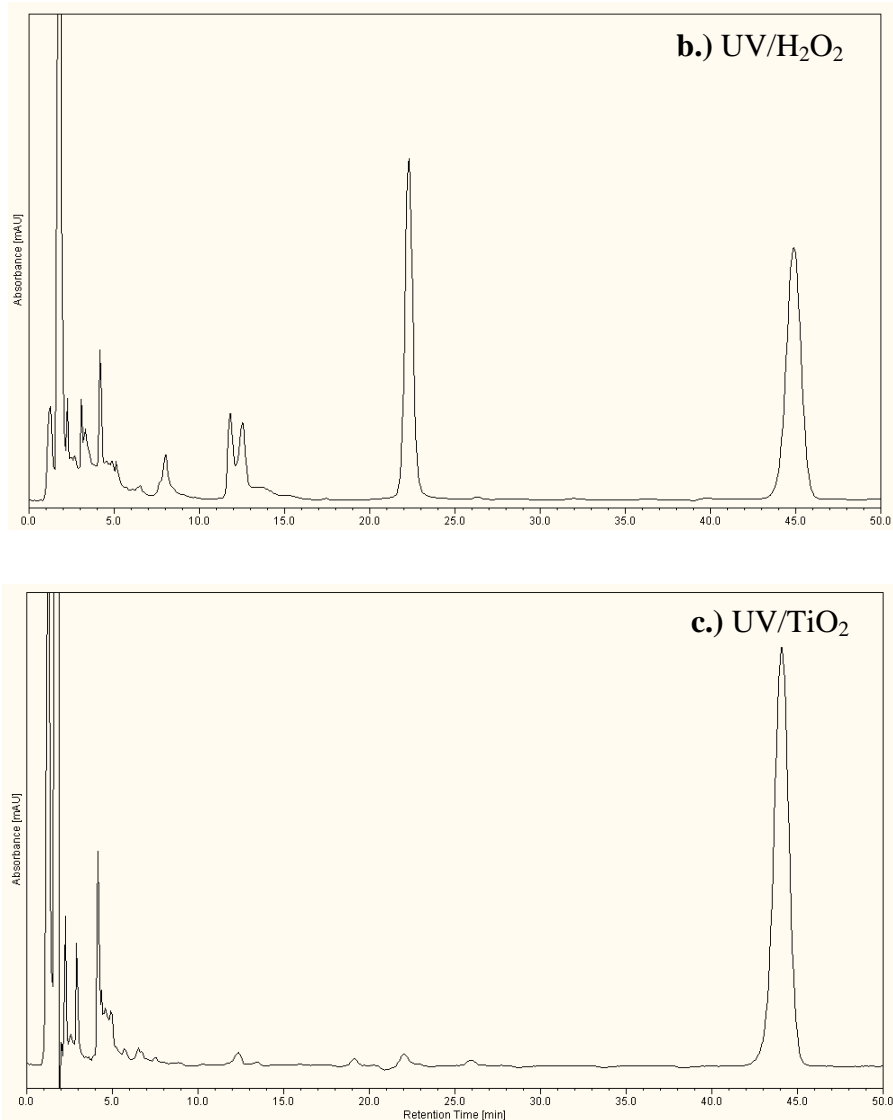
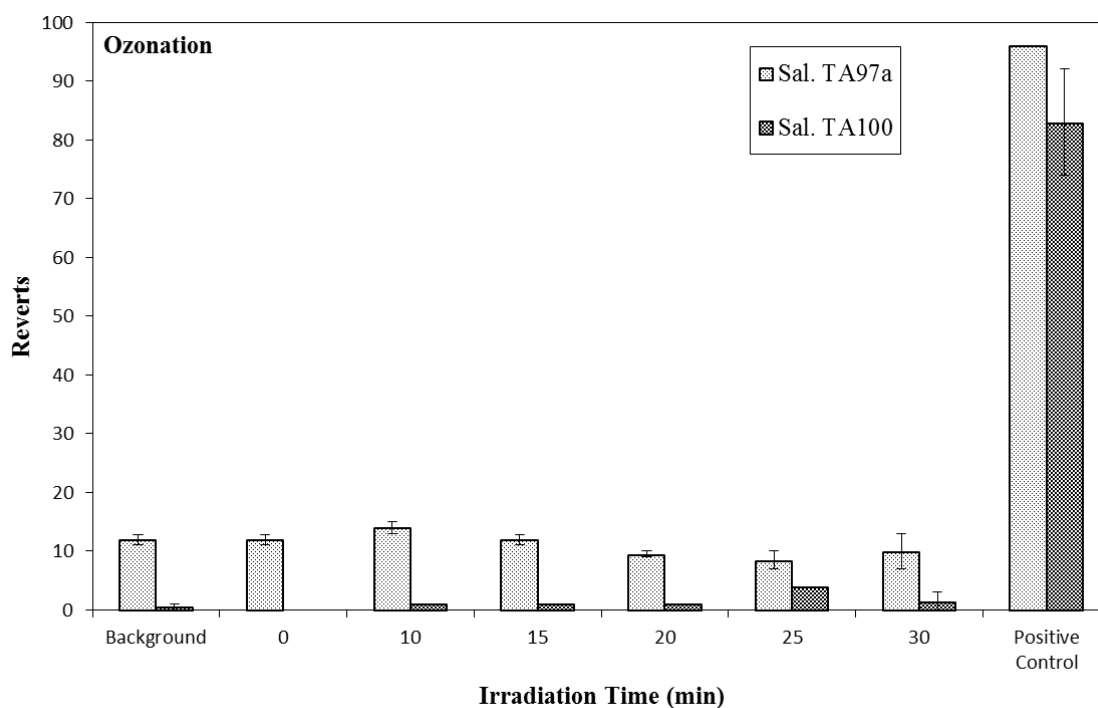


Figure 4.7: HPLC chromatogram of BPA degradation: a.) ozonation at t=30 min, b.) UV/H₂O₂ at t=10 min, and c.) UV/TiO₂ at t=16 min.

4.3.3 Mutagenicity Comparison

While the BPA degradation in all of the above AOPs was more than 80%, the slow rate of TOC degradation warrants further evaluation of water quality without undertaking major chemical analyses. Quick bioassays can provide valuable information about the safety of resultant water from a specific AOP. The mutagenicity for the degradation of BPA in each AOP was evaluated at multiple concentration values of BPA remaining. To avoid complications due to complex consecutive reactions undergoing in AOPs, sampling

times for genotoxicity for each type of AOP tested were determined a-priori based on initial kinetic experiments (Fig. 4.5); the points were selected based on similar extents of BPA conversion for each AOP. The determination of mutagenicity is based on the statistical deviation of the number of reverts relative to the background; any deviation up to 15% is considered a negative response. The Ames Test results for each AOP for both strains of Salmonella are shown in Fig. 4.8. There were no samples that resulted in probable mutagenicity for either strain over the entire tested range of BPA conversion. In the study of BPA biodegradation, Ike et al. (2002) identified several intermediates: p-hydroxyacetophenone, phydroxybenzaldehyde, and p-hydroxybenzoic acid, which have also been identified in photocatalytic oxidation of BPA (Fukahori et al., 2003). The mutagenicity of these compounds was analyzed using the Ames test with no positive toxicity (Ike et al., 2002).



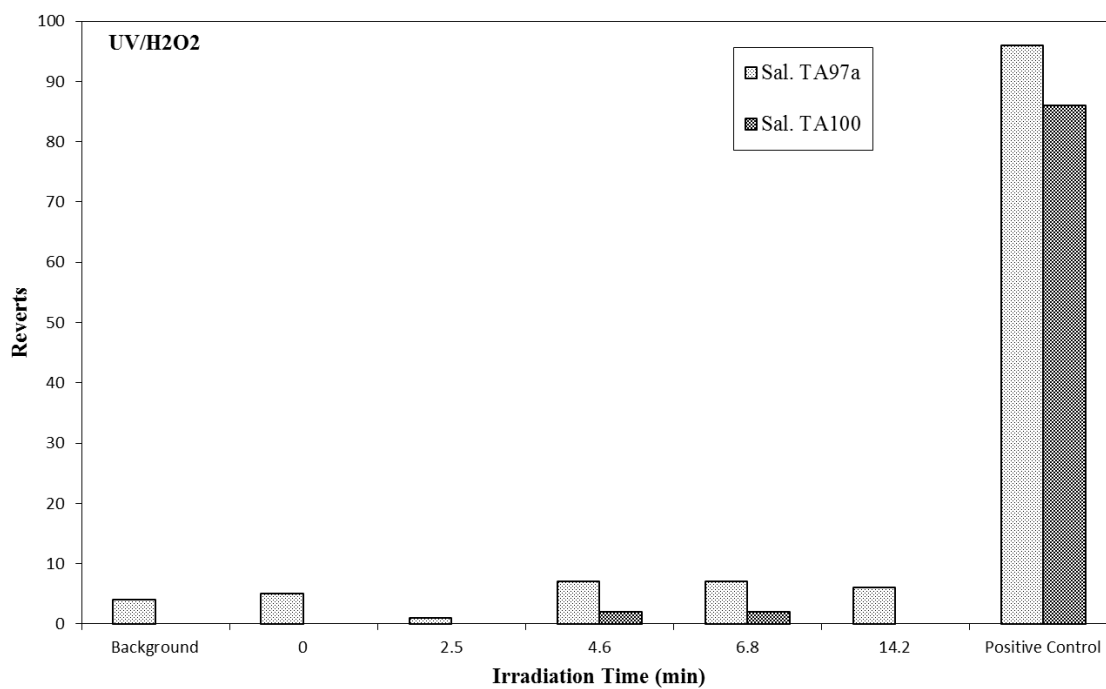
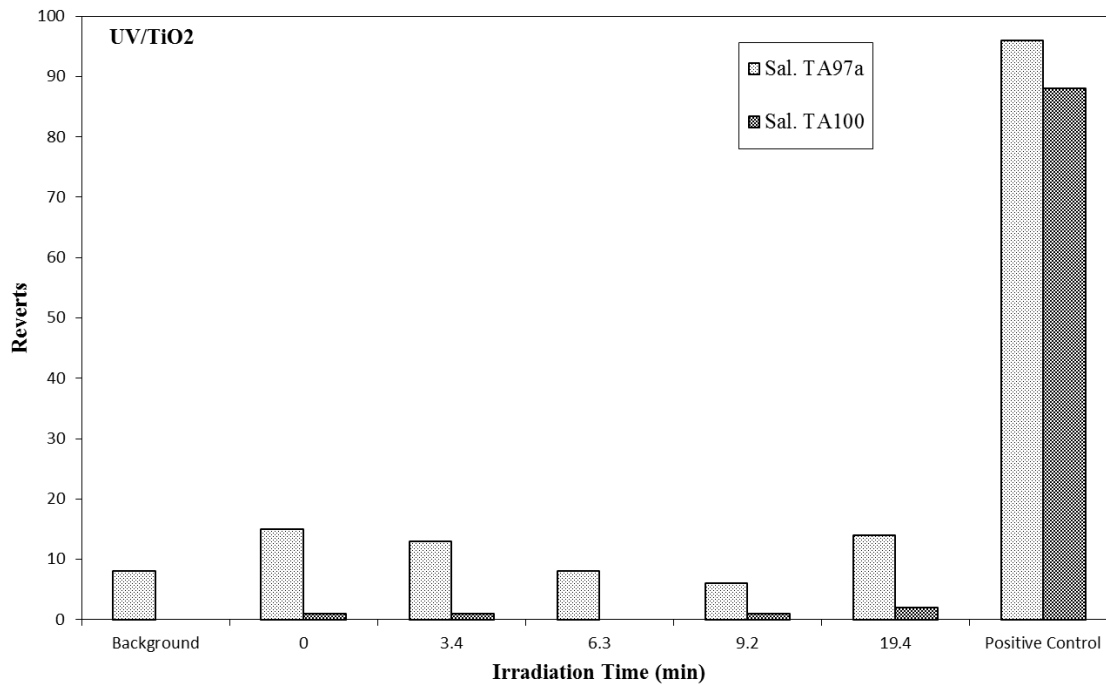


Figure 4.8: Mutagenicity analysis using the Ames Test for BPA degradation in different advanced oxidation processes.

4.3.4 Removal of Estrogenicity

The removal of total estrogenic activity is shown in Fig. 4.9, and is plotted in terms of the normalized equivalent estrogenicity ($EEQ/EEQ_{t=0}$) versus the percent BPA conversion. The overall trend is a steady decrease in estrogenicity, up to ~50% conversion, where at this point the estrogen activity was much lower at ~15%, but further removal of BPA did not reduce the EEQ, even up to 95% removal of BPA along with the limited removal of TOC; this indicated the potential formation of slightly estrogenic intermediates. Chen et al. (2006) investigated the estrogenicity of BPA following treatment with UV/H₂O₂ using a YES assay, showed that the normalized estrogenicity decreased at a lower rate when compared to the disappearance of BPA, and concluded that minor estrogenic transformation products had been formed. BPA biodegradation intermediates such as p-hydroxyacetophenone and p-isopropenylphenol had a slight estrogenic activity (Ike et al., 2002); these intermediates are also expected under chemical oxidation. UV/TiO₂ treatment resulted in the steady removal of the estrogenic activity with seemingly no levelling off, which is in agreement with TOC removal and lack of significant intermediate concentration in the solution. Ohko et al. (2001) also found that the removal of EEQ was in line with BPA conversion and a high rate of TOC removal. No estrogenic intermediates were found.

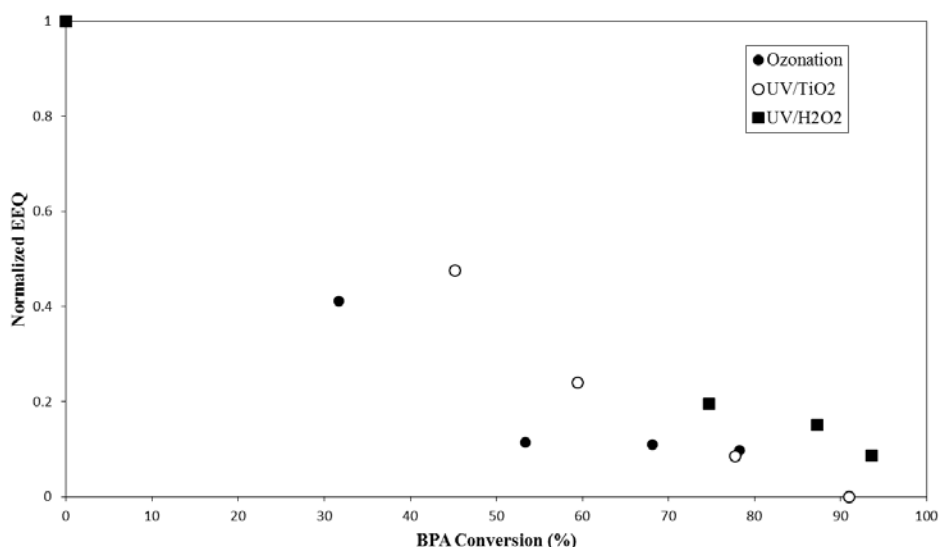


Figure 4.9: Analysis of estrogenic activity of BPA in aqueous solution.

Chapter 5

5 Conclusions and Recommendations

5.1 Conclusions

From the first stage of research in Chapter 3, the major conclusions are as follows:

- (i) The proprietary VN-TiO₂ catalyst and commercial catalyst Aeroxide P25 could be coated onto a glass support, but very thin films were formed. Subsequent dipping cycles with high temperature intermediate calcination stages would be required for thicker films.
- (ii) By dip coating a fibreglass support into the VN-TiO₂ solution optimal catalyst loading were achieved with only two dipping cycles and required only one calcination stage. The coated fibreglass was mechanically robust in the reactor with minimal loss of mass in subsequent use and maintained its shape and configuration.
- (iii) At optimal loadings, P25 on fibreglass had a reaction rate 4.5 times higher than on the glass disk, indicating fibreglass to be an effective support.
- (iv) Films formed from VN-TiO₂ were mesoporous with a very narrow pore size distribution at an average pore size of 4.7 nm. The films had very high surface area ~80 m²/g as compared to ~10 m²/g for films formed from standard sol-gel solutions.
- (v) VN-TiO₂ coated fibreglass had a photocatalytic degradation rate for methylene blue of about 50% lower than Aeroxide P25.
- (vi) Hybridization by adding only 10% P25 into the VN-TiO₂ solution improved the reaction rate of VN-TiO₂ by 40% and increased the surface area to ~95m²/g. The hybrid films maintained the mechanical properties of the pure VN-TiO₂ films.
- (vii) Long-term performance testing showed that both the VN-TiO₂ and P25 coated fibreglass suffered from catalyst fouling and inactivation. Regeneration of the catalyst only recovered the rate by ~50%, although the mechanism of degradation of methylene blue remained the same.

(viii) Overall, a hybrid catalyst of VN-TiO₂ with 10% P25 coated on fibreglass performed the best for methylene blue degradation in terms of photocatalytic activity, mechanical strength, and durability. The major advantage of VN-TiO₂ over P25 is that it is available in a form that can be easily coated on the support resulting in a uniform film without agglomeration.

The following conclusions can be drawn from the second stage of the project presented in Chapter 4.

- (i) All three tested AOPs effectively degraded BPA within 30 min of reaction time, however, UV/H₂O₂ and ozone could only remove 10% of the TOC after 30 min whereas UV/TiO₂ removed 50%.
- (ii) Several intermediate peaks were detected in the HPLC chromatographs for UV/H₂O₂ and ozone at the same retention times, but with different relative peak size compared to the parent BPA peak demonstrating the difference in reaction kinetics of the intermediates. UV/TiO₂ only produced very minor peaks with no intermediate buildup as found from TOC analysis.
- (iii) At all points analysed over the 30 min testing period for each AOP no significant mutagenicity was detected either for pure BPA or for the intermediates.
- (iv) UV/TiO₂ steadily removed the estrogenicity in line with BPA removal below the detection limit. UV/H₂O₂ and ozone reduced estrogenic activity to 15% of the starting solution at 50% conversion of BPA, but further BPA degradation did not significantly change the estrogenicity indicating the possible formation of weakly estrogenic intermediates.
- (v) Based on the removal of intermediates and estrogenicity of BPA, UV/TiO₂ was the most effective AOP.

5.2 Recommendations

The results obtained from each stage of the study were very promising and as a result several recommendations are presented below:

- (i) Available doped versions of the VN-TiO₂ which are active in the visible range should be tested for effectiveness in a lab scale solar photocatalytic reactor using the fibreglass dip coating procedure.
- (ii) Based on common immobilised reactor designs which have prescribed support configurations within the reactor, the fibreglass should be configured to the required shape and coated using the VN-TiO₂ catalyst to determine if at larger scales the mechanical properties would hold.
- (iii) Cost-benefit analysis comparing the coating procedures of VN-TiO₂ vs. a standard sol-gel method for fibreglass support at an industrial scale, including estimates for regular replacement of immobilised support, should be considered.
- (iv) Complete the same set of bioassay evaluations for the degradation of other prominent EDCs (e.g., E1, E2, and EE2) in the three AOPs.
- (v) Further testing to include assays to monitor in-vivo mutagenicity and estrogenicity should be carried out.
- (vi) Experiments should be conducted for BPA degradation in AOPs with bioassay analysis for spiked wastewater/drinking water samples to evaluate complex matrix effects on toxic by product formation.

References

- Abdelmelek, S. B., Greaves, J., Ishida, K. P., Cooper, W. J., & Song, W. (2011). Removal of pharmaceutical and personal care products from reverse osmosis retentate using advanced oxidation processes, *Environmental Science and Technology*, 45(8) 3665–3671.
- Ali, S., Angove, M. J., Wells, J. D., & Johnson, B. B. (2006). Aqueous Solubilities of Estrone, 17 β -Estradiol, 17 α -Ethinylestradiol, and Bisphenol A. *Journal of Chemical and Engineering Data*, 51(3), 879-881.
- Al-Sayyed, G., D'Oliveira, J-C., & Pichat, P. (1991). Semiconductor-sensitized photodegradation of 4-chlorophenol in water. *Journal of Photochemistry & Photobiology A: Chemistry*, 58(1), 99-114.
- Ames, B. N., Mccann J., & Yamasaki, E. (1975). Methods for detecting carcinogens and mutagens with the Salmonella/mammalian-microsome mutagenicity test. *Mutation Research*, 31(6), 347-364.
- Anderson, D., Goh, J. B., & Dinglasan, J. A. (2008). *Patent No. 7,501,180*. United States of America.
- Andreozzi, R., Caprio, V., Insola, A., & Marotta, R. (1999). Advanced oxidation processes (AOP) for water purification and recovery. *Catalysis Today*, 53(1), 51-59.
- Asakura, H., Matsuto, T., & Tanaka, N. (2004). Behavior of endocrine-disrupting chemicals in leachate from MSW landfill sites in Japan. *Waste Management*, 24(6), 613-622.
- Ashby, J., & Tennant, R. W. (1988). Chemical structure, Salmonella mutagenicity and extent of carcinogenicity as indicators of genotoxic carcinogenesis among 222 chemicals tested in rodents by the U.S. NCI/NTP. *Mutation Research/Genetic Toxicology*, 204(1), 17-115.
- Bakardjieva, S., Šubrt, J., Štengl, V., Dianež, M. J., & Sayagues, M. J. (2005). Photoactivity of anatase–rutile TiO₂ nanocrystalline mixtures obtained by heat treatment of homogeneously precipitated anatase. *Applied Catalysis B: Environmental*, 58(3-4), 193-202.
- Balasubramanian, G., Dionysiou, D. D., & Suidan, M. T. (2003). Titania powder modified sol-gel process for photocatalytic applications. *Journal of Materials Science*, 38(4), 823-831.

- Bischoff, B. L., & Anderson, M. A. (1995). Peptization Process in the Sol-Gel Preparation of Porous Anatase (TiO₂). *Chem. Mater.*, 7(10), 1772-1778.
- Boorman, G. A., Dellarco, V., Dunnick, J. K., Chapin, R. E., Hunter, S., Hauchman, F., Gardner, H., Cox, M., & Sills, R. C. (1999). Drinking water disinfection byproducts: review and approach to toxicity evaluation. *Environ Health Perspect.*, 107((Suppl 1)), 207-217.
- Brezova, V., Blazkova, A., Breznan, M., & Kottas, P. (1994). Phenol Degradation on Glass Fibres with Immobilized Titanium Dioxide Particles. *Collection of Czechoslovak Chemical Communications*, 60(5), 788-794.
- Brinker, C. J., Frye, G. C., Hurd, A. J., & Ashley, C. S. (1991). Fundamentals of sol-gel dip coating. *Thin Solid Films*, 201(1), 97-108.
- Burridge, E. (2008, October 12). *Chemical profile: bisphenol A*. Retrieved from ICIS Chemical Business: <http://www.icis.com/Articles/2008/10/13/9162868/chemical-profile-bisphenol-a.html>
- Byrne, J. A., Eggins, B. R., Brown, N. M. D., McKinney, B., & Rouse, M. (1998). Immobilisation of TiO₂ powder for the treatment of polluted water. *Applied Catalysis B: Environmental*, 17(1-2), 25-36.
- Caliman, F. A., & Gavrilescu, M. (2009). Pharmaceuticals, Personal Care Products (PPCP) and Endocrine Disrupting Agents in the Environment – A Review. *CLEAN – Soil, Air, Water*, 37(4-5), 277–303.
- Cantavenera, M. J., Catanzaro, I., Loddo, V., Palmisano, L., & Sciandrello, G. (2007). Photocatalytic degradation of paraquat and genotoxicity of its intermediate products. *Journal of Photochemistry and Photobiology A: Chemistry*, 185(2-3), 277-282.
- Carp, O., Huisman, C. L., & Reller, A. (2004). Photoinduced reactivity of titanium dioxide. *Progress in Solid State Chemistry*, 32(1-2), 33-177.
- Chen, D. & Ray, A. K. (1999). Photocatalytic kinetics of phenol and its derivatives over UV irradiated TiO₂. *Applied Catalysis B: Environmental*, 23(2-3), 143-157.
- Chen, D., Fengmei, L., & Ray, A. K. (2000a). Effect of mass transfer and catalyst layer thickness on photocatalytic reaction. *AIChE Journal*, 46(5), 1034-1045.
- Chen, D., Sivakumar, M., & Ray, A. K. (2000b). Heterogeneous Photocatalysis in Environmental Remediation. *Developments in Chemical Engineering and Mineral Processing*, 8(5-6), 505-550.

- Chen, P.-J., Linden, K. G., Hinton, D. E., Kashiwada, S., Rosefeldt, E. J., & Kullman, S. W. (2006). Biological assessment of bisphenol A degradation in water following direct photolysis and UV advanced oxidation. *Chemosphere*, *65*(7), 1094-1102.
- Chen, P.-J., Rosefeldt, E. J., Kullman, S. W., Hinton, D. E., & Linden, K. G. (2007). Biological assessments of a mixture of endocrine disruptors at environmentally relevant concentrations in water following UV/H₂O₂ oxidation. *Science of the Total Environment*, *376*(1-3), 18-26.
- Chen, Y. & Dionysiou, D. D. (2006a). TiO₂ photocatalytic films on stainless steel: The role of Degussa P-25 in modified sol-gel methods. *Applied Catalysis B: Environmental*, *62*(3-4), 255-264.
- Chen, Y. & Dionysiou, D. D. (2006b). Effect of calcination temperature on the photocatalytic activity and adhesion of TiO₂ films prepared by the P-25 powder-modified sol-gel method. *Journal of Molecular Catalysis A: Chemical*, *244*(1-2), 73-82.
- Chen, Y. & Dionysiou, D. D. (2008). Bimodal mesoporous TiO₂-P25 composite thick films with high photocatalytic activity and improved structural integrity. *Applied Catalysis B: Environmental*, *80*(1-2), 147-155.
- Chen, Y., & Dionysiou, D. D. (2007). A comparative study on physicochemical properties and photocatalytic behavior of macroporous TiO₂-P25 composite films and macroporous TiO₂ films coated on stainless steel substrate. *Applied Catalysis A: General*, *317*(1), 129-137.
- Chiang, K., Lim, T. M., Tsen, L., & Lee, C. C. (2004). Photocatalytic degradation and mineralization of bisphenol A by TiO₂ and platinumized TiO₂. *Applied Catalysis A: General*, *261*(2), 225-237.
- Choi, H., Stathatos, E., & Dionysiou, D. D. (2007). Effect of surfactant in a modified sol on the physicochemical properties and photocatalytic activity of crystalline TiO₂ nanoparticles. *Topics in Catalysis*, *44*(4), 513-521.
- Choi, W., & Ryu, J. (2008). Substrate-Specific Photocatalytic Activities of TiO₂ and Multiactivity Test for Water Treatment Application. *Environmental Science and Technology*, *42*(1), 294-300.
- Chong, M. N., Jin, B., Chow, C. W. K., & Saint, C. (2010). Recent developments in photocatalytic water treatment technology: A review. *Water Research*, *44*(10), 2997-3027.

- Comninellis, C., Kapalka, A., Malato, S., Parsons, S. A., Poullos, I., & Mantzavinos, D. (2008). Advanced oxidation processes for water treatment: advances and trends for R&D. *Journal of Chemical Technology and Biotechnology*, 83(6), 769-776.
- Davis, R. H., & Weller, S. G. (1998). *The Gist Of Genetics: Guide To Learning And Review*. London: Jones & Bartlett Learning.
- Deborde, M., Rabouan, S., Duguet, J-P., & Legube, B. (2005). Kinetics of Aqueous Ozone-Induced Oxidation of Some Endocrine Disruptors. *Environmental Science & Technology*, 39(16), 6086-6092.
- Deborde, M., Rabouan, S., Mazellier, P., Duguet, J-P., Legube, B. (2008). Oxidation of bisphenol A by ozone in aqueous solution. *Water Research*, 42, 4209-4308.
- Diamanti-Kandarakis, E., Bourguignon, J-P., Giudice, L. C., Hauser, R., Prins, G. S., Soto, A. M., Soeller, R. T., & Gore, A. C. (2009). Endocrine-Disrupting Chemicals: An Endocrine Society Scientific Statement. *Endocrine Reviews*, 30(4), 293-342.
- Environment Canada. (2009, March 12). *Pharmaceuticals and Personal Care Products in the Canadian Environment: Research and Policy Directions*. Retrieved from <http://www.ec.gc.ca/inre-nwri/default.asp?lang=En&n=C00A589F-1&offset=3&toc=show>
- Falconer, I. R., Chapman, H. F., Moore, M. R., & Ranmuthugala, G. (2006). Endocrine-disrupting compounds: A review of their challenge to sustainable and safe water supply and water reuse. *Environmental Toxicology*, 21(2), 181-191.
- Francis, S., Varshney, L., & Sabharwal, S. (2007). Thermal degradation behavior of radiation synthesized polydiallyldimethylammonium chloride. *European Polymer Journal*, 43(6), 2525-2531.
- Fretwell, R., & Douglas, P. (2001). An active, robust and transparent nanocrystalline anatase TiO₂ thin film — preparation, characterisation and the kinetics of photodegradation of model pollutants. *Journal of Photochemistry and Photobiology A: Chemistry*, 143(2-3), 229-240.
- Fu, P., Luan, Y., & Dai, X. (2004). Preparation of activated carbon fibers supported TiO₂ photocatalyst and evaluation of its photocatalytic reactivity. *Journal of Molecular Catalysis A: Chemical*, 221(1-2), 81-88.
- Fukahori, S., Ichiura, H., Kitaoka, T., & Tanka, H. (2003). Capturing of bisphenol A photodecomposition intermediates by composite TiO₂-zeolite sheets. *Applied Catalysis B: Environmental*, 46(3), 453-462.

- Galindo, C., Jacques, P., & Kalt, A. (2000). Photodegradation of the aminoazobenzene acid orange 52 by three advanced oxidation processes: UV/H₂O₂, UV/TiO₂ and VIS/TiO₂: Comparative mechanistic and kinetic investigations. *Journal of Photochemistry and Photobiology A: Chemistry*, 130(1), 35-47.
- Garoma, T., Matsumoto, S. A., Wu, Y., & Klinger, R. (2010). Removal of Bisphenol A and its Reaction-Intermediates from Aqueous Solution by Ozonation. *Ozone: Science and Engineering*, 32(5), 338-343.
- Gelover, S., Mondragón, P., & Jiménez, A. (2004). Titanium dioxide sol-gel deposited over glass and its application as a photocatalyst for water decontamination. *Journal of Photochemistry and Photobiology A: Chemistry*, 165(1-3), 241-246.
- Goh, C. M., Dinglasan, J. A., Goh, J. B., Loo., R., & Veletanlic, E. (2009). *Patent No. 7,534,490*. United States of America.
- Gottschalk, C., Libra, J. A., & Saupe, A. (2010). *Ozonation of Water and Waste Water: A Practical Guide to Understanding Ozone and its Applications, 2nd Edition*. Germany: John Wiley & Sons.
- Guillard, C., Lachheb, H., Houas, A., Ksibi, M., Elalouis, E., & Herrmann, J-M. (2003). Influence of chemical structure of dyes, of pH and of inorganic salts on their photocatalytic degradation by TiO₂ comparison of the efficiency of powder and supported TiO₂. *Journal of Photochemistry and Photobiology A: Chemistry*, 158(1), 27-36.
- Gunten, U. von & Hoigne, J. (1994). Bromate Formation during Ozonation of Bromide-Containing Waters: Interaction of Ozone and Hydroxyl Radical Reactions. *Environmental Science and Technology*, 28(7), 1234-1242.
- Guo, C., Ge., M., Liu, L., Gao, G., Feng, Y., & Wang, Y. (2010). Directed Synthesis of Mesoporous TiO₂ Microspheres: Catalysts and Their Photocatalysis for Bisphenol A Degradation. *Environmental Science and Technology*, 44(1), 419-425.
- Guzzella, L., Feretti, D., & Monarca, S. (2002). Advanced oxidation and adsorption technologies for organic micropollutant removal from lake water used as drinking-water supply. *Water Research*, 36(17), 4307-4318.
- Henderson, M. A. (2011). A surface science perspective on TiO₂ photocatalysis. *Surface Science Reports*, 66(6-7), 185-297.
- Heringa, M. B., Harmsen, D. J. H., Beerendonk, E. F., Reus, A. A., Krul, C. A. M., Metz, D. H., & Ijpelaar, G. F. (2011). Formation and removal of genotoxic activity during UV/H₂O₂-GAC treatment of drinking water. *Water Research*, 45, 366-374.

- Herrmann, J.-M. (1999). Heterogeneous photocatalysis: fundamentals and applications to the removal of various types of aqueous pollutants. *Catalysis Today*, 53(1), 115-129.
- Hing-Biu, L., & Peart, T. E. (2000). Bisphenol a contamination in Canadian municipal and industrial wastewater and sludge samples. *Water quality research journal of Canada*, 35(2), 283-298.
- Höfer, T., Gerner, I., Gundert-Remy, U., Liebsch, M., Schulte, A., Spielmann, H., Vogel, R., & Wettig, K. (2004). Animal testing and alternative approaches for the human health risk assessment under the proposed new European chemicals regulation. *Archives of Toxicology*, 78(10), 549-564.
- Hoigne, J. (1998). Chemistry of Aqueous Ozone and Transformation of Pollutants by Ozonation and Advanced Oxidation Processes. *Handbook of Environmental Chemistry*, 83-142.
- Horikoshi, S., Watanabe, N., Onishi, H., Hidaka, A., & Serpone, N. (2002). Photodecomposition of a nonylphenol polyethoxylate surfactant in a cylindrical photoreactor with TiO₂ immobilized fiberglass cloth. *Applied Catalysis B, Environmental*, 37(2), 117-129.
- Houas, A., Lachheb, H., Ksibi, M., Elaloui, E., Guillard, C., & Herrmann, J.-M. (2001). Photocatalytic degradation pathway of methylene blue in water. *Applied Catalysis B: Environmental*, 31(2), 145-157.
- Hubbard, S. A., Green, M. H. L., Gatehouse, D., & Bridges, J. W. (1984). In B. J. Kilbey, M. Legartor, W. Nichols, & C. Ramel (Eds.), *Handbook of Mutagenicity Test Procedures, 2nd Edition* (pp. 141-160). Amsterdam: Elsevier.
- Huber, M. M. (2004). *Elimination of pharmaceuticals during oxidative treatment of drinking water and wastewater: Application of ozone and chlorine dioxide* (Doctoral Dissertation). Retrieved From <http://e-collection.library.ethz.ch/eserv/eth:27680/eth-27680-02.pdf>
- Hurum, D. C., Agrios, A. G. & Gray, K. A. (2003). Explaining the Enhanced Photocatalytic Activity of Degussa P25 Mixed-Phase TiO₂ Using EPR. *The Journal of Physical Chemistry B*, 107(19), 4545-4549.
- Ike, M., Chen, M.-Y., Jin, C.-S., & Fujita, M. (2002). Acute toxicity, mutagenicity, and estrogenicity of biodegradation products of bisphenol-A. *Environmental Toxicology*, 17(5), 457-461.

- Ioan, I., Wilson, S., Lundances, E., & Neculai, A. (2007). Comparison of Fenton and sono-Fenton bisphenol A degradation. *Journal of Hazardous Materials*, 142(1-2), 559-563.
- Irmak, S., Erbatur, O., & Akgerman, A. (2005). Degradation of 17 β -estradiol and bisphenol A in aqueous medium by using ozone and ozone/UV techniques. *Journal of Hazardous Materials*, 126(1-3), 54-62.
- Katsumata, H., Kewabe, S., Kaneco, S., Suzuki, T., & Ohta, K. (2004). Degradation of bisphenol A in water by the photo-Fenton reaction. *Journal of Photochemistry and Photobiology A: Chemistry*, 162(2-3), 297-305.
- Kidd, K. A., Blanchfield, P. J., Mills, K. H., Palace, V. P., Evans, R. E., Lazorchak, J. M., & Flick, R. W. (2007). Collapse of a fish population after exposure to synthetic estrogen. *Proceedings of the National Academy of Sciences*, 104, 8897-8901.
- Kim, D. J., Hahn, S. H., Oh, S. H., & Kim, E. J. (2002). Influence of calcination temperature on structural and optical properties of TiO₂ thin films prepared by sol-gel dip coating. *Materials Letters*, 57(2), 355-360.
- Kim, S. H., Kwaka, S-Y., Sohn, B-H., & Park, T. H. (2003). Design of TiO₂ nanoparticle self-assembled aromatic polyamide thin-film-composite (TFC) membrane as an approach to solve biofouling problem. *Journal of Membrane Science*, 211(1), 157-165.
- Kirkland, D., Reeve, L., Gatehouse, D., & Vanparys, P. (2011). A core in vitro genotoxicity battery comprising the Ames Test plus the in vitro micronucleus test is sufficient to detect rodent carcinogens and in vivo genotoxins. *Mutation Research/Genetic Toxicology and Environmental Mutagenesis*, 721(1), 27-73.
- Klavarioti, M., Mantzavinos, D., & Kassinos, D. (2009). Removal of residual pharmaceuticals from aqueous systems by advanced oxidation processes. *Environment International*, 35(2), 402-417.
- Konstantinou, I., & Albanis, T. A. (2004). TiO₂-assisted photocatalytic degradation of azo dyes in aqueous solution: kinetic and mechanistic investigations: A review. *Applied Catalysis B: Environmental*, 49(1), 1-14.
- Kwon, C. H., Shin, H., Kim, J. H., Choi, W. S., & Yoon, K. H. (2004). Degradation of methylene blue via photocatalysis of titanium dioxide. *Materials Chemistry and Physics*, 86(1), 78-82.

- Lakshmi, S., Renganathan, R., & Fujita, S. (1995). Study on TiO₂-mediated photocatalytic degradation of methylene blue. *Journal of Photochemistry and Photobiology, A: Chemistry*, 88(2-3), 163-167.
- Lee, J-C., Kim, M-S., & Kim, B-W. (2002). Removal of paraquat dissolved in a photoreactor with TiO₂ immobilized on the glass-tubes of UV lamps. *Water Research*, 36(7), 1776-1782.
- Legrini, O., Oliveros, E., & Braun, A. M. (1993). Photochemical processes for water treatment. *Chemical Reviews*, 93(2), 671-698.
- Li, H., Helm, P. A., & Metcalfe, C. D. (2010). Sampling in the Great Lakes for pharmaceuticals, personal care products, and endocrine-disrupting substances using passive polar organic chemical integrative sampler. *Environmental Toxicology and Chemistry*, 29, 751-762.
- Ling, C. M., Mohamed, A. R., & Bhatia, S. (2004). Performance of photocatalytic reactors using immobilized TiO₂ film for the degradation of phenol and methylene blue dye present in water stream. *Chemosphere*, 57(7), 547-554.
- Liuxuea, Z., Xiolian, W., Peng, L., & Zhixing, S. (2007). Photocatalytic activity of anatase thin films coated cottonfibers prepared via a microwave assisted liquid phase deposition process. *Surface and Coatings Technology*, 201(18), 7607-7614.
- Luria, S. E., & Delbrück, M. (1943). Mutations of Bacteria from Virus Sensitivity to Virus Resistance. *Genetics*, 28(6), 491-511.
- Maniero, M. G., Bila, D. M., & Dezotti, M. (2008). Degradation and estrogenic activity removal of 17β-estradiol and 17α-ethinylestradiol by ozonation and O₃/H₂O₂. *Science of the Total Environment*, 407(1), 105-115.
- Martijn, A. J., & Kruithof, J. C. (2012). UV and UV/H₂O₂ Treatment: The Silver Bullet for By-product and Genotoxicity Formation in Water Production. *Ozone: Science & Engineering: The Journal of the International Ozone Association*, 34(2), 92-100.
- Martínez-Huitle, C. A., & Brillas, E. (2009). Decontamination of wastewaters containing synthetic organic dyes by electrochemical methods: A general review. *Applied Catalysis B: Environmental*, 87(3-4), 105-145.
- McCann, J., Choi, E., Yamasaki, E., & Ames, B. N. (1975). Detection of Carcinogens as Mutagens in the Salmonella/Microsome Test: Assay of 300 Chemicals. *Proceedings of the National Academy of Sciences of the United States of America*, 72(12), 5135-5139.

- Medina-Valtierra, J., García-Servín, J., Frausto-Reyes, C., & Calixto, S. (2006). The photocatalytic application and regeneration of anatase thin films with embedded commercial TiO₂ particles deposited on glass microrods. *Applied Surface Science*, 252(10), 3600-3608.
- Mikula, M., Brezová, V., Čěppan, M., Pach, L., & Karpinský, Ľ. (1995). Comparison of photocatalytic activity of sol-gel TiO₂ and P25 TiO₂ particles supported on commercial fibreglass fabric. *Journal of Materials Science Letters*, 14(9), 615-616.
- Mills, A., Hill, G., Bhopal, S., Parkin, I. P., & O'Neill, S. A. (2003). Thick titanium dioxide films for semiconductor photocatalysis. *Journal of Photochemistry and Photobiology*, 160(3), 185-194.
- Mills, A., Hill, G., Crow, M., & Hodgen, S. (2005). Thick titania films for semiconductor photocatalysis. *Journal of Applied Electrochemistry*, 35(7-8), 641-653.
- Mortelmans, K., & Zeiger, E. (2000). The AmesSalmonella/microsomes mutagenicity assay. *Mutation Research/Fundamental and Molecular Mechanisms of Mutagenesis*, 455(1-2), 29-60.
- Mukherjee, P. S., & Ray, A. K. (1999). Major Challenges in the Design of a Large-Scale Photocatalytic Reactor for Water Treatment. *Chemical engineering & technology*, 22(3), 253-260.
- Muneer, M., Theurich, J., & Bahnemann, D. (2001). Titanium dioxide mediated photocatalytic degradation of 1,2-diethyl phthalate. *Journal of Photochemistry and Photobiology A: Chemistry*, 143(2-3), 213-219.
- Nakada, N., Nyunoya, H., Nakamura, M., Hara, A., Iguchi, T., & Takada, H. (2004). Identification of estrogenic compounds in wastewater effluent. *Environmental toxicology and chemistry*, 23(12), 2807-2815.
- Ohe, T., Watanabe, T., & Wakabayashi, K. (2004). Mutagens in surface waters: a review. *Mutation Research/Reviews in Mutation Research*, 567(2-3), 109-149.
- Ohko, Y., Ando, I., Niwa, C., Tatsuma, T., Yamamura, T., Nakashima, T., Kubota, Y., & Fujishima, A. (2001). Degradation of Bisphenol A in Water by TiO₂ Photocatalyst. *Environmental Science and Technology*, 35(11), 2365-2368.
- Ohtani, B., Ogawa, Y., & Nishimoto, S. (1997). Photocatalytic Activity of Amorphous-Anatase Mixture of Titanium(IV) Oxide Particles Suspended in Aqueous Solutions. *The Journal of Physical Chemistry B*, 101(19), 3746-3752.

- Onesios, K. M., Yu, J. T., & Bouwer, E. J. (2009). Biodegradation and removal of pharmaceuticals and personal care products in treatment systems: a review. *Biodegradation*, 20(4), 441–466.
- Peill, N. J., & Hoffmann, M. R. (1996). Chemical and Physical Characterization of a TiO₂-Coated Fiber Optic Cable Reactor. *Environmental Science and Technology*, 30(9), 2806-2812.
- Pera-Titus, M., García-Molina, V., Baños, M. A., Giménez, J., & Esplugas, S. (2004). Degradation of chlorophenols by means of advanced oxidation processes: a general review. *Applied Catalysis B: Environmental*, 47(4), 219-256.
- Petala, M., Samaras, P., Zouboulis, A., Kungolos, A., & Sakellaropoulos, G. P. (2008). Influence of ozonation on the in vitro mutagenic and toxic potential of secondary effluents. *Water Research*, 42, 4929-4940.
- Platzek, T., Lang, C., Grohmann, G., Gi, U-S., & Baltes, W. C. (1999). Formation of a carcinogenic aromatic amine from an azo dye by human skin bacteria in vitro. *Human & Experimental Toxicology*, 18(9), 552-559.
- Pozzo, R. L., Baltanás, M. A., & Cassano, A. E. (1997). Supported titanium oxide as photocatalyst in water decontamination: State of the art. *Catalysis Today*, 39(3), 219-231.
- Pozzo, R. L., Giombi, J. L., Baltanás, M. A., & Cassano, A. E. (2000). Performance in a fluidized bed reactor of photocatalysts immobilized onto inert supports. *Catalysis Today*, 62(2-3), 175-187.
- Pruden Childs, L. & Ollis, D. F. (1981). Photoassisted heterogeneous catalysis: Rate equations for oxidation of 2-methyl-2-butyl-alcohol and isobutane. *Journal of Catalysis*, 67(1), 35-48.
- Rao, K. V. S., Subrahmanyam, M., & Boule, P. (2004). Immobilized TiO₂ photocatalyst during long-term use: decrease of its activity. *Applied Catalysis B: Environmental*, 49(4), 239-249.
- Ray, A. K., & Beenackers, A. A. C. M. (1998). Development of a new photocatalytic reactor for water purification. *Catalysis Today*, 40(1), 73-83.
- Ray, A. K., & Beenackers, A. A. C. M. (1997). Novel swirl-flow reactor for kinetic studies of semiconductor photocatalysis. *AIChE Journal*, 43(10), 2571-2578.
- Reuters. (2012). Climate, food pressures require rethink on water: UN [Press release]. Retrieved from <http://www.reuters.com/article/2012/03/11/water-study-idUSL5E8E9ANL20120311>

- Rice, R. G., Robson, C. M., Miller, G. W., & Hill, A. G. (1981). Uses of Ozone in Drinking Water Treatment. *Journal AWWA*, 73(1), 44-57.
- Richardson, S. D., Plewa, M. J., Wagner, E. D., Schoeny, R., & DeMarini, D. M. (2007). Occurrence, genotoxicity, and carcinogenicity of regulated and emerging disinfection by-products in drinking water: A review and roadmap for research. *Mutation Research/Reviews in Mutation Research*, 636(1-3), 178-242.
- Rivera-Utrilla, J., Sánchez-Polo, M., Mondaca, M. A., & Zaror, C. A. (2002). Effect of ozone and ozone/activated carbon treatments on genotoxic activity of naphthalenesulfonic acids. *Journal of Chemical Technology and Biotechnology*, 77(8), 883-890.
- Rizzo, L. (2011). Bioassays as a tool for evaluating advanced oxidation processes in water and wastewater treatment. *Water Research*, 45(15), 4311-4340.
- Rodgers-Gray, T. P., Jobling, S., Morris, S., Kelly, C., Kelly, C., Kirby, S., Janbakhsh, A., Harries, J. E., Waldock, M. J., Sumpter, J. P., & Tyler, C.R. (2000). Long-Term Temporal Changes in the Estrogenic Composition of Treated Sewage Effluent and Its Biological Effects on Fish. *Environmental Science and Technology*, 34(8), 1521-1528.
- Rodriguez, P., Meille, V., Pallier, S., & Al Sawah, M. A. (2009). Deposition and characterisation of TiO₂ coatings on various supports for structured (photo)catalytic reactors. *Applied Catalysis A, General*, 360(2), 154-162.
- Rosenfeldt, E. J., & Linden, K. G. (2004). Degradation of Endocrine Disrupting Chemicals Bisphenol A, Ethinyl Estradiol, and Estradiol during UV Photolysis and Advanced Oxidation Processes. *Environmental Science and Technology*, 38(20), 5476-5483.
- Rouquerol, F., Rouquerol, J., & Sing, K. (1999). *Adsorption by Powders and Porous Solids Principles, Methodology and Applications*. London: Academic Press.
- Routledge, E. J., & Sumpter, J. P. (1996). Estrogenic activity of surfactants and some of their degradation products assessed using a recombinant yeast screen. *Environmental Toxicology and Chemistry*, 15(3), 241-248.
- Routledge, E. J., & Sumpter, J. P. (2005). Endocrine Disrupters in the Aquatic Environment: An Overview. *Acta hydrochimica et hydrobiologica*, 33(1), 9-16.
- Saint-Gobain Vetrotex Deutschland GmbH (2002, March). *Glass Composition, Glass Types*. Retrieved from Statistical Calculation and Development of Glass Properties: http://glassproperties.com/glasses/E_R_and_D_glass_properties.pdf

- Schrader, T. J., Langlois, I., Soper, K., & Cherry, W. (2002). Mutagenicity of bisphenol A (4,4'-isopropylidenediphenol) in vitro: effects of nitrosylation. *Teratogenesis, Carcinogenesis, and Mutagenesis*, 22(6), 425-441.
- Schweickl, H., Schmalz, G., & Rackebrandt, K. (1998). The mutagenic activity of unpolymerized resin monomers in *Salmonella typhimurium* and V79 cells. *Mutation Research/Genetic Toxicology and Environmental Mutagenesis*, 415(1-2), 119-130.
- Serpone, N., Borgarello, E., Harris, R., Cahill, P., & Borgarello, M. (1986). Photocatalysis over TiO₂ supported on a glass substrate. *Solar Energy Materials*, 14(2), 121-127.
- Shan, A. Y., Ghazi, T. I. M., & Rashid, S. A. (2010). Immobilisation of titanium dioxide onto supporting materials in heterogeneous photocatalysis: A review. *Applied Catalysis A: General*, 389(1-2), 1-8.
- Sharma, K. P., Sharma, S., Sharma, S., Singh, P. K., Kuma, S., Grover, R., & Sharma, P. K. (2007). A comparative study on characterization of textile wastewaters (untreated and treated) toxicity by chemical and biological tests. *Chemosphere*, 69(1), 48-54.
- Sivakumar, S., Pillai, P. K., Mukundan, P., & Warriar, K. G. K. (2002). Sol-gel synthesis of nanosized anatase from titanyl sulfate. *Materials Letters*, 57(2), 330-335.
- Snyder, S. A., Westerhoff, P., Yoon, Y., & Sedlak, D. L. (2003). Pharmaceuticals, Personal Care Products, and Endocrine Disruptors in Water: Implications for the Water Industry. *Environmental engineering science*, 20(5), 449-469.
- Sonawane, R. S., Hegde, S. G., & Dongare, M. K. (2003). Preparation of titanium(IV) oxide thin film photocatalyst by sol-gel dip coating. *Materials Chemistry and Physics*, 77(3), 744-750.
- Stahelin, J., & Hoigne, J. (1985). Decomposition of ozone in water in the presence of organic solutes acting as promoters and inhibitors of radical chain reactions. *Environmental Science and Technology*, 19(12), 1206-1213.
- Su, C., Hong, B-Y., & Tseng, C-M. (2004). Sol-gel preparation and photocatalysis of titanium dioxide. *Catalysis Today*, 96(3), 119-126.
- Tanaka, Y., & Suganuma, M. (2001). Effects of Heat Treatment on Photocatalytic Property of Sol-Gel Derived Polycrystalline TiO₂. *Journal of Sol-Gel Science and Technology*, 22(1-2), 83-89.

- Tennant, R. W., Margolin, B. H., Shelby, M. D., Zeiger, E., Haseman, J. K., Spalding, J., Caspary, W., Resnick, M., Stasiewicz, S., & Anderson, B. (1987). Prediction of chemical carcinogenicity in rodents from in vitro genetic toxicity assays. *Science*, 236(4804), 933-941.
- The Dow Chemical Company. (2012, January 23). *Product Safety - Product Safety Assessment Finder*. Retrieved from: http://msdssearch.dow.com/PublishedLiteratureDOWCOM/dh_088c/0901b8038088c783.pdf?filepath=productsafety/pdfs/noreg/233-00250.pdf&fromPage=GetDoc
- Torres, R. A., Pétrier, C., Combet, E., Carrier, M., & Pulgarin, C. (2008). Ultrasonic cavitation applied to the treatment of bisphenol A. Effect of sonochemical parameters and analysis of BPA by-products. *Ultrasonics Sonochemistry*, 15(4), 605-611.
- United States Environmental Protection Agency. (2011, September 06). *Endocrine Disruptors Research*. Retrieved from EPA: <http://www.epa.gov/ncer/science/endocrine/index.html>
- United States National Library of Medicine. (2012, July 30). *Handbook Illustrations*. Retrieved from Genetics Home Reference: <http://ghr.nlm.nih.gov/handbook/illustrations/frameshift>
- Watanabe, N., Horikoski, S., Kawabe, H., Sugie, Y., Zhao, J., & Hidaka, H. (2003). Photodegradation mechanism for bisphenol A at the TiO₂/H₂O interfaces. *Chemosphere*, 52(5), 851-859.
- Xagas, A. P., Androulaki, E., Hiskia, A., & Falaras, P. (1999). Preparation, fractal surface morphology and photocatalytic properties of TiO₂ films. *Thin Solid Films*, 357(2), 173-178.
- Yamamoto, T., Yasuhara, A., Shiraishi, H., & Nakasugi, O. (2001). Bisphenol A in hazardous waste landfill leachates. *Chemosphere*, 42(4), 415-418.
- Yu, J., Wang, X., & Fu, X. (2004). Pore-Wall Chemistry and Photocatalytic Activity of Mesoporous Titania Molecular Sieve Films. *Chemistry of Materials*, 16(8), 1523-1530.
- Yu, J., Yu, H., Cheng, B., Zhou, M., & Zhao, X. (2006). Enhanced photocatalytic activity of TiO₂ powder (P25) by hydrothermal treatment. *Journal of Molecular Catalysis A: Chemical*, 253(1-2), 112-118.

- Yu, J., Zhao, X., & Zhao, Q. (2000). Effect of surface structure on photocatalytic activity of TiO₂ thin films prepared by sol-gel method. *Thin Solid Films*, 349(1-2), 7-14.
- Yu, J-G., Yu, H-G., Cheng, B., Zhao, X-J., Yu, J. C., & Ho, W-K. (2003). The Effect of Calcination Temperature on the Surface Microstructure and Photocatalytic Activity of TiO₂ Thin Films Prepared by Liquid Phase Deposition. *The Journal of Physical Chemistry B*, 107(50), 13871-13879.
- Zeiger, E. (1987). Carcinogenicity of Mutagens: Predictive Capability of the Salmonella Mutagenesis Assay for Rodent Carcinogenicity. *Cancer Research*, 47(5), 1287-1296.
- Zhang, T., Oyama, T., Aoshima, A., Hidaka, H, Zhao, J., & Serpone, N. (2001). Photooxidative N-demethylation of methylene blue in aqueous TiO₂ dispersions under UV irradiation. *Journal of Photochemistry and Photobiology A: Chemistry*, 140(2), 163-172.

Curriculum Vitae

Name: Charles Gilmour

Post-secondary Education and Degrees: Ryerson University
Toronto, Ontario, Canada
2005-2010 B.Eng

The University of Western Ontario
London, Ontario, Canada
2010-2012 M.E.Sc.

Honours and Awards: Western Graduate Research Scholarship
2010-2012

Dean's List
Ryerson University
2010

Related Work Experience Teaching Assistant
The University of Western Ontario
2010-2012

Process Engineer
Suncor Energy
2009

Industrial Research Intern
Electro-Pack Inc.
2008